

E. coli trends in Waikato streams

Exploration of drivers and alternative trend analysis

Prepared by:

Simon Woodward, Sandy Elliott, Rob Davies-Colley and Rebecca Stott (National Institute of Water & Atmospheric Research Ltd (NIWA))

For:

Waikato Regional Council
Private Bag 3038
Waikato Mail Centre
HAMILTON 3240

June 2022

Disclaimer

This internal series report has been prepared for the use of Waikato Regional Council as a reference document and as such does not constitute Council's policy.

Council requests that if excerpts or inferences are drawn from this document for further use by individuals or organisations, due care should be taken to ensure that the appropriate context has been preserved, and is accurately reflected and referenced in any subsequent spoken or written communication.

While Waikato Regional Council has exercised all reasonable skill and care in controlling the contents of this report, Council accepts no liability in contract, tort or otherwise, for any loss, damage, injury or expense (whether direct, indirect or consequential) arising out of the provision of this information or its use by you or any other party.

E. coli trends in Waikato streams

Exploration of drivers and alternative trend analysis

Prepared for Waikato Regional Council

January 2022

Prepared by:
Simon Woodward
Sandy Elliott
Rob Davies-Colley
Rebecca Stott

For any information regarding this report please contact:

Simon Woodward
Water Quality Modelling Scientist
Freshwater and Estuaries
+64 7 856 1717
simon.woodward@niwa.co.nz

National Institute of Water & Atmospheric Research Ltd
PO Box 11115
Hamilton 3251

Phone +64 7 856 7026

NIWA CLIENT REPORT No: 2021347HN
Report date: January 2022
NIWA Project: EVW21208

Quality Assurance Statement		
	Reviewed by:	Neale Hudson
	Formatting checked by:	Carole Evans
	Approved for release by:	Michael Bruce

© All rights reserved. This publication may not be reproduced or copied in any form without the permission of the copyright owner(s). Such permission is only to be given in accordance with the terms of the client's contract with NIWA. This copyright extends to all forms of copying and any storage of material in any kind of information retrieval system.

Whilst NIWA has used all reasonable endeavours to ensure that the information contained in this document is accurate, NIWA does not give any express or implied warranty as to the completeness of the information contained herein, or that it will be suitable for any purpose(s) other than those specifically contemplated during the Project or agreed by NIWA and the Client.

Contents

- Contents 3**
- Tables 5**
- Figures 5**
- Executive summary 8**

- 1 Introduction 11**
 - 1.1 Trends of concern for river water quality in the Waikato 11
 - 1.2 Objective and scope..... 11
 - 1.3 Overview of this report..... 13

- 2 *E. coli* as an indicator of faecal contamination 14**

- 3 Summary of factors expected to affect faecal contamination 15**
 - 3.1 Sources of faecal contamination 16
 - 3.2 Naturalised *E. coli* 17
 - 3.3 Modifiers of faecal contamination 17
 - 3.4 Observed stream faecal contaminant concentrations 19

- 4 Trend analysis methods 20**
 - 4.1 Traditional trend analysis approach (Sen slope) 20
 - 4.2 Alternative trend analysis approach (GAM) 20

- 5 Summary of types of data used 23**

- 6 *E. coli* data 24**
 - 6.1 Water quality sites 24
 - 6.2 Data preparation..... 27
 - 6.3 Data censoring and banding correction..... 29
 - 6.4 Data skew and outlier correction 30
 - 6.5 Effect of change in sampling frequency..... 31

- 7 Factors related to faecal pollution trends, and relationships to *E. coli* concentrations..... 32**
 - 7.1 Water quality variables other than *E. coli* 32
 - 7.2 Air temperature and rainfall 33

7.3	Livestock density.....	38
7.4	Land use area.....	42
7.5	Fencing.....	43
7.6	Point source discharges.....	43
7.7	Flow.....	43
8	Estimation of <i>E. coli</i> trends.....	48
8.1	Time window selection.....	48
8.2	Traditional methods (based on Sen slope).....	49
8.3	Alternative methods (based on GAM).....	49
8.4	Uncertainty, significance and strength of evidence.....	52
8.5	Example 1 (Waihou River at Whites Road, no flow data).....	53
8.6	Example 2 (Waitoa River at Landsdowne Road, flow data).....	57
8.7	<i>E. coli</i> trends for all sites.....	63
8.8	<i>E. coli</i> trends by subregion.....	75
8.9	<i>E. coli</i> trends overall summary.....	75
8.10	Comparison of GAM Models.....	81
9	Turbidity and visual clarity trends in relation to <i>E. coli</i> trends.....	83
9.1	Waihou and Waitoa examples.....	83
9.2	Trends for all sites and summary.....	88
10	Interpretation of <i>E. coli</i> trends.....	90
10.1	Livestock density.....	90
10.2	Land use and regional variations.....	92
10.3	Point sources.....	92
10.4	Fencing.....	95
11	Discussion.....	96
12	Conclusion.....	98
13	Supplementary material.....	100
14	Acknowledgements.....	101
15	Glossary of abbreviations and terms.....	102
16	References.....	104

Tables

Table 1:	Categorisation of sources and modifiers affecting faecal contamination, with notes.	15
Table 2:	List of water quality monitoring sites analysed in this study (N = 82).	25
Table 3:	Intergovernmental Panel on Climate Change likelihood categories (from McBride, 2019).	52
Table 4:	Explanation of statistics included in the trend plots.	55
Table 5:	Summary of Waikato <i>E. coli</i> trends (%/year) assessed using Thiel-Sen analysis.	78
Table 6:	Summary of Waikato <i>E. coli</i> trends (%/year) assessed using GAM analysis.	80

Figures

Figure 1:	<i>E. coli</i> state and trends in the Waikato-Waipā catchment (2015-2019), as assessed by LAWA (Land, Air, Water Aotearoa).	12
Figure 2:	Summary of anthropogenic and natural factors that affect <i>E. coli</i> concentrations and trends.	19
Figure 3:	Map of the Waikato Region showing WRC water quality and flow site locations, as well as major point source discharges.	24
Figure 4:	Raw <i>E. coli</i> data at 82 WRC SOE sites.	28
Figure 5:	Annual median <i>E. coli</i> concentration (CFU/100 mL) at 82 WRC SOE sites.	29
Figure 6:	Raw <i>E. coli</i> data at Waikato River at Taupo Control Gates (site 1131_127).	30
Figure 7:	Distribution of optimal Box-Cox lambda values used to transform <i>E. coli</i> data at the 82 WRC sites used in this study.	31
Figure 8:	Correlation between <i>E. coli</i> and other water quality variables.	33
Figure 9:	Correlation between <i>E. coli</i> and turbidity at all 82 WRC SOE sites.	34
Figure 10:	Correlation between <i>E. coli</i> and visual clarity at the 79 WRC SOE sites that had clarity data.	35
Figure 11:	Correlation between <i>E. coli</i> and VCSN daily catchment rainfall (mm).	36
Figure 12:	Correlation between <i>E. coli</i> and VCSN catchment daily average temperature (°C).	37
Figure 13:	Catchment annual total rainfall (mm) (top) and annual average temperature (°C) (bottom) for the 82 WRC SOE sites.	38
Figure 14:	WRC (AgriBase) livestock density data (SU/ha).	39
Figure 15:	Correlation between long term <i>E. coli</i> and WRC (AgriBase) livestock density (SU/ha).	40
Figure 16:	CLUES (LCDB) land use data, showing proportional area of six types of land use in each of the 82 catchments.	41
Figure 17:	Correlation between <i>E. coli</i> and CLUES (AgriBase/LCDB3) land use area.	42

Figure 18:	Changes in proportions of fenced streambank adjacent to drystock (sheep-beef) pastures, across subregions and stream orders.	44
Figure 19:	Changes in proportions of fenced streambank adjacent to dairy pastures, across subregions and stream orders.	45
Figure 20:	Correlation between <i>E. coli</i> concentrations at stream monitoring sites and total upstream point source yield.	46
Figure 21:	Annual average flow (m ³ /s) at 38 WRC flow sites.	46
Figure 22:	Correlation between <i>E. coli</i> and flow (m ³ /s) at a nearby flow gauge.	47
Figure 23:	Trends and 5-year changes in <i>E. coli</i> concentrations for the Waihou River at Whites Road (no adjustment).	56
Figure 24:	Trends and 5-year changes in <i>E. coli</i> concentrations from the Waihou River at Whites Road (seasonal adjustment).	56
Figure 25:	Trends and 5-year changes in <i>E. coli</i> concentrations from the Waihou River at Whites Road (seasonal, rain and temperature adjustment).	57
Figure 26:	GAM residuals and model terms for <i>E. coli</i> at Waihou River at White's Road (seasonal, rain and temperature adjustment).	59
Figure 27:	Trends and 5-year changes in <i>E. coli</i> concentrations from the Waitoa River at Landsdowne Road (no adjustment).	60
Figure 28:	Trends and 5-year changes in <i>E. coli</i> concentrations from the Waitoa River at Landsdowne Road (flow adjustment).	60
Figure 29:	GAM residuals and model terms for <i>E. coli</i> at Waitoa River at Landsdowne Road (flow adjustment).	61
Figure 30:	Trends and 5-year changes in <i>E. coli</i> concentrations from the Waitoa River at Landsdowne Road (seasonal and flow adjustment).	62
Figure 31:	Trends and 5-year changes in <i>E. coli</i> concentrations from the Waitoa River at Landsdowne Road (seasonal, flow, rain and temperature adjustment).	62
Figure 32:	Trends and 5-year changes in <i>E. coli</i> concentrations from the Waitoa River at Landsdowne Road (seasonal, rain and temperature adjustment).	63
Figure 33:	Five-year trends in <i>E. coli</i> concentration (% increase/year) in the Waikato River and regional streams according to subcatchment groupings.	73
Figure 34:	Summary of statistical significance of GAM covariate terms.	74
Figure 35:	Summary of 5-year trends in <i>E. coli</i> concentration (% increase/year) by subregion (Thiel-Sen Slope Estimator).	76
Figure 36:	Summary of 5-year trends in <i>E. coli</i> concentration (% increase/year) by subregion (GAM).	77
Figure 37:	Map of 2015-2019 <i>E. coli</i> trends (%/year) assessed using Thiel-Sen analysis (with seasonal adjustment).	79
Figure 38:	Map of 2015-2019 <i>E. coli</i> trends (%/year) assessed using a GAM model (seasonal, rain and temperature adjustment).	81
Figure 39:	Comparison of model fit to <i>E. coli</i> data (NSE) for the GAM models with different covariates.	82
Figure 40:	Trends and 5-year changes in Turbidity from the Waihou River at Whites Road (seasonal, rain and temperature adjustment).	84
Figure 41:	Trends and 5-year changes in visual clarity from the Waihou River at Whites Road (seasonal, rain and temperature adjustment).	84

Figure 42:	Trends and 5-year changes in Turbidity from the Waitoa River at Landsdowne Road (seasonal, rain and temperature adjustment).	85
Figure 43:	Trends and 5-year changes in Visual Clarity from the Waitoa River at Landsdowne Road (seasonal, rain and temperature adjustment).	85
Figure 44:	Summary of 5-year trends in Turbidity (% increase/year) by subregion (GAM).	86
Figure 45:	Summary of 5-year trends in Visual Clarity (%/year) by subregion (GAM).	87
Figure 46:	Map of 2015-2019 Turbidity trends (%/year) assessed using a GAM model (seasonal, rain and temperature adjustment).	88
Figure 47:	Map of 2015-2019 Visual Clarity trends (%/year) assessed using a GAM model (seasonal, rain and temperature adjustment).	89
Figure 48:	<i>E. coli</i> “raingam” trend estimates from Figure 36 against median livestock density (stock units per hectare).	91
Figure 49:	<i>E. coli</i> “raingam” trend estimates from Figure 36 against 5-year percent change in livestock density (stock units per hectare).	91
Figure 50:	<i>E. coli</i> “raingam” trend estimates from Figure 36 against land use type and fraction of catchment area.	94
Figure 51:	Comparison of methods for handling censored data in trend analysis.	112

Executive summary

Routine monitoring of concentrations of the microbial indicator *Escherichia coli* across the Waikato region between 2008 and 2017 indicated that faecal contamination of streams and rivers was generally decreasing (important improvements were identified at 16 out of 114 sites over time compared with important deteriorations at only 4 sites; Vant, 2018). These positive trends may have been due to efforts made to reduce the impact of land use on water quality, such as limiting pastoral intensification, improving effluent management, and excluding stock from waterways by fencing.

More recent monitoring of Waikato streams (2015-2019¹), however, indicates that concentrations of *E. coli* are increasing at most river monitoring sites, indicating a deterioration in water quality. For example, data downloaded from <https://www.lawa.org.nz> (LAWA— Land, Air, Water Aotearoa) on 10 March 2021 indicated that in the five year period 2015-2019, *E. coli* concentrations were decreasing at three of 70 sites (4%) in the Waikato-Waipā catchment, increasing at 59 sites (84%), and indeterminate or not assessed at 5 sites (12%). This situation is of concern to Waikato Regional Council (WRC) given the effort expended in policy development and implementation, and the expense that farmers have incurred to meet regional plan requirements. These reported trends are also of concern considering the requirements of the National Policy Statement for Freshwater Management (NPS-FM) 2020, which requires councils to ensure river water quality meets or exceeds threshold attribute values (thereby enhancing water quality, including recreational water quality, over time).

Waikato Regional Council (WRC) wish to better understand the cause(s) of the apparent deteriorating trend in microbial water quality across the region, and commissioned NIWA to undertake a desktop assessment of historical data and provide advice. NIWA was tasked with:

- Assessing trends in microbial water quality across the entire Waikato Region over the preceding 25-year period, with emphasis on the most recent 10- and 5-year periods.
- Trend assessment was to use standard best-practice trend assessment methods, as well as alternative modelling approaches.
- Within the limits imposed by available data, these assessments were intended to determine:
 - which factors (including rainfall, streamflow, temperature, solar radiation, climate variability, livestock density, land use and point source discharges) were responsible for recently observed trends in *E. coli* concentrations, and
 - their relative contribution to these trends.
- There was also interest in examining the relationship between *E. coli* and other water quality variables – turbidity and visual clarity – which are often advocated as proxy measurements for *E. coli*.

Trends in *E. coli* concentrations in Waikato streams were analysed using the traditional Thiel-Sen method, as well as Generalized Additive Model (GAM) approaches. The 82 Waikato Regional Council monitoring sites where sufficient data were available comprised ten sites along the Waikato River mainstem and 72 regional stream sites.

¹ The period denoted by '2015-2019' covers the 5-year period from the start of 2015 to the end of 2019.

Using both the Thiel-Sen and GAM methods, *E. coli* trends were estimated for four consecutive 5-year periods: 2000–2004, 2005–2009, 2010–2014 and 2015–2019. These periods correspond to the periods of interest, the period of available data, the periods reported by LAWA, and allow straightforward comparison between analysis methods. The effects of month (season), flow, water temperature, air temperature and rainfall were explored as possible explanatory variables.

Both approaches used for trend analysis confirmed that, after generally decreasing trends were observed in 2010–2014, *E. coli* concentrations have increased at most monitoring sites in the 2015–2019 period over a wide range of catchment characteristics and *E. coli* concentrations. For example, GAM analysis indicated that *E. coli* likely decreased at 39 (48%) and increased at 15 (18%) of 82 sites in 2010–2014, but decreased at 7 (9%) and increased at 60 (73%) of the same sites in 2015–2019 (after adjusting for season, temperature and rainfall). The unadjusted median rate of change was -1% per year in the 2010–2014 period compared with +6% per year in the 2015–2019 period (GAM method results). Changes in flow, water temperature, air temperature and rainfall at or prior to the time of sampling did not account for the observed increasing trend — in fact, after correcting for these variables, the median trend was estimated to be -2% per year in the 2010–2014 period and +7% per year in the 2015–2019 period.

The increases in *E. coli* concentrations were not significantly correlated with changes in livestock density or land use, and were of similar relative magnitude in predominantly pastoral, forested, or urban catchments. The increase in faecal contamination occurred in streams across all major land uses in the Waikato region, including native and plantation forest, making it unlikely that the general trend is related to management actions on livestock farms. Ongoing improvements in stock exclusion on pastoral farms continued in the 2015–2019 period. Although the input of faecal contaminants to streams was expected to decrease through these efforts, increased concentrations were observed across the region. The increases in *E. coli* concentration were unlikely to be related to changes in point source discharges (wastewater treatment plants or dairy sheds); previous investigations indicated that point sources make a small contribution to the contaminant load measured at most stream monitoring sites. The load discharged from these point sources is also expected to decrease over time rather than increase because of improvements in wastewater treatment.

Increases in the extent of stream shading arising from riparian protection programmes have been small over the recent period, so reductions of solar radiation (and light-induced disinfection) were likely to be small or negligible, and unlikely to explain the increase in *E. coli* concentrations observed.

Turbidity and visual clarity – often considered as proxies for *E. coli* because of co-mobilization of fine particles and faecal matter – did *not* show similar direction of trend in water quality to *E. coli*, according to the GAM analysis after adjustment for season, temperature and rainfall. Turbidity likely improved at 45 of 82 sites (55%) in the 2015–2019 period and visual clarity likely improved at 31 of 75 sites (41%), whereas there was widespread deterioration in microbial water quality over the same period.

Using the data and information available, we were unable to identify causes of the recent increases in *E. coli* concentrations in Waikato streams.

We have identified several areas where further investigation may help explain the trend of increasing *E. coli* concentrations; these include:

- Undertaking a similar exercise using data from other regions to see whether recent increases in concentrations of faecal bacteria is Waikato-specific, or a more

widespread phenomenon. National data has already been collected by LAWA and will be published in an upcoming update to the previous Ministry for the Environment report (i.e., Larned et al., 2019).

- Refining the statistical models developed in this project to address long-term, gradual variations in temperature as a specific covariate.
- Including the effects of solar radiation in extended models.
- Reviewing the literature to identify whether naturalised populations of *E. coli*, or other strains of microbe that are not of faecal origin but are enumerated in the *E. coli* analysis, could be involved with recently observed trends.
- Reviewing the scientific literature to identify whether temperature changes (related to climate change) may influence the growth of organisms in faecal matter in pastures and in riparian areas, as well as in naturalised populations, thereby increasing *E. coli* concentrations in surface waters.
- Although highly unlikely to be the cause of the observed trend, for completeness we suggest a desktop review of sample collection, storage and analysis procedures used by WRC; this would be done to identify factors that might have a systematic effect on measured microbial concentrations and apparent trends.

1 Introduction

1.1 Trends of concern for river water quality in the Waikato

As part of their ongoing State of the Environment (SOE) reporting, Waikato Regional Council (WRC) regularly assesses state and trends in water quality indicators in Waikato rivers. This includes measuring concentrations of *Escherichia coli* (*E. coli*), an indicator of micro-organisms of faecal origin. *E. coli* concentrations are reported as colony-forming units (CFU) per 100 millilitres of water (CFU/100 mL). While *E. coli* are not generally pathogenic (disease-causing), they are correlated with pathogenic organisms such as *Campylobacter* which do have human health implications (McBride et al. 2020). Sections 3.18 to 3.20 of the National Policy Statement for Freshwater Management 2020 (NPS-FM 2020, New Zealand Government, 2020) require analysis of trends in water quality, and if deteriorating trends are detected, the cause of the trend must be investigated. If the trend is the result of other than naturally occurring processes, then steps must be taken to halt or reverse the degradation.

A period of declining *E. coli* concentrations was observed in Waikato rivers during 1993-2017 (Vant et al. 2018), matching the national trends for the 1998-2017 period reported by Larned et al. (2019). However, recent monitoring (2015-2019) of microbiological water quality appears to show increasing *E. coli* concentrations in many Waikato catchments, indicating a deterioration in water quality. This deterioration is shown in Figure 1, which is an excerpt from the state and trend analysis carried out by LAWA (Land, Air, Water Aotearoa) for Waikato-Waipā monitoring sites for the 2015-2019 period using the Mann-Kendall Slope Test (LAWA, 2021a; <https://www.lawa.org.nz/explore-data/waikato-region/river-quality>). State is indicated by colour (e.g., blue = best/lowest 25% of sites) and five-year trend by a white arrow (e.g., downward = deteriorating = increasing *E. coli* concentrations). The analysis summarised in this figure indicated that *E. coli* concentrations were decreasing (water quality was improving) at 3 of 70 sites (4%), concentrations were increasing at 59 sites (84%), and were indeterminate or not assessed at 8 sites (12%). These trends occurred despite increased efforts to improve land use practices, such as restricting livestock access to waterways (reference to regional plan). Given the effort that farmers have made to meet regional plan requirements and considering the requirements of the NPS-FM 2020, WRC are interested in better understanding the cause(s) of the apparent deteriorating trend in microbial water quality across the region.

1.2 Objective and scope

WRC requested advice from NIWA as to why *E. coli* concentrations are apparently increasing, including statistical considerations and the potential influence of causal factors. The time period of interest for this analysis is the last 25 years, especially the last 10- and 5-year periods. The spatial area of interest is the entire Waikato Region.

To answer this question, we considered multiple possible causes of water quality trends, including rainfall, streamflow, temperature, solar radiation, climate variations (SOI, Southern Oscillation Index), livestock density, land use and point source discharges (Donnison et al. 2008; Harmel et al. 2010; Figure 2). Available stocking rate, land use and point source information were provided by WRC (described below).

There was also interest in examining the relationship between *E. coli* and turbidity and visual clarity as potential proxy measurements. These variables are amenable to continuous monitoring, and visual clarity is also strongly related to swimming quality (Davies-Colley et al. 2018; New Zealand Government, 2020).

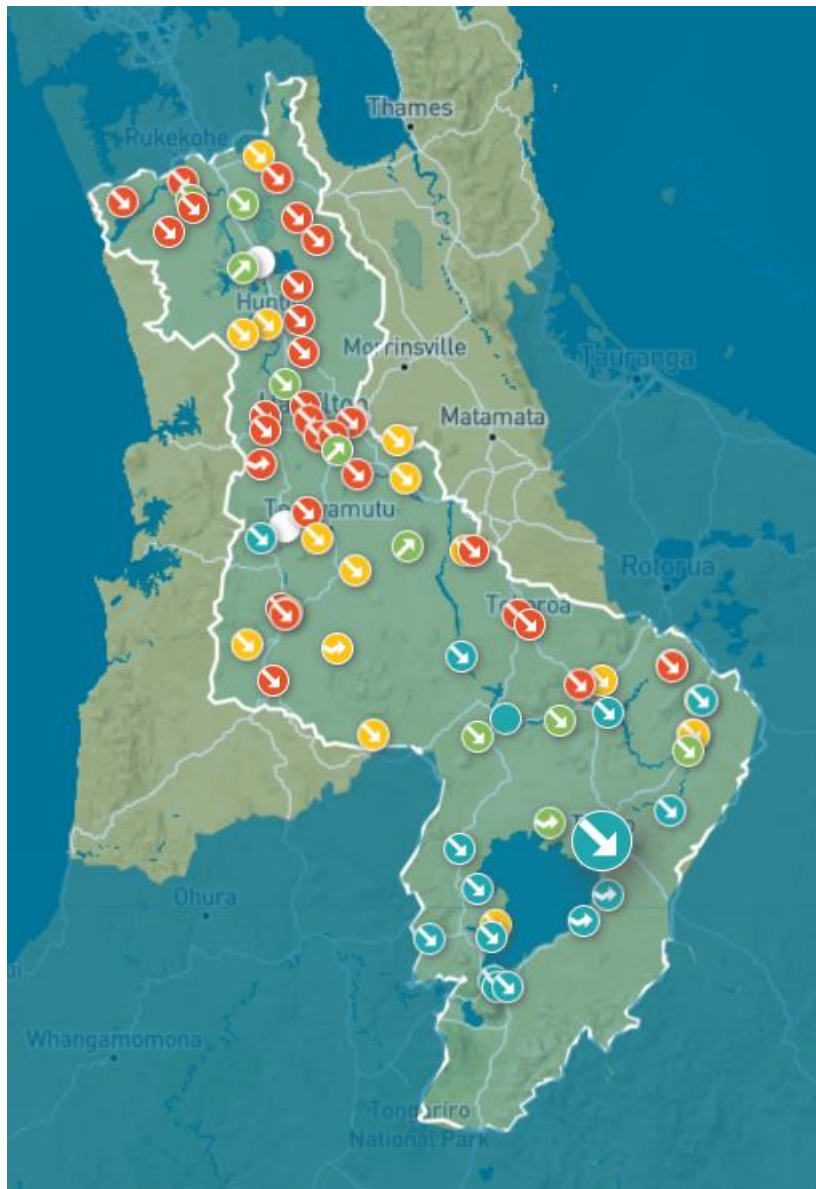


Figure 1: *E. coli* state and trends in the Waikato-Waipā catchment (2015-2019), as assessed by LAWA (Land, Air, Water Aotearoa). Figure downloaded from <https://www.lawa.org.nz> on 10 May 2021. Marker colour indicates state, i.e., quartiles of 5-year median *E. coli* concentration (blue = best/lowest 25%, green = best/lowest 50%, orange = worst/highest 50%, red = worst/highest 25%, white = insufficient data). White arrows indicate trends, upward = improving (declining *E. coli* concentrations), wiggly = indeterminate, downward = deteriorating (increasing *E. coli* concentrations), none = not assessed. The larger circle is the site that was selected at the time the figure was downloaded. Note the prevalence of downward arrows, indicating predominance of sites with deteriorating water quality (increasing *E. coli* concentrations).

1.3 Overview of this report

This report is structured as follows:

- Section 2 describes *E. coli* and its use as an indicator.
- Section 3 summarises current scientific understanding of the biological and physical causes of faecal contamination of surface waters (particularly by *E. coli*), with emphasis on factors that may cause trends.
- Section 4 briefly describes the current “best-practice” statistical trend analysis method, as well as an alternative method that was selected as being more appropriate for the current study.
- Section 5 lists the water quality, catchment and environmental data used in the study.
- Section 6 describes the *E. coli* data in greater detail, including data collation and processing steps, and the location of sample sites.
- Section 7 describes data that were investigated to explain observed *E. coli* trends, and correlations with *E. coli* concentrations are examined.
- Section 8 describes the *E. coli* trend analysis method in detail and presents the results for individual catchments and subregions.
- Section 9 compares the *E. coli* trend results with trends of turbidity and visual clarity, and assess their value as proxy measurements for *E. coli*.
- In Section 10 *E. coli* trend results are interpreted using in environmental and land use factors as potential explanatory variables.
- Finally, potential explanations for the observed *E. coli* trends are discussed in Section 11.

2 *E. coli* as an indicator of faecal contamination

E. coli bacteria are naturally present in the gut (and hence faeces) of a wide range of animals (e.g., birds, livestock, wildlife, humans, domestic pets). The presence of *E. coli* in water is therefore considered an indicator of faecal contamination, and *E. coli* are referred to as “faecal indicator bacteria” (FIB). Although most *E. coli* strains are non-pathogenic, the presence of *E. coli* is indicative of the potential presence of enteric (‘gut’) pathogens, which are of public health concern.

To manage the health risks to communities and individuals exposed to contaminated water and to safeguard human health for recreational and cultural use of waters, tolerable levels of *E. coli* in freshwater are defined in New Zealand Microbiological Water Quality Guidelines for Marine and Freshwater Recreational Areas (MFE and MOH, 2003) and the National Policy Statements for Freshwater Management 2020 (NPS-FM 2020, New Zealand Government 2020). Defined threshold levels of *E. coli* depend on whether monitoring is being used to check the suitability of water for recreational use (surveillance monitoring), or if monitoring is being undertaken for longer term grading of microbiological water quality.

Surveillance monitoring entails weekly sampling of water from a recreational site and comparing *E. coli* concentrations in these single samples with MFE and MOH (2003) guideline values of *E. coli* levels acceptable for primary contact (e.g., swimming). These data may also be used to meet the requirements of the NPS-FM 2020 (Section 3.27 and Table 22 of that document). Grading of water is based on analysis from multiple samples taken over an extended period and using statistical metrics (e.g., median, 95th percentile values) to categorise a water body into various grades or attribute states according to grading criteria.

Monthly water samples collected for SOE monitoring, are used for grading purposes and to understand progress towards desired environmental outcomes and reporting against national microbiological water quality objectives defined in the NPS-FM 2020. WRC also use the SOE monitoring results for *E. coli* (and visual clarity) to provide a grading assessment of whether a site is excellent, satisfactory or unsatisfactory for swimming. For WRC sites, water is considered unsuitable for swimming if the 95th percentile exceeds 550 *E. coli* per 100 millilitres of water because of the potential elevated health risks.

E. coli are measured as colony forming units (CFU) or most probable number (MPN) per 100 millilitres of water (CFU/100 mL or MPN/100 mL respectively) reflecting the different types of culture-based methods used for enumeration. The detection limit will depend on the volume of water analysed but is generally a minimum of 1 *E. coli* / 100 mL if 100 mL of water is analysed (or 10 *E. coli* / 100mL if 10 mL water is analysed etc.). The WRC uses the CFU method, which is based on filtering a sample of water and counting cultures on the filter after incubation.

3 Summary of factors expected to affect faecal contamination

Following review of major review articles and NZ research (e.g., Collins et al. 2007; Hipsey et al. 2008; Bradford et al. 2013; Pandey et al. 2014), we identified and summarised key factors that affect concentrations of microbial indicators in freshwater, shown in Table 1 and Figure 2. Here we give a brief overview of these factors, divided into “sources” and “modifiers”. The influence of soils or topography is not considered, because they are fixed over time.

Table 1: Categorisation of sources and modifiers affecting faecal contamination, with notes.

Source/modifier	Notes on effects	Expected relation to trends
Land use (source)	Land use affects the source of faecal material. Urban land uses contribute faecal pollution from domestic and feral animals (defecating on streets and roofs) as well as human sources (e.g., sewer leaks, wastewater plant discharges). Pastoral land uses contribute faecal pollution mainly from livestock, including dairy parlour washings via treatment ponds or land irrigation. Feral animals, and birds are important in all land uses, and septic tanks with onsite disposal systems may be significant in rural land. Plantation and conservation forests typically contribute far less faecal pollution (principally from feral mammals and birds).	Changes from forest to intensive land use such as pasture and urban, or increases in domestic or feral animal populations, are expected to increase concentrations in freshwater.
Point sources (source)	Municipal and industrial discharges can influence microbial concentrations. Improved wastewater treatment reduces loading to freshwater. Historically, dairy-shed wastewater was a significant contributor to stream microbial contamination, but direct discharges to streams are now relatively rare.	Reductions in discharge and improved treatment will decrease concentrations.
Livestock access to waters (source/modifier)	Livestock access to stream channels and wetlands in pasture greatly increases faecal contamination (in all states of flow) by direct faecal deposition. Restricting stock access, particularly by riparian fencing/livestock exclusion, eliminates direct faecal deposition (by cattle in particular) and reduces wash-in from riparian zones.	Stock exclusion is expected to decrease concentrations.
Rainfall (modifier)	In rural areas, rainfall mobilises faecal deposits on land and some of this faecal material may reach channels in overland flow, although much is intercepted by vegetation or soils on infiltration. Heavy rainfall may also lead to sewage overflows. Rainfall also drives streamflow (see below). In urban areas, heavy rainfall may also lead to sewage overflows.	Increased rainfall increases losses of microbes and increases stream flow, which is likely to increase concentrations.
Streamflow (modifier)	Faecal pollution usually correlates positively with streamflow because overland flow can wash-in faecal matter from land, and accelerating currents on the rising limb of the hydrograph can mobilise in-channel stores of faecal microbes. The latter are notably from the hyporheic zone, but also from biofilms on in-stream surfaces such as aquatic plants, and entrainment of faecal matter deposited in riparian areas that are inundated.	Increased stream flow likely to increase concentrations.

Temperature (modifier)	Faecal pollution relates complicatedly to temperature. Temperature increase increases rates of reaction, which includes both <i>E. coli</i> die-off processes and <i>E. coli</i> growth rate (in environmental reservoirs). For example, with increase in temperature <i>E. coli</i> growth rate increases in (freshly-deposited) dung deposits within which bacteria are buffered from die-off, but <i>E. coli</i> die-off rate increases where the bacteria are exposed to various environmental stressors and/or predation.	Unclear: positive and negative influences.
Sunlight exposure (modifier)	Faecal pollution usually correlates negatively with sunlight exposure owing to the powerful disinfecting properties of (mainly UV wavelengths in) solar radiation. Several mechanisms of sunlight action affect <i>E. coli</i> simultaneously, including direct DNA damage by UVB (skin-burning) wavelengths in sunlight and indirect damage by strongly oxidizing species produced photo-chemically by UV and blue-visible wavelengths, both within bacterial cells and externally.	Increased sunlight expected to reduce concentrations. Increased shading by riparian vegetation could increase shading and increase concentrations.

3.1 Sources of faecal contamination

The ultimate source of faecal contamination of waters is the faeces of warm-blooded animals, both mammals and birds (Soller et al. 2010; Moriarty et al. 2011; Moriarty, 2015). Some land uses intrinsically involve large densities of humans (urban land use) or livestock (pastoral land use) and are thus important sources of faecal pollution (Schreiber et al. 2015). Wildfowl may also contribute to faecal pollution in rural catchments. Birds and feral mammals are typically the only sources in forest land, which explains why *E. coli* concentrations are relatively low in streams draining forest. In areas of urban land use, wastewater treatment usually controls human faecal pollution, but sewer leaks and overflows during rainstorms may cause faecal pollution of waters.

Faecal pollution of waters strongly reflects land use and densities of warm-blooded animals and birds (Kay et al. 2008). Mammals generally have greater significance to the human health risk of surface waters than birds (including waterfowl that can sometimes cause intense local water contamination), because mammalian faeces have a higher prevalence of pathogenic organisms likely to infect humans than bird faecal matter (Soller et al. 2010).

Point sources can make a significant contribution to microbial indicator concentrations in streams, especially when the discharge is inadequately treated and/or discharge occurs into a small stream. Over time the treatment of municipal wastewater has improved, and land application has been introduced in many cases, factors which have reduced stream microbial concentrations. In addition, historical discharge of treated dairy shed waste directly into streams has largely been replaced by land application (Wilcock et al. 2013).

Cattle are attracted to water and stock access to stream channels causes considerable faecal pollution, due to direct defaecation in the stream, plus wash-off of faeces from riparian areas. Fencing of channels has been demonstrated to greatly reduce faecal pollution of streams in pastoral catchments (Bragina et al. 2017; Kay et al. 2018).

Faecal pollution of streams draining forest land, including plantation forest as well as native forest, is generally relatively low and can be attributed mainly to feral animals and birds (Donnison and Ross, 1999). For example, faecal pollution of the Waihaha River on the western shore of Lake Taupo, which has a catchment almost entirely in native and exotic forest, is very low (median *E. coli* c. 10 CFU/100 mL from 23 years of WRC sampling).

Statistical and mass balance modelling in the Waikato Region has identified that pastoral areas are associated with higher microbial loads and concentrations in streams, although Hamilton City was also associated with high loading (Semadeni-Davies et al. 2015, 2016). A recent analysis of national data showed that stream catchments with predominantly urban land cover had worse microbial quality than pastoral catchments, which were in turn had worse microbial water quality than forested catchments (LAWA, 2021b).

Waterfowl can sometimes be the dominant source of faecal pollution, but this source has comparatively lower health risk compared, say, to cattle pollution (Soller et al. 2010). However, contamination of water by avian faeces may still represent a potentially substantial human health risk (Wood et al. 2018).

3.2 Naturalised *E. coli*

The assumption that *E. coli* are exclusively found in the gut of animal hosts has been increasingly challenged by the recognition of environmentally-adapted (“naturalised”) *E. coli* populations (derived from aged faecal material, as well as non-enteric “*E. coli*-like” strains) (Byappanahalli et al. 2006; Ishii et al. 2006; Devane et al. 2020). These strains are tolerant to a range of environmental conditions (Perchec-Merien and Lewis, 2012) and are able to persist and grow in conditions of low temperature (e.g., >7°C) and limited nutrient availability (Berthe et al. 2013; Byappanahalli et al. 2003). If environmental conditions are becoming more conducive to survival of naturalised populations, then concentrations of *E. coli* could increase; this is an area of current research (Devane et al. 2020).

In New Zealand, persistent environmental strains reported in water and sediments have been identified as either belonging to several phylogroups of enteric *E. coli* derived from aged faecal material, or *Escherichia* species not derived from faecal material but which are “*E. coli*-like” (Devane, 2019). Both types of environmentally-adapted strains can numerically dominate in water (Devane, 2019), however, they cannot be discriminated from *E. coli* arising from recent faecal deposition using culture-based enumeration methods.

Sediments may act as a habitat for environmentally persistent strains from which strains may transfer to the water column (Devane, 2019). In river systems, microbes in sediment reservoirs may be resuspended into the water column following disturbance during high flow events. Microbes from these sources may also be entrained under baseflow conditions by hyporheic exchange across the water/sediment interface.

The presence of environmentally adapted aged-enteric and non-enteric strains may confound the use of *E. coli* as a faecal indicator and use of this organism for assessment of faecal contamination in rivers. We also speculate that increases in measured indicators may be related to changes in environmental conditions that favour environmentally-adapted strains, rather than changes in fresh enteric sources. The health implications of these strains is currently unknown.

3.3 Modifiers of faecal contamination

Factors that increase or decrease faecal pollution of waters include: mobilisation and transport of faecal matter (e.g., rainfall and consequent streamflow), inactivation or immobilisation of faecal microbes (e.g., sunlight, hyporheic uptake and deposition), or dilution.

Faecal microbial contaminants reach waterways through several pathways, including direct deposition, effluent discharges and surface runoff (Collins et al. 2007).

E. coli concentrations often correlate positively with rainfall because of four phenomena:

1. Rainfall generates overland flow, entraining faecal matter from dung deposits, resulting in some faecal bacteria reaching channels.
2. Increased rain increases flow through artificial drains which can be an important flow pathway for microbes (e.g., Monaghan et al. 2007).
3. Rainfall increases streamflow, and the currents on the rising limb of the resulting hydrograph can entrain *E. coli* from in-channel stores such as biofilms on surfaces of aquatic plants and pore water within streambed sediments (i.e., the hyporheic zone).
4. Faecal material previously deposited in riparian zones may be mobilized into the flow following inundation of the riparian zone.

On the other hand, rainfall may dilute inputs from point sources, reducing their contribution to observed concentrations, although we expect this effect to be minor given the predominance of non-point sources in the Waikato region.

Riparian buffers are generally expected to reduce concentrations of microbial indicators, because they promote infiltration of surface runoff and help exclude stock from wet riparian areas prone to runoff. There is little direct experimental evidence of effectiveness of riparian buffers at catchment scale (apart from stream stock exclusion effects), and estimates of their effectiveness are variable (e.g., Muller and Stephens 2021). However, extensive riparian restoration in Taranaki was associated with significant *reductions* in *E. coli* concentrations (Graham et al. 2018). Similarly, we would expect improved microbial water quality in the Waikato with increasing riparian restoration (Norris et al., 2020).

Survival of *E. coli* (on land and in water) is influenced by both abiotic factors (e.g., temperature, UV radiation in sunlight) and biotic factors (e.g., effects of grazing from bacterivorous predators). A negative correlation of *E. coli* survival with temperature is often reported from experimental and statistical studies (e.g., see summary in Hipsey et al. 2008; Vermeulen and Hofstra, 2014), although the relationship is complicated by *E. coli* growth rates which increase with temperature in the range of 20°C–~35°C (Ratkowsky et al. 1983). Under fluctuating environmental conditions, gross bacterial die-off will occur if the die-off rate exceeds the growth rate. Increased die-off at higher temperatures may also be attributable to faster growth rates of bacterial predators (in particular free-living protozoa) increasing proportionally with temperature up to an optimum (McCambridge and McMeekin, 1980; Geller, 1993; Davies et al. 1995) and to competition with indigenous bacteria for limited nutrient resources (Craig et al. 2004).

Sunlight is a powerful bactericide (Nelson et al. 2018), and several mechanisms of sunlight action occur simultaneously, mostly related to the ultraviolet (UV) content of sunlight. Recognising the powerful disinfecting action of sunlight suggests a potential downside of riparian planting and increased stream shade, namely reduced sunlight disinfection of stream water. However, the negative effect of this mechanism is probably outweighed by positive effects of riparian restoration on microbial water quality, such as reduced stock access and increased infiltration in riparian areas (see earlier discussion of riparian buffers). Overall we expect reduced microbial contamination in riparian-restored streams.

3.4 Observed stream faecal contaminant concentrations

In addition to the sources and modifiers of faecal contamination already discussed, in-stream concentrations are also affected by hydrological transport processes including wash-off during rain events, drain discharge and dilution from groundwater discharge, and finally measured concentrations depend on sampling and laboratory procedures (Figure 2).

The interactions between factors that eventually determine measured *E. coli* values means that the effects of land management or mitigation practices may be difficult to separate from the effects of other factors at event (e.g., rainfall), seasonal (e.g., temperature, groundwater dilution) and climate time scales. The influence of many factors that operate at various timescales makes selection and application of suitable trend detection methods both essential and challenging.

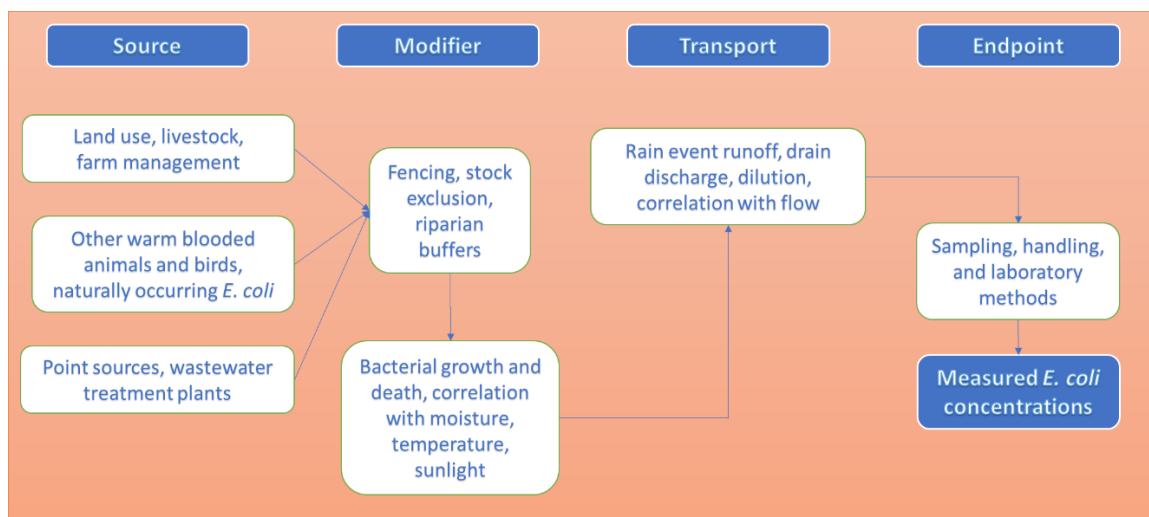


Figure 2: Summary of anthropogenic and natural factors that affect *E. coli* concentrations and trends.

4 Trend analysis methods

4.1 Traditional trend analysis approach (Sen slope)

Traditional approaches for detecting and estimating changes in water quality data, including *E. coli*, assume the effects of event and seasonal factors can be considered as “random noise”, the distribution of which does not change over time. Statistical evidence for an underlying linear trend with a non-zero slope is then tested using the non-parametric rank-order Mann-Kendall Slope Test. Following this, the linear slope of any trend is estimated using the semi-parametric Thiel-Sen Slope Estimator (“Sen slope”). In addition, McBride (2019) provided a framework for determining a “strength of evidence” for this estimated trend, which is more meaningful than simply reporting a p-value for statistical significance. These methods were recently reviewed by Fraser et al. (in prep.).

Commonly-used extensions of these methods include seasonal blocking and/or flow adjustment. Seasonal blocking typically considers the values in each calendar month as a separate time series (block), and only compares values within the same block; other blocking strategies may also be used. This results in an analysis which is robust to seasonal patterns but has less statistical power overall (i.e., reduces our ability to reliably detect change), due to the lower sample size in each block.

Flow adjustment typically involves development of a regression relationship between streamflow at time of sampling and measured water quality. This is often done using LOESS (locally estimated scatterplot smoothing). The regression assumes that the residuals will be normally distributed with a mean of zero, so that flow-adjusted trend estimation is no longer non-parametric and may be sensitive to the distribution of the data. It also assumes that the concentration-discharge relationship does not change with time. These requirements are not always checked. The water quality data are then adjusted by removing the predicted difference in water quality due to flow being above or below its long-term median value, and trend detection and estimation is carried out on the adjusted values.

The traditional approach has the following characteristics:

1. Can handle non-normally distributed data and/or seasonal data and/or randomly missing values and/or outliers and/or irregularly spaced samples.
2. Can only identify a *linear* trend (a single slope estimate is provided), even if the true trend is nonlinear. This is particularly a drawback for longer time series, say, several decades.
3. Trend estimation breaks down in the presence of large numbers (more than 29%) of outliers and/or censored values, which can occur in some water quality time series.
4. In the flow-adjusted case, the residuals are assumed to be normally distributed with a mean of zero and the flow relationship is assumed to remain the same over time. These assumptions are not required in the original tests and are not always checked.

4.2 Alternative trend analysis approach (GAM)

The traditional trend estimation method described above can address only some of the objectives of the current study. In particular, our brief was to explore recent changes in long term data, which is best modelled using non-linear trends.

Furthermore, the traditional method cannot easily incorporate the effects of multiple, interacting or time-varying environmental covariates (potential factors).

These objectives can be met using a Generalised Additive Model (GAM) approach (Hastie and Tibshirani, 1986, 1990; Yang and Moyer, 2020). GAMs are an extension of multiple regression. Instead of a sum of linear terms, GAMs fit the data using a sum of generalised smooth semi-parametric non-linear terms (e.g., smoothing splines, tensor product smooths). Each smooth term is constructed from the sum of simpler basis functions (e.g., cubic polynomials). In contrast to the similar LOESS (locally estimated scatterplot smoothing) method, which requires subjective tuning, the GAM method (as implemented in the `mgcv` package in R) provides *automated smoothness estimation* as well as rejection of terms that are not statistically supported by the data.

Compared with the traditional non-parametric approach, the GAM approach has the following characteristics:

1. It assumes that the residuals are normally distributed with a mean of zero and few outliers.
2. It can handle seasonal data and/or randomly missing values and/or irregularly spaced samples.
3. It can identify non-linear trends, which is desirable for longer (e.g., multi-decadal) time series.
4. Adjusting for covariates such as flow is straightforward, as well as interactions between covariates. Correlations between covariates are handled as in multiple regression models.

GAM models are specified as a sum of non-linear terms, one for each potential covariate of interest, and optionally including interaction terms. Each non-linear term is a smooth semi-parametric function that is determined during model calibration. The approach can also be extended to include categorical variables (GAMM, generalised additive mixed models). The GAM models used in the current study were of the form:

$$y \sim f_1(\text{time}) + f_2(\text{month}) + f_3(\text{flow0}) + f_4(\text{flow1}) + f_5(\text{flow2}) + f_6(\text{flow3}) \\ + f_7(\text{rain0}) + f_8(\text{rain1}) + f_9(\text{rain2}) + f_{10}(\text{rain3}) + f_{11}(\text{wt}) + f_{12}(\text{at}) + \varepsilon$$

for example, where

- y is the measured *E. coli* value (CFU/100 mL) transformed as described in Section 6.4,
- f_i is a smooth semi-parametric function of the particular covariate (e.g., a regression spline; Simpson, 2018),
- time is the continuous decimal time in years,
- month is the continuous decimal time within a year,
- flow0 is the mean flow (m^3/s) on the day of water quality sampling. Mean flow 1, 2 or 3 days previously were also included as additional covariates (flow1 , flow2 , flow3). We applied a natural log transformation for all flow covariates—while not strictly necessary, it is convenient for variables that may vary over many orders of magnitude.

- rain0, rain1, rain2, rain3 are the average daily catchment rainfall (mm) on the day of sampling and the three previous days,
- wt is the water temperature (°C) at the time of water quality sampling,
- at is the average daily catchment air temperature (°C) on the day of sampling, and
- ε is the residual (unexplained variance).

Each function $f_i()$ is a generalised smooth function. The coefficients of these functions are simultaneously determined by linear regression to the data. More complex smooths are able to more closely fit complex patterns in the data but also require more data to fit. The implementation of GAM in the mgcv package in R includes the option to automatically simplify the $f_i()$ functions if the data do not support a more complex form. Interaction terms may also be added (e.g., $f_{13}(\text{time, month})$), but require more data to fit and may be more difficult to interpret. Interaction terms were not included in the current study.

Like the traditional non-parametric trend approach, GAM does not require equally spaced points, although sampling should not be biased in time (e.g., sampling only in summer). *Unlike* the traditional non-parametric trend approach, GAM assumes that the model residuals are independent, identically distributed Gaussian random numbers. This means that an appropriate transformation may be required to achieve data symmetry (e.g., Box-Cox; Fischer, 2016), and the influence of outliers must be considered.

Use of GAMs to analyse trends in environmental data and separate the effects of one or more potential drivers is becoming increasingly common. For example, Fewster et al. (2000) used GAMs to identify and compare trends in farmland bird species abundance data in the United Kingdom. Similarly, Simpson (2018) describes the use of GAMs to model paleoecological time series with irregular observations. In the water quality space, Beck and Murphy (2017) applied GAMs to modelling chlorophyll-a concentrations in the Patuxent River estuary in terms of salinity, flow, and day of year. Yang and Moyer (2020) likewise used GAMs to infer water temperature, turbidity and conductance trends in the James River on the basis of flow and seasonal drivers.

5 Summary of types of data used

In this section, we summarise the main data sources. Later sections provide more details on the data.

The primary data source for this study was WRC's long-term stream water quality monitoring data, which included *E. coli* measurements (quarterly prior to 2014, then monthly). In addition to this, environmental and land use data were collected from several sources. "Sites" refer to stream monitoring locations, unless otherwise stated.

Water quality data (especially *E. coli*) were drawn from two sources:

- WRC monthly water quality records (especially *E. coli*, turbidity, visual clarity (from black disk sighting distance), water temperature) from 136 sites (Vant, 2018).
- NIWA water quality records (6 sites) were checked, but were not used in the analysis, as these largely overlapped with the WRC data.

Each site was associated with a river segment on version 2.5 of the New Zealand River Environment Classification (NZREC) national drainage network (Snelder et al. 2010).

Supporting data (used to explain *E. coli* trends) were drawn from a range of data sources:

- WRC continuous streamflow data from 39 sites. Each water site was associated with a nearby flow site, following Vant (2018).
- WRC livestock layer for the catchments of 136 WRC water quality sites. These were spatial data for livestock type and density in the entire upstream catchment of each site at four points in time (2008, 2012, 2019, 2021). The density was derived from AgriBase data.
- WRC point source loads from 40 point source discharge locations (e.g., sewage treatment outflows, treated wastewater discharges from dairy factories and meat works) (Vant, 2014).
- WRC fencing survey records from 613 longitudinal stream bank transects (Norris et al. 2020). These were distributed independently of the water quality monitoring sites, and only 50 of the water quality catchments contained fence survey transects.
- NIWA Virtual Climate Station Network (VCSN) daily weather data, spatially averaged over the upstream catchment for each of the 136 WRC water quality sites, to give a daily average rainfall and daily mean temperature for each catchment.
- NIWA CLUES land use data for each of the 136 water quality site catchments. These were spatial data for land use in the entire upstream catchment of each site at two points in time (2008, 2018), and are based on AgriBase and the New Zealand Land Cover Database LCDB3. This data set summarises the legal property areas associated with each land use as surveyed in 2008 and 2018, including dairy, sheep/beef (sb), exotic, native, urban and other (e.g., other livestock, arable, horticulture, scrub).

6 *E. coli* data

6.1 Water quality sites

The 82 water quality sites that had *E. coli* data at least covering the period from 2010 to 2019 were used in this study (Figure 3; Table 2). Of these, 56 were able to be associated with a nearby flow site. These streamflow recording sites are also shown in Figure 3 and listed in Table 2. Each water quality site also had other water quality measurements (e.g., black disk visibility, turbidity, water temperature), and virtual climate station network (VCSN), WRC livestock density, and CLUES land use data were available for the catchment upstream.

WRC stream sites are identified with a numerical code. For example, site 1131_328 is at the Waikato River at Narrows Boat Ramp, south of Hamilton. The first part of the code is the river number and the second part of the code is the unique monitoring site number on that river.

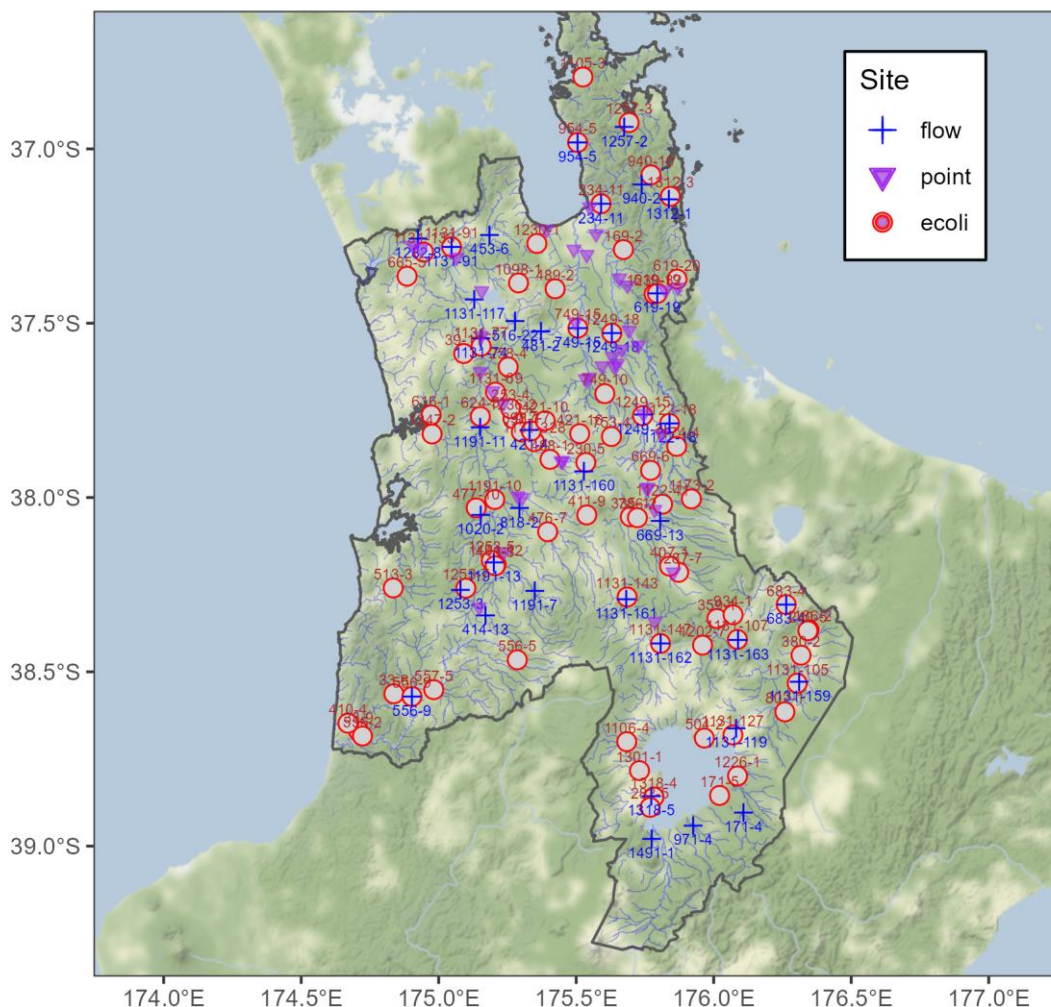


Figure 3: Map of the Waikato Region showing WRC water quality and flow site locations, as well as major point source discharges. Red circles = water quality sites, blue crosses = flow sites, purple triangles = point sources. Water quality site details are given in Table 2.

Table 2: List of water quality monitoring sites analysed in this study (N = 82). These sites had *E. coli* data at least covering the periods from 2010 to 2019. Sites with a nearby flow data site are indicated. NZSEG is the NZREC river segment ID.

Key	River	Station	From	To	N	Ncens	NZSEG	Long	Lat	Flow
1098_1	Waerenga Stm	Taniwha Rd	1998	2020	151	0	3050816	175.2905	-37.3838	-
1105_3	Waiau River	E309 Rd Ford	1998	2020	151	0	3037301	175.5244	-36.7939	954_5
1106_4	Waihaha River	SH32	1998	2020	150	10	3136644	175.6827	-38.7002	-
1122_18	Waihou River	Okauia	1998	2020	153	0	3064061	175.8394	-37.7874	1122_18
1122_41	Waihou River	Whites Rd	1998	2020	150	0	3078605	175.8141	-38.0193	669_13
1131_105	Waikato River	Ohaaki Br	1998	2020	269	6	3123400	176.3037	-38.5328	1131_159
1131_107	Waikato River	Ohakuri Tailrace Br	1998	2020	269	56	3111845	176.0861	-38.407	1131_163
1131_127	Waikato River	Taupo Control Gates	1998	2020	269	86	3135527	176.0699	-38.6811	1131_119
1131_133	Waikato River	Tuakau Br	1998	2020	268	0	3048245	174.9452	-37.296	1131_91
1131_143	Waikato River	Waipapa Tailrace	1998	2020	268	15	3099935	175.6852	-38.2855	1131_161
1131_147	Waikato River	Whakamaru Tailrace	1998	2020	260	18	3112254	175.8063	-38.4187	1131_162
1131_328	Waikato River	Narrows Boat Ramp	1998	2020	161	1	3066645	175.3477	-37.8396	1131_160
1131_69	Waikato River	Horotiu Br	1998	2020	268	3	3059280	175.2068	-37.6977	1131_74
1131_77	Waikato River	Huntly-Tainui Br	1998	2020	267	1	3055438	175.1543	-37.5662	1131_74
1131_91	Waikato River	Mercer Br	1998	2020	269	0	3047923	175.0467	-37.2813	1131_91
1173_2	Waiohotu Stm	Waiohotu Rd	1998	2020	150	2	3077848	175.9193	-38.0038	669_13
1174_4	Waiomou Stm	Matamata-Tauranga Rd	1998	2020	153	0	3067934	175.8655	-37.8533	1122_18
1186_2	Waiotapu Stm	Campbell Rd Br	1998	2020	149	60	3109925	176.3462	-38.3805	-
1191_10	Waipa River	Pirongia-Ngutunui Rd Br	1998	2020	95	0	3076838	175.2039	-38.0058	1191_11
1191_12	Waipa River	SH3 Otorohanga	1998	2020	151	1	3091406	175.2086	-38.1922	1191_13
1202_7	Waipapa Stm	Tirohanga Rd Br	1998	2020	150	0	3112853	175.9597	-38.4228	-
1226_1	Waitahanui River	Blake Rd	1998	2020	148	4	3144485	176.0862	-38.7981	-
1230_1	Waitakaruru River	Coxhead Rd Br	1998	2020	152	0	3047683	175.3579	-37.2724	481_2
1236_2	Waitawhiriwhiri Stm	Edgecumbe Street	1998	2020	150	1	3062685	175.2701	-37.773	421_4
1239_32	Waitekauri River	U/S Ohinemuri Conflu	1998	2020	150	0	3051680	175.7832	-37.4167	619_19
1247_2	Waitetuna River	Te Uku-Waingaro Rd	1998	2020	150	0	3064930	174.9752	-37.8181	-
1249_15	Waitoa River	Landsdowne Rd Br	1998	2020	152	2	3062720	175.7412	-37.7653	1249_38
1249_18	Waitoa River	Mellon Rd Recorder	1998	2020	152	0	3054693	175.6292	-37.5296	1249_18
1253_5	Waitomo Stm	SH31 Otorohanga	1998	2020	150	0	3090304	175.1923	-38.1808	1253_3
1253_7	Waitomo Stm	Tumutumu Rd	1998	2020	151	0	3096865	175.0988	-38.2602	1253_3
1257_3	Waiwawa River	SH25 Coroglen	1998	2020	151	0	3039645	175.6932	-36.924	1257_2
1287_7	Whakauru Stm	U/S SH1 Br	1998	2020	149	1	3093674	175.8718	-38.2145	-
1301_1	Whanganui Stm	Lakeside Lake Taupo T8	2001	2020	136	1	3143172	175.731	-38.7829	1318_5
1312_3	Wharekawa River	SH25	1998	2020	151	0	3044647	175.842	-37.1357	1312_1

Key	River	Station	From	To	N	Ncens	NZSEG	Long	Lat	Flow
1318_4	Whareroa Stm	Lakeside Lake Taupo T9	2001	2020	138	1	3149001	175.7827	-38.8593	1318_5
169_2	Hikutaia River	Old Maratoto Rd	1998	2020	151	0	3048567	175.671	-37.2896	234_11
171_5	Hinemaiaia River	SH1	1998	2020	148	4	3149003	176.0207	-38.854	171_4
230_5	Karapiro Stm	Hickey Rd Bridge - Cambridge	1998	2020	152	1	3070130	175.5349	-37.8996	-
234_11	Kauaeranga River	Smiths Cableway/Recorder	1998	2020	150	1	3044978	175.5905	-37.1574	234_11
240_5	Kawaunui Stm	SH5 Br	1998	2020	150	0	3110340	176.3426	-38.3822	-
253_4	Kirikiroa Stm	Tauhara Dr	1998	2020	151	0	3061405	175.2615	-37.745	421_4
258_4	Komakorau Stm	Henry Rd	1998	2020	152	0	3056992	175.2531	-37.6262	-
282_5	Kuratau River	Te Rae Street T10	2001	2020	139	2	3151224	175.7686	-38.8887	-
33_6	Awakino River	Gribbon Rd	1998	2020	150	0	3123054	174.8371	-38.5631	-
33_9	Awakino River	SH3 Awakau Rd Junction	1998	2020	149	2	3131731	174.709	-38.6724	-
335_1	Little Waipa Stm	Arapuni - Putaruru Rd	1998	2020	150	0	3081097	175.6968	-38.0553	-
359_1	Mangaharakeke Stm	SH30	1998	2020	150	0	3106095	176.0118	-38.3472	-
380_2	Mangakara Stm	SH5	1998	2020	150	0	3116290	176.3175	-38.4526	-
39_11	Awaroa Stm	Sansons Br at Rotowaro-Huntly Rd	1998	2020	152	0	3056003	175.091	-37.587	481_2
398_1	Mangakotukutuku Stm	Peacockes Rd	1998	2020	151	0	3064979	175.3005	-37.8118	421_4
407_1	Mangamingi Stm	Paraonui Rd Br	1998	2020	150	0	3091783	175.8394	-38.1969	-
410_4	Manganui River	Off Manganui Rd	1998	2020	148	0	3130367	174.6692	-38.6442	-
411_9	Mangaohoi Stm	South Branch Maru Rd	1998	2020	152	3	3079677	175.5382	-38.0509	818_2
417_7	Mangaone Stm	Annebrooke Rd Br	1998	2020	150	1	3064673	175.3363	-37.8092	421_4
421_10	Mangaonua Stm	Hoeka Rd	1998	2020	152	0	3063144	175.3875	-37.7793	421_4
421_16	Mangaonua Stm	Te Miro Rd	1998	2020	144	0	3065476	175.5126	-37.8171	421_4
443_3	Mangapu River	Otorohanga	1998	2020	150	0	3091562	175.2053	-38.1959	1191_13
476_7	Mangatutu Stm	Walker Rd Br	1998	2020	151	0	3083539	175.3961	-38.0982	818_2
477_10	Mangauika Stm	Te Awamutu Borough W/S Intake	1998	2020	150	14	3077698	175.1374	-38.0305	-
488_1	Mangawhero Stm	Cambridge-Ohaupo Rd	1998	2020	151	1	3069532	175.4049	-37.8898	421_4
489_2	Mangawhero Stm	Mangawara Rd	1998	2020	150	0	3051409	175.4244	-37.4008	481_2
504_2	Mapara Stm	Off Mapara Rd T1	1998	2020	149	0	3136377	175.9664	-38.6904	971_4
513_3	Marokopa River	Speedies Rd	1998	2020	151	0	3095966	174.8347	-38.2594	-
556_2	Mokau River	Awakau Rd	1998	2020	150	0	3133606	174.7243	-38.6848	556_9
556_5	Mokau River	Mangaokewa Rd	1998	2020	151	0	3115276	175.2862	-38.4656	414_13
556_9	Mokau River	Totoro Rd Recorder	1998	2020	150	0	3123396	174.9048	-38.5716	556_9
557_5	Mokauiti Stm	Three Way Point - Aria	1998	2020	150	0	3122377	174.9814	-38.5507	556_9

Key	River	Station	From	To	N	Ncens	NZSEG	Long	Lat	Flow
616_1	Ohautira Stm	Waingaro Te Uku Rd	1998	2020	150	0	3061831	174.9725	-37.7632	-
619_19	Ohinemuri River	Queens Head	1998	2020	151	0	3051991	175.7944	-37.4146	619_19
619_20	Ohinemuri River	SH25 Br	1998	2020	150	1	3050858	175.8667	-37.3734	619_19
624_5	Ohote Stm	Whatawhata/Horotiu Rd	1998	2020	151	0	3062320	175.1509	-37.7679	-
665_5	Opuatia Stm	Ponganui Rd	1998	2020	150	0	3050086	174.885	-37.3653	1282_8
669_6	Oraka Stm	Lake Rd	1998	2020	150	0	3071941	175.7706	-37.9221	669_13
683_4	Otamakokore Stm	Hossack Rd	1998	2020	150	0	3103240	176.2637	-38.3072	683_4
749_10	Piako River	Kiwitahi	1998	2020	152	1	3059826	175.6038	-37.7023	749_15
749_15	Piako River	Paeroa-Tahuna Rd Br	1998	2020	149	0	3054261	175.5063	-37.5135	749_15
753_4	Piakonui Stm	Piakonui Rd	1998	2020	152	0	3066020	175.6301	-37.827	-
786_2	Pokaiwhenua Stm	Arapuni - Putaruru Rd	1998	2020	150	0	3081022	175.7225	-38.0579	-
802_1	Pueto Stm	Broadlands Rd Br	1998	2020	147	1	3129762	176.2585	-38.613	-
934_1	Tahunaatara Stm	Ohakuri Rd	1998	2020	150	0	3105500	176.0705	-38.3378	-
940_10	Tairua River	Morrisons Br Hikuai	1998	2020	151	1	3043115	175.7709	-37.0744	940_2
954_5	Tapu River	Tapu-Coroglen Rd	1998	2020	151	0	3040973	175.5051	-36.9816	954_5

6.2 Data preparation

E. coli was measured quarterly at most sites prior to 2013, usually in March, June, September and December. From 2013 onwards, measurements were made monthly. Prior to analysis, these data were checked thoroughly, and several small amendments were made:

- Some of the WRC sites had been relocated and/or renamed, so the data from these were combined (1191_10 into 1191_2, 1131_101 into 1131_328, 414_12 into 414_6, 971_4 into 971_5).
- Only *E. coli* results derived using method 507 were used (*E. coli* by membrane filtration, count on MFC agar, confirmation by NA-MUG. APHA 9222 G. CFU/100 mL). The few data points using the older 506 method were removed.
- Data from the 6 NIWA National River Water Quality Network (NRWQN) sites were considered for inclusion, but after examining the data and comparing it with data from nearby WRC sites, we felt it did not add anything significant to the data set.
- Sites with short data records were excluded from the analysis, leaving 82 sites with available *E. coli* data starting between May 1998 and March 2001 and finishing between October 2020 and December 2020.

Figure 4 shows the raw *E. coli* data for the 82 sites analysed, plotted as a time series with a simple smoothed curve (2-year rolling median) to indicate trend. The annual medians of the raw *E. coli* concentrations for the 82 sites and a regional annual median are shown in Figure 5. The low number and high variability of samples in each year results in high variation in the year to year median.

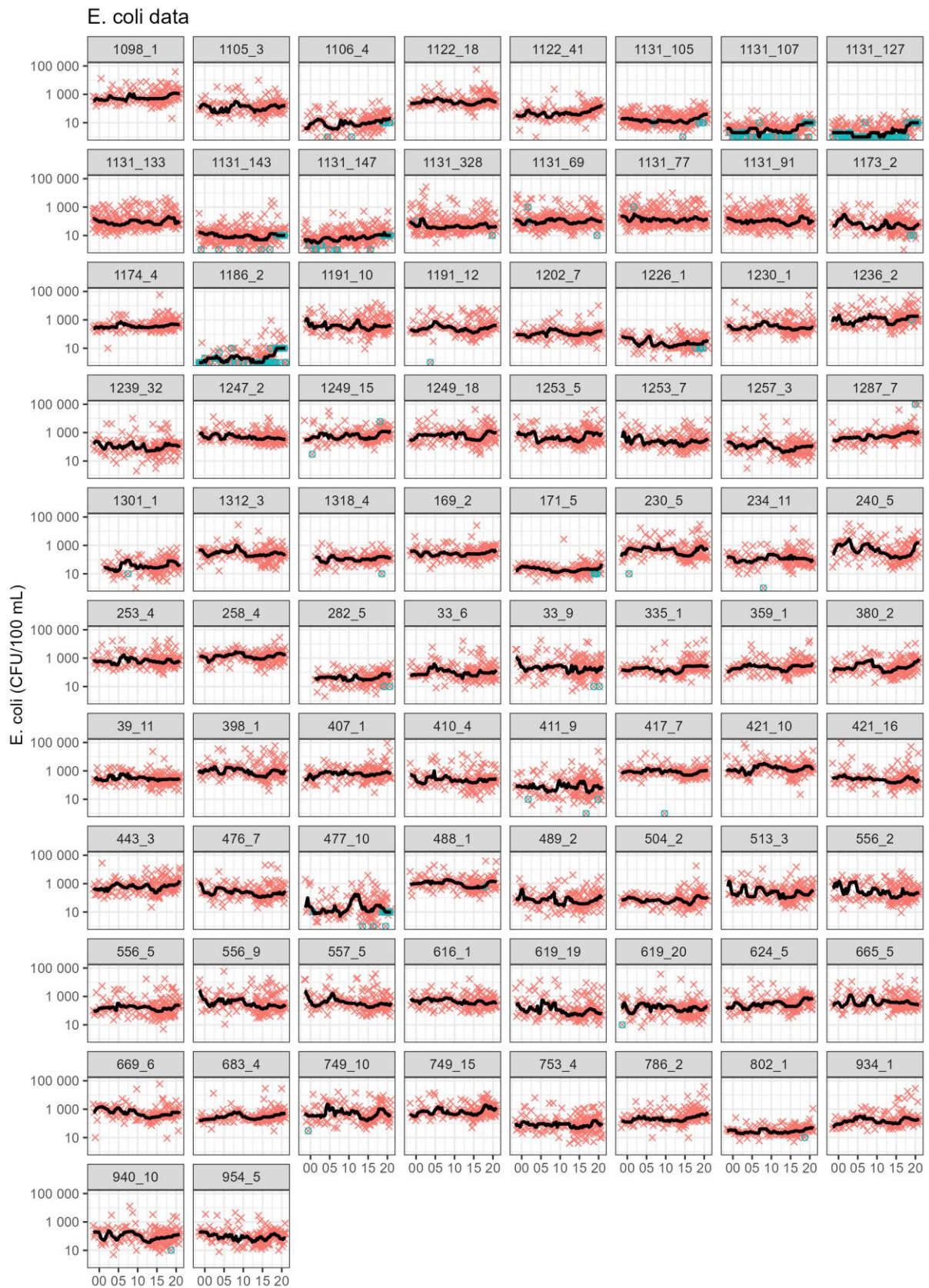


Figure 4: Raw *E. coli* data at 82 WRC SOE sites. Censored values are highlighted in blue. A simple trendline has been superimposed (2-year rolling median). The x-scale is years.

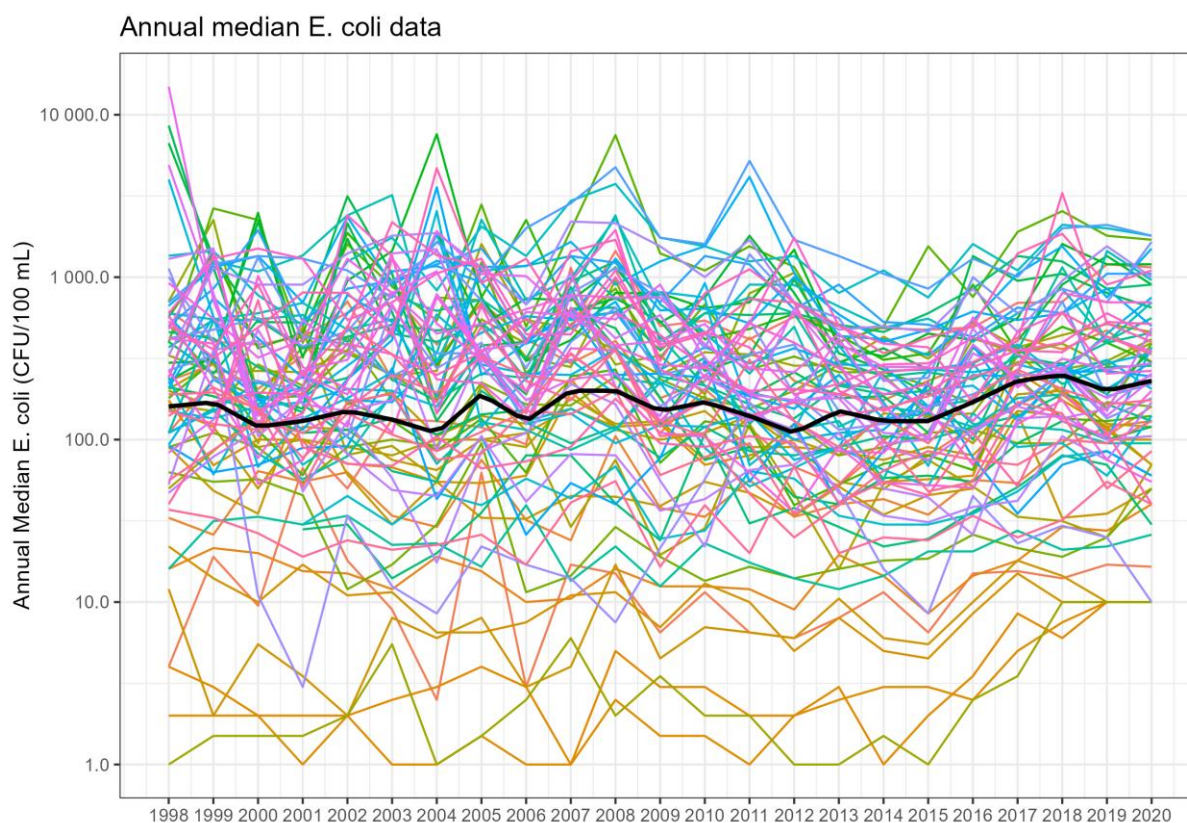


Figure 5: Annual median *E. coli* concentration (CFU/100 mL) at 82 WRC SOE sites. The black curve plots the annual median across all sites.

6.3 Data censoring and banding correction

Approximately 1.2% of *E. coli* 507 values were censored (mostly low values that were left-censored), although the fraction was as high as 40.2% at some sites. Censored values can cause problems with trend analysis, especially at sites where generally low levels of *E. coli* occur and a large proportion of the observations are left-censored (i.e., reported as being “less than” a certain value). The WRC *E. coli* data contained a range of censorship levels, the majority being left-censored (“< 1”, “< 2”, “< 5”, “< 10”, “< 30”, “< 100”, “< 1000”) as well as a few right-censored values (“> 600”, “> 6000”, “> 100000”). At some sites, censorship levels changed over time.

Seven sites had more than 5% censored values (blue data points, Figure 4). These included four upper Waikato River sites (site codes starting with 1131), as well as Waiotapu Stream at Campbell’s Road Bridge (1186_2), Waihaha River at State Highway 32 (1106_4) and Mangauika Stream at Te Awamutu Water Intake (477_10). An increase in the left-censorship level (from < 1 to < 10 CFU/100 mL) can be seen in the data across all sites from about October 2017 onwards (i.e., an upward shift in the blue data points towards the right-hand end of the time series).

For example, Figure 6 shows detail from Figure 4 for a site with very low faecal contamination (site 1131_127, Waikato River at Taupo Control Gates). The impact of censorship (blue markers) and banding (lines of discrete y-values) are both clear, including the marked change in censorship level after October 2017.

Censored values can cause artefactual trends (illustrated in Figure 6), where the apparent upward trend is influenced by the change in censorship level. To avoid this, censored values must be adjusted to reduce artefacts. Several approaches to handling censored values are discussed in Appendix A. The method adopted in the current study is “imputation”, in which the censored values are adjusted to restore, as far as possible, the mean of the original data set without censoring. In this approach, censored values are replaced with the mean of measured values outside the censored value (or with the censoring limit itself if there are no measurements outside the censored value).

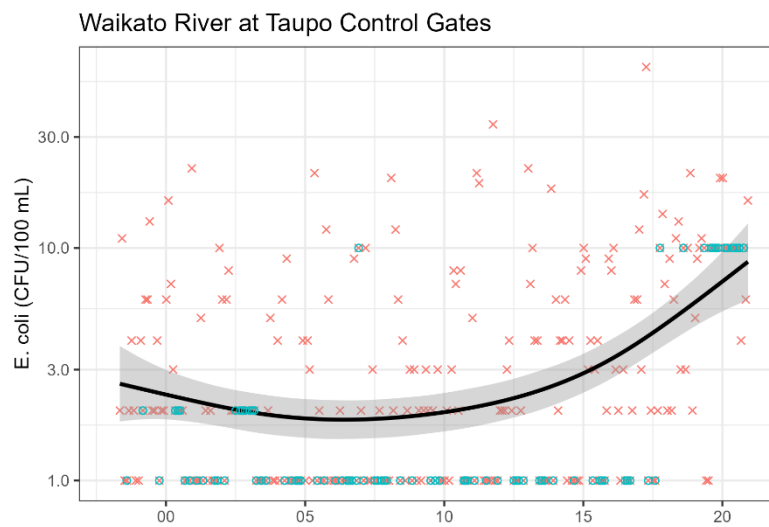


Figure 6: Raw *E. coli* data at Waikato River at Taupo Control Gates (site 1131_127). Censored values are shown as blue points. A simple trendline has been superimposed (calculated using a simple GAM).

Banding (e.g., due to reporting of low count data as numbers with 1 significant digit in Figure 6) can be also a problem for the traditional non-parametric method described above, because calculation of both the Mann-Kendall and Thiel-Sen statistics both rely on comparing values in the time series. Banded causes over-representation of several equal values, which must be handled carefully to avoid a biased Mann-Kendall statistic or Theil-Sen slope estimate (Helsel et al., 2020). The GAM approach is not sensitive to banding provided the measurement error is similar for all measurements, which is approximately true for log-transformed *E. coli* data (Harmel et al. 2016).

6.4 Data skew and outlier correction

The traditional trend estimation methods described above are robust for non-normally distributed (e.g., highly skewed) data and/or outliers. However, the GAM method that we wish to use to determine the influence of multiple factors on *E. coli* trends is a regression method that relies on symmetrically distributed residuals.

Achieving normally distributed residuals (and satisfying the requirements of the model) can be accomplished using a data transformation (Lee, 2020). Although log transformation is useful in some cases, the more general Box-Cox transformation may be more effective for highly skewed data (Fischer, 2016). Box-Cox is a scaled power transformation with a parameter lambda (λ):

$$y' = \begin{cases} \frac{y^\lambda - 1}{\lambda}, & \lambda \neq 0 \\ \log(y), & \lambda = 0 \end{cases}$$

In the special case where lambda equals zero, Box-Cox is the same as a log transformation. The `boxcox()` function in R was used to determine the maximum likelihood value of lambda for each WRC *E. coli* data series (Figure 7). In most cases maximum likelihood values of lambda were less than 0, indicated that the data were more skewed than a log-normal distribution (Davies-Colley et al. 2019). This suggests that Box-Cox transformation is more appropriate for the WRC *E. coli* data than log transformation.

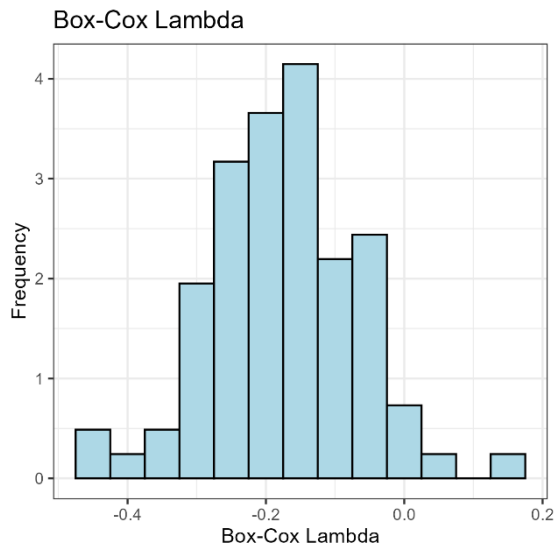


Figure 7: Distribution of optimal Box-Cox lambda values used to transform *E. coli* data at the 82 WRC sites used in this study.

Normality of the transformed data and also of the model residuals was checked using a Shapiro-Wilk test (`shapiro.test()` in R). The p-value from the test represents the probability that the data are sampled from a normal distribution.

After GAM model fitting to the transformed data, the residuals were checked for extreme outliers. Extreme outliers are defined as data points that are further than 3 times the interquartile range outside the quartiles of the data (SAS, 2009). Extreme outliers were identified using the `is extreme()` function of the `rstatix` package in R. Extreme outliers were uncommon, and so were counted and marked, but not removed.

6.5 Effect of change in sampling frequency

Change point analysis carried out using the `EnvCpt` package in R (Killick et al., 2012, 2021) determined that the change from quarterly to monthly sampling from 2013 onwards was not associated with a step change in observed *E. coli* concentrations. Since both the traditional and alternative trend analysis methods allow irregularly spaced data, the main effect of the increase in sampling frequency from 2013 onwards was expected to be seen as lower uncertainty in the trend estimates after this time.

7 Factors related to faecal pollution trends, and relationships to *E. coli* concentrations

This section presents the data on covariates that could be related to faecal pollution trends, and simple correlations between these covariates and *E. coli* concentrations. In addition, relationships between *E. coli* and other water quality variable are explored to see whether they could give insight into reasons for trends, or patterns observed in trends.

7.1 Water quality variables other than *E. coli*

The WRC water quality monitoring programme includes a range of other water quality variables in addition to *E. coli* concentration. Turbidity, water temperature and black disk visual clarity were also examined. Turbidity and visual clarity often co-vary with *E. coli* (e.g., Davies-Colley et al. 2018), while temperature is often found to correlate because of its effects on biological and chemical processes.

Only turbidity (NTU) data derived from measurement method 69 was used (Nephelometry, Portable Hach 16800, R.J. Hill Laboratories). There were few data points using the older 65 method, and it is not advisable to use turbidity measurements from different instruments since these may be weakly comparable (Davies-Colley et al. 2021). Water temperature (°C) measured with methods 15 and 1274 were combined, because these methods are considered equivalent. Black disk visual clarity (m) measured with methods 18 to 23 were also combined.

Davies-Colley et al. (2018, 2021, 2021 *in press*) propose that visual clarity is a more meaningful measure of optical water quality than is turbidity because it is a physical quantity expressed in SI units, and reported values are not instrument-independent. Visual clarity may also be directly related to swimmability. However, it is recognised that reasonably robust local (site-specific) relationships between turbidity and visual clarity may be demonstrated, and on this basis turbidity can be used under the National Objectives Framework of the National Policy Statement for Freshwater Management (NPS-FM 2020; New Zealand Government, 2020).

Figure 8 shows the correlation between *E. coli* and other water quality variables considered in the current study. Davies-Colley et al. (2018) found Pearson's correlation coefficients of -0.53 and 0.53 for *E. coli* against visual clarity and turbidity respectively, on a log-log scale. Pearson correlations were similar at -0.57 and 0.62 respectively for the WRC data in the current study. The relationship with water temperature is non-linear, with a maximum at approximately 16 °C.

Turbidity is of particular interest as a potential indicator of *E. coli* concentrations, due to ease of automated high-frequency measurement. *E. coli*-turbidity responses by site were plotted in Figure 9. Most sites showed a positive correlation between turbidity and *E. coli*, so there is a strong likelihood that turbidity trends will align with *E. coli* trends. The equivalent plot for visual clarity is given in Figure 10. In contrast to turbidity, most sites showed a negative correlation between visual clarity and *E. coli*. Therefore, it is likely that visual clarity trends will be opposite to those of *E. coli*. This reflects the typical strong inverse relationship of visual clarity and turbidity shown in Figure 8 (Davies-Colley et al. 2018). The relationships between *E. coli* and turbidity or visual clarity give some insights into potential drivers of trends. For example, increased rainfall and flow are likely to increase turbidity and decrease visual clarity. On the other hand, there may be drivers which increase *E. coli* without affecting turbidity. For example, increased temperature is likely to affect *E. coli* numbers without affecting turbidity. Similarly, a point source may be high in *E. coli* but with low associated turbidity.

The relationship between *E. coli* and water temperature shows that a non-monotonic relationship exists. Interpretation of this relationship requires consideration of factors such as the correlation between land use and altitude, and land use practices and season.

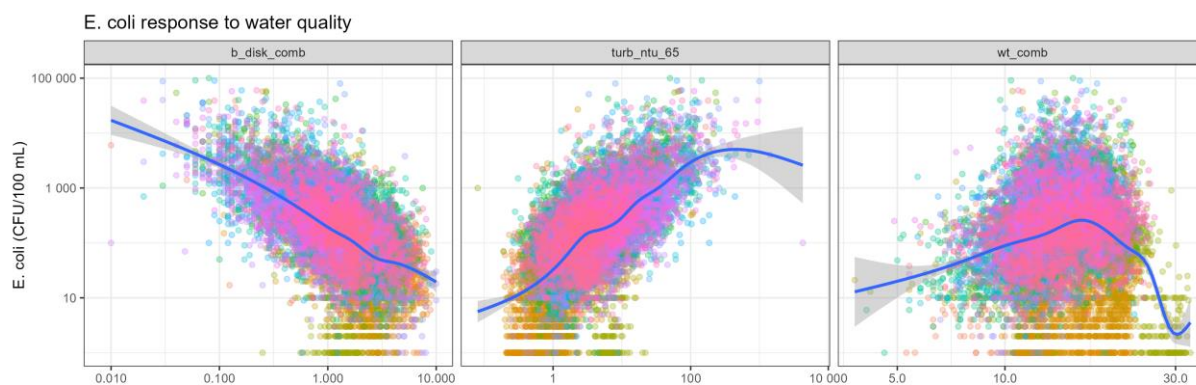


Figure 8: Correlation between *E. coli* and other water quality variables. Black disk visibility (left), turbidity (middle) and water temperature (right). Points are coloured by site, and a smoothed response curve is shown for each variable (calculated using a simple GAM), with uncertainty bands indicated as grey shading. Note log₁₀ scale for all axes.

7.2 Air temperature and rainfall

Catchment weather variables were estimated from the NIWA Virtual Climate Station Network (VCSN) data set. This daily (midnight to midnight) weather data set is interpolated from physical stations onto an approximately 5 × 5 km grid across the whole of New Zealand. For the current study, catchment daily rainfall (mm) and air temperature (°C) at the time of each water sample was calculated as the average of daily values from all of the VCSN grid points contained within the catchment.

Correlations between measured *E. coli* concentrations and rainfall are shown in Figure 11. At many sites, there are positive correlations between *E. coli* and rainfall, and there are very few sites with negative correlation. That means for a given catchment, days with higher rainfall tend to have higher *E. coli* counts. As explained in Section 3.3, we expect the positive correlation of *E. coli* with rainfall as seen at most sites, because resulting runoff can wash faecal matter from land into streams, and consequent stream flow increase can entrain channel stores of *E. coli* (e.g., Stott, 2011).

Correlations between measured *E. coli* concentrations and air temperature are shown in Figure 12. Generally positive correlations exist between *E. coli* and air temperature. That means for a given catchment, days with higher temperature tend to have higher *E. coli* counts. The increase of *E. coli* with temperature is complicated. *E. coli* might be expected to decrease with temperature, because die-off is greater at higher temperatures, and higher temperatures may also be associated with greater UV-induced decay and smaller flows in summer when temperatures are high. However, increased temperature could also be associated with increased growth in some sub-environments, such as faecal deposits on land and increased survival of naturalised *E. coli* in soil and in water (see Section 3).

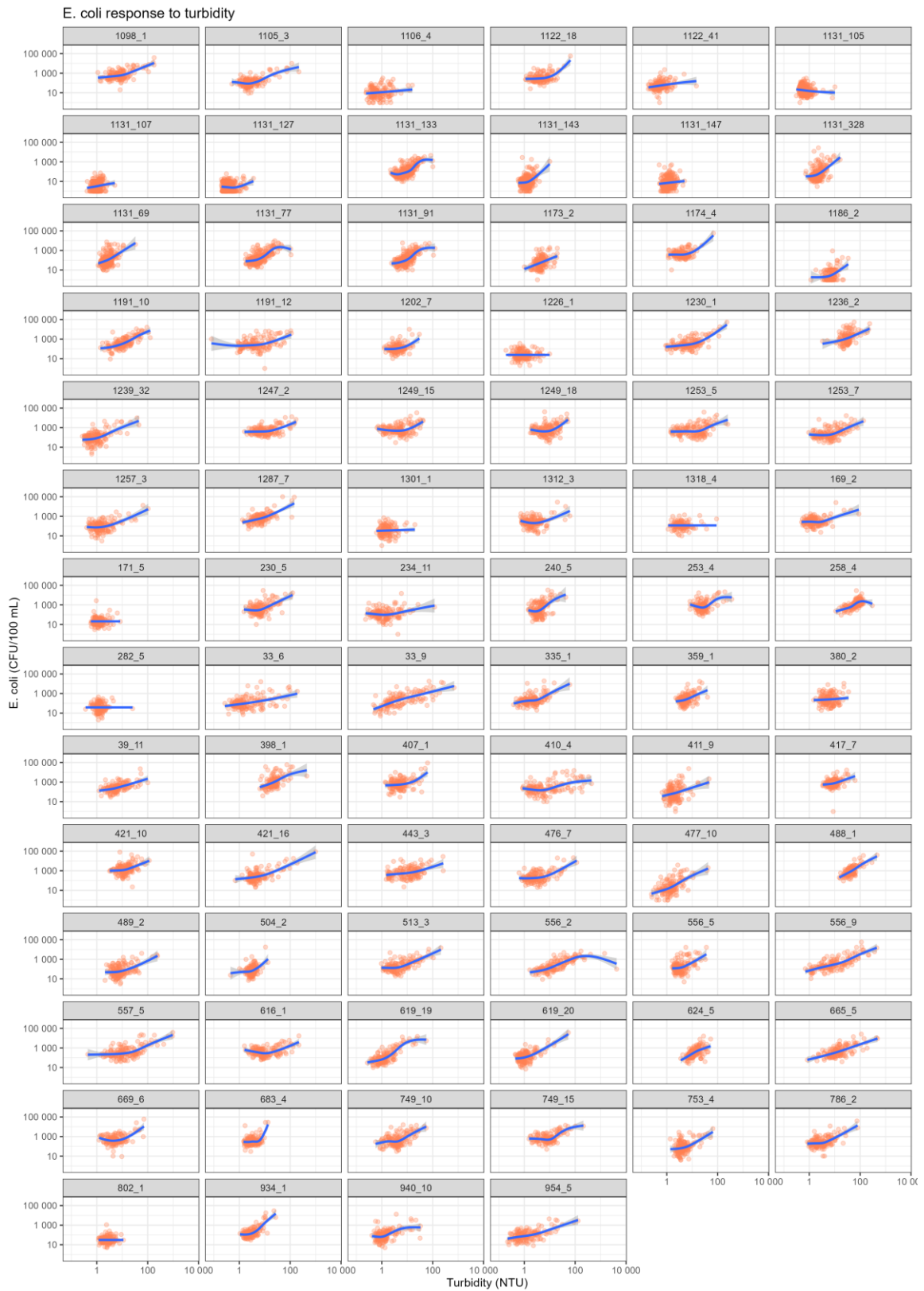


Figure 9: Correlation between *E. coli* and turbidity at all 82 WRC SOE sites. A smoothed response curve is shown for each site (calculated using a simple GAM), with uncertainty bands for the average response indicated as grey shading.

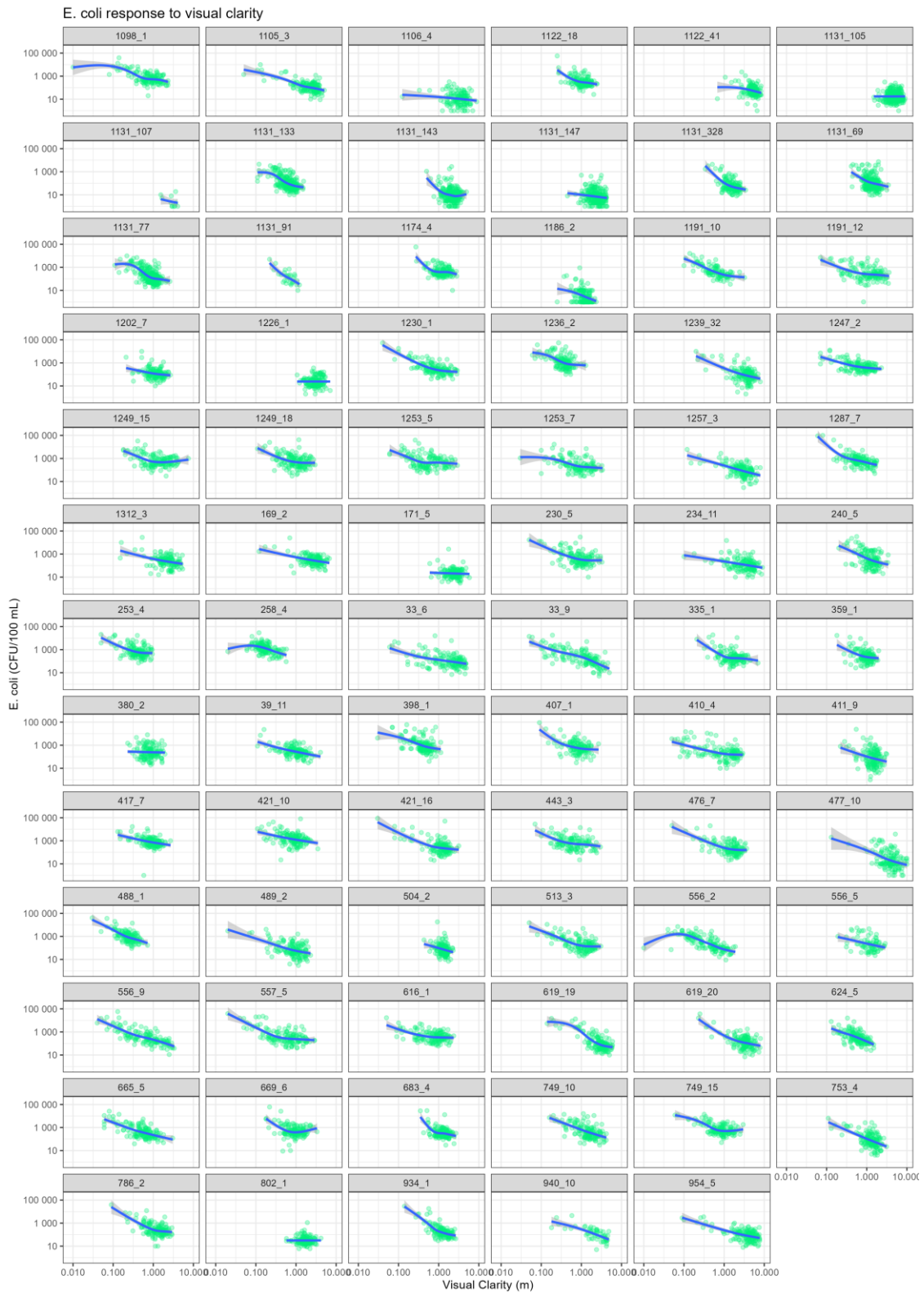


Figure 10: Correlation between *E. coli* and visual clarity at the 79 WRC SOE sites that had clarity data. A smoothed response curve is shown for each site (calculated using a simple GAM), with uncertainty bands indicated as grey shading.



Figure 11: Correlation between *E. coli* and VCSN daily catchment rainfall (mm). A smoothed response curve is shown for each site (calculated using a simple GAM), with uncertainty bands indicated as grey shading.

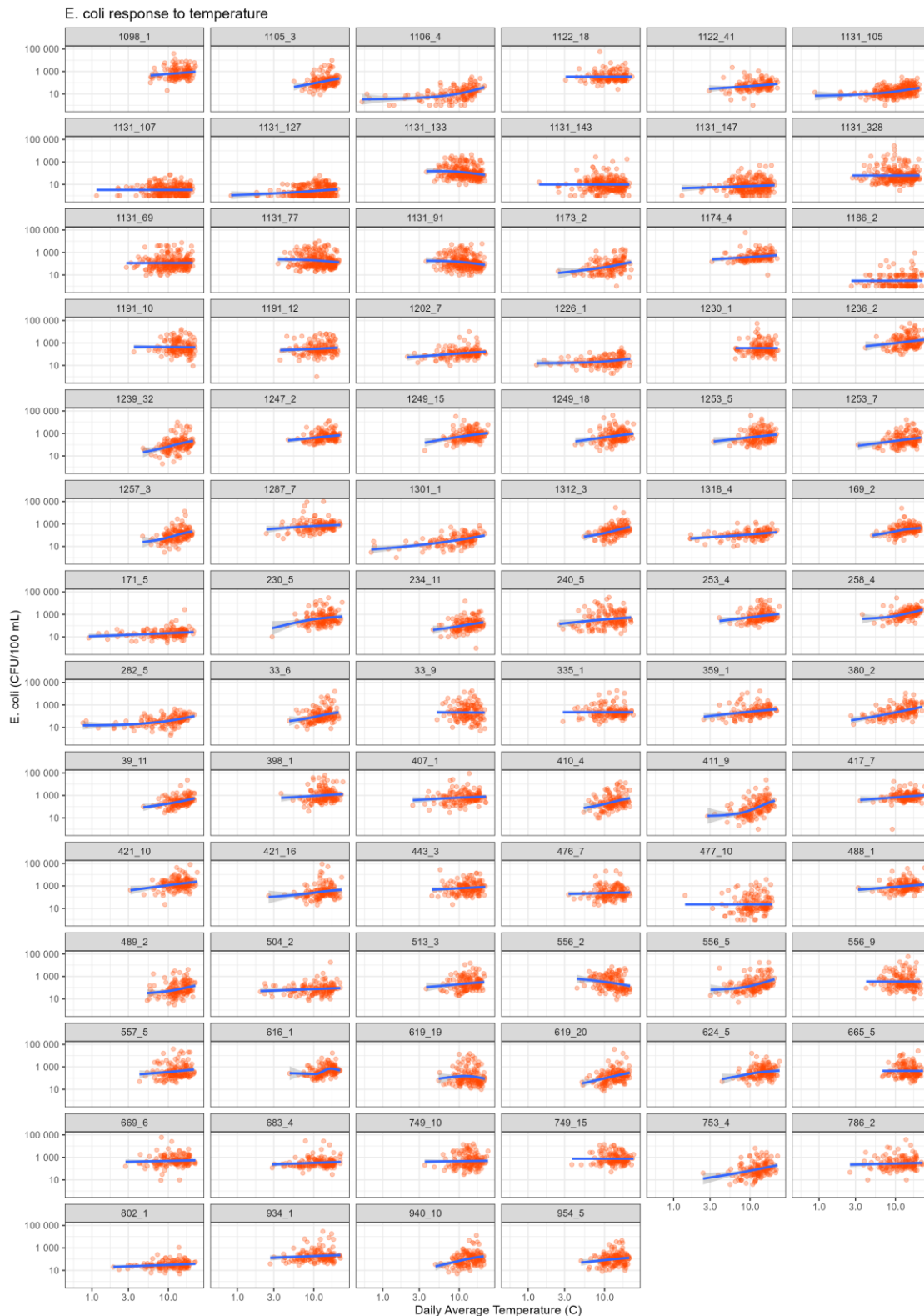


Figure 12: Correlation between *E. coli* and VCSN catchment daily average temperature (°C). A smoothed response curve is shown for each site (calculated using a simple GAM), with uncertainty bands indicated as grey shading.

Since *E. coli* levels are correlated with rainfall and temperature within a catchment, it is important to know whether the long term rainfall and/or temperature data show any patterns that could explain trends in the *E. coli* data (Figure 4). Annual total rainfall and annual average temperatures for each catchment are shown in Figure 13. The high degree of similarity in the patterns between sites is a result of the VCSN data being generated by interpolating and smoothing data from physical stations.

Both rainfall and the temperature data show changing (and different) trends over time, suggesting that inclusion of longer term rainfall and temperature in the analysis could help explain the observed trends in the *E. coli* data. We recommend this as a potential area for further investigation.

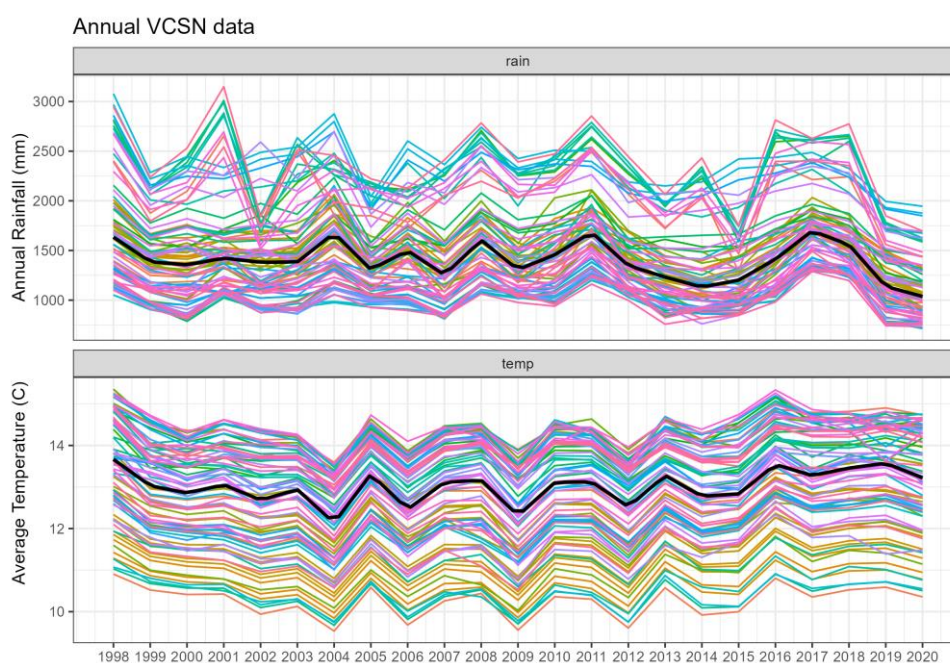


Figure 13 Catchment annual total rainfall (mm) (top) and annual average temperature (°C) (bottom) for the 82 WRC SOE sites. Traces are coloured by site, and data are averaged over VCSN points within the catchment of each *E. coli* monitoring site. The black curve plots the annual median value across all sites.

7.3 Livestock density

Land use type and intensity are known to be primary drivers of *E. coli* concentrations (see Section 3). Two sets of land use data were available: livestock types and numbers from WRC, and land use type and extent of cover from CLUES. Although the livestock density and land use data are only available at a few points in time, they can be used to see whether *E. coli* concentrations or *E. coli* concentration trends are correlated with the density of the different types of livestock or with land use or *changes* in the density of stock or land use.

Figure 14 show the changes in land use from the WRC data set, which gives livestock numbers in each catchment as surveyed in 2008, 2012, 2019 and 2021, expressed as “stock units” per hectare (SU/ha). The “stock units” metric scales animal numbers to allow different livestock types to be compared (e.g., 1 breeding ewe = 1 SU, 1 dairy cow = 7 SU, 1 beef cow = 5.5 SU, etc., Waikato Regional Council, 2019).

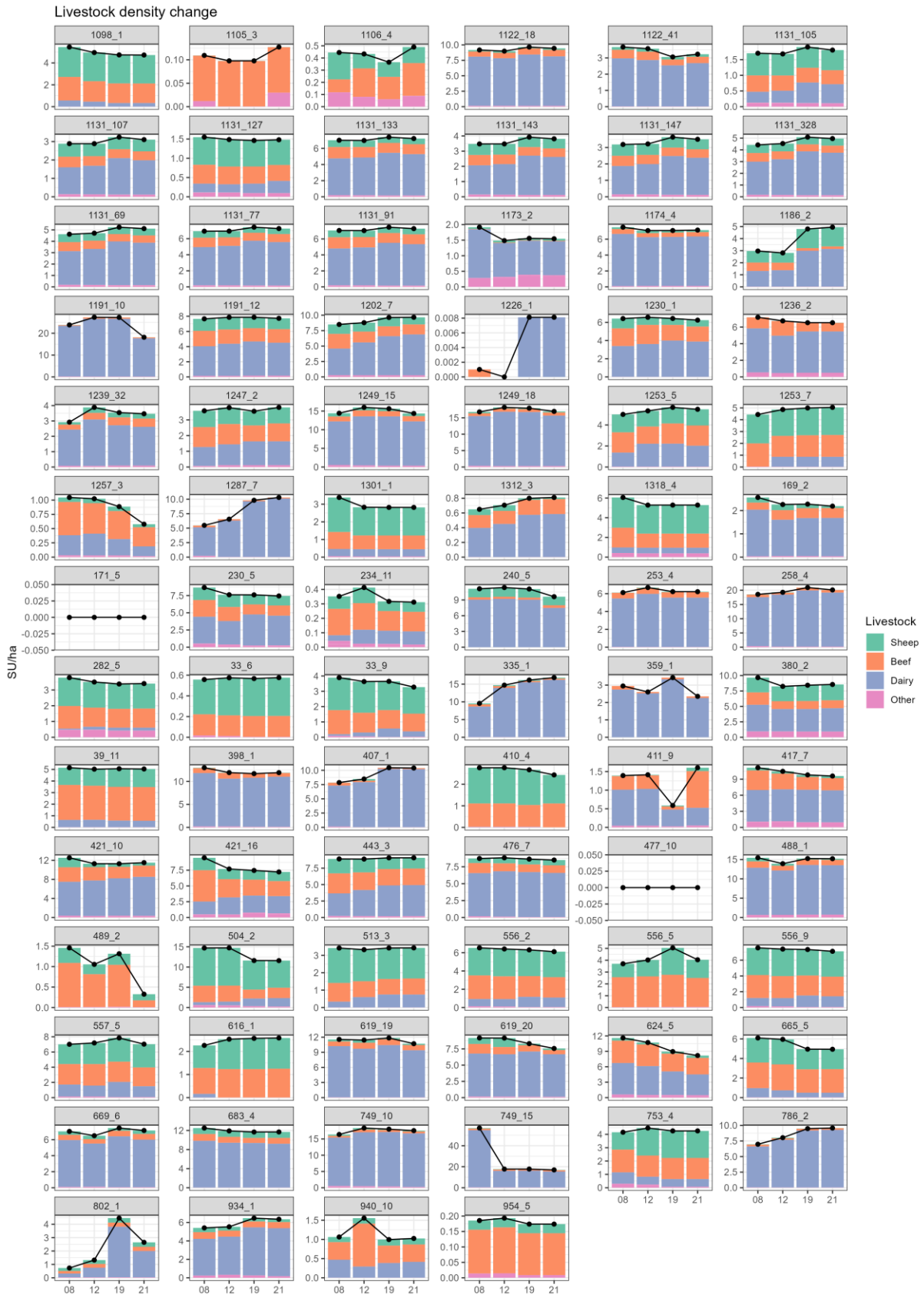


Figure 14: WRC (AgriBase) livestock density data (SU/ha). Total SU/ha is shown in black, and the x-axis shows the survey year.

No livestock were recorded in two fully forested catchments (Hinemaiaia River 171_5 and Mangauika Stream 477_10). Several other catchments show unusual patterns that may be data errors, but these are yet to be fixed. Apart from a few subcatchments, there have not been major changes in stocking rates. Exceptions include the Pueto Stream (802_1) and Whakauru Stream (1287_7), which both had an increase in stock number following pasture establishment.

Figure 15 shows the simple correlation between long-term median *E. coli* concentration and long-term median livestock density of different types. Median *E. coli* concentrations generally increase with beef and dairy cattle densities (stock units per hectare, SU/ha), although there is considerable variation, presumably due to other land uses in the catchment and environmental factors such as land form, geology or average catchment rainfall and temperature. Surprisingly, median *E. coli* concentrations are not strongly correlated with sheep numbers, despite the fact that sheep faeces are known to contain high *E. coli* counts (Wilcock, 2006). However, this could be due to the generally low numbers of sheep in these catchments, with only one catchment having > 4 sheep SU/ha (Mapara Stream, Lake Taupo, 504_2) compared with dairy numbers. Other livestock types were only present in low numbers.

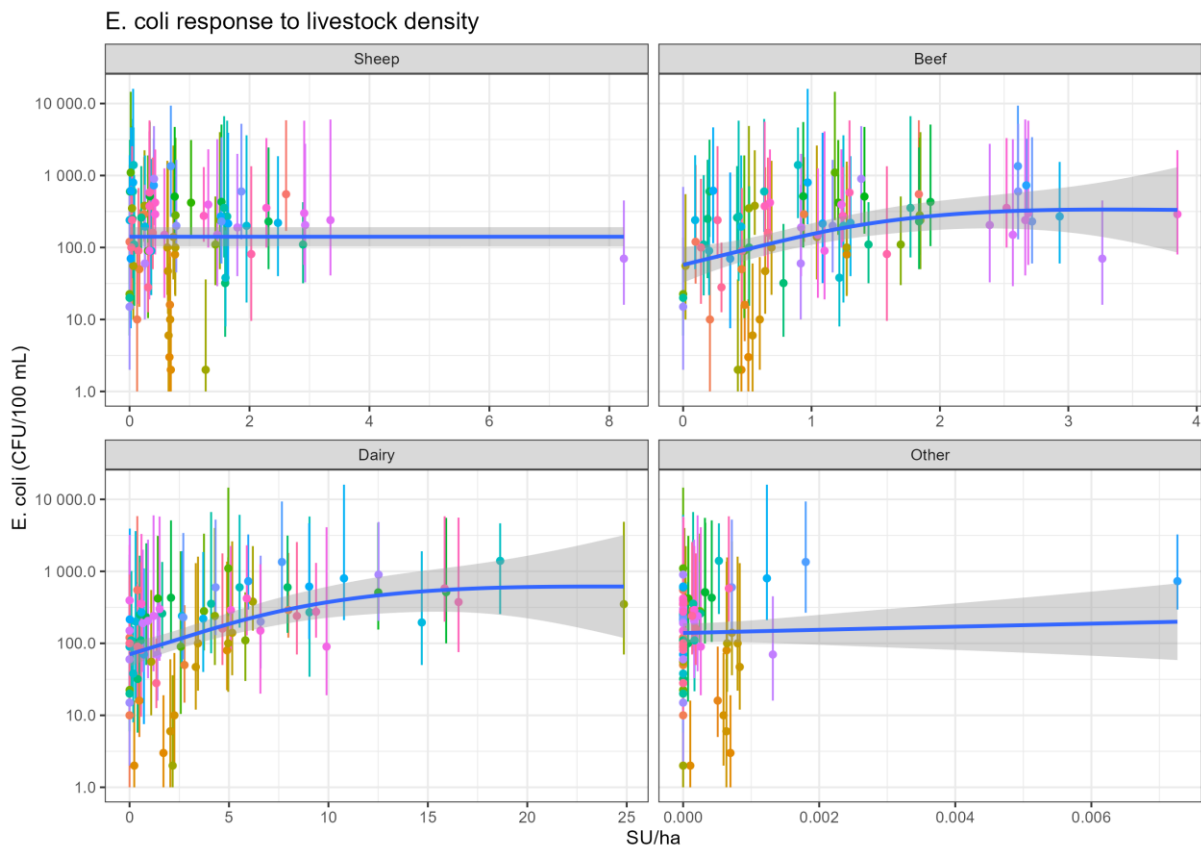


Figure 15: Correlation between long term *E. coli* and WRC (AgriBase) livestock density (SU/ha). Points are coloured by site, and median *E. coli* points and 5-95% quantile ranges are plotted for each site and a smoothed response curve is shown.

7.4 Land use area

The second land use data set comes from the CLUES model (based on AgriBase and the New Zealand Land Cover Database LCDB3) (Figure 16). This data set summarises the legal property areas associated with each land use as surveyed in 2008 and 2018. Unlike the WRC livestock density data, the CLUES data report the proportion of catchment area in each land use and distinguish native from plantation (“exotic”) forest. Land use categories include dairy, sheep/beef (sb), exotic, native, urban and other (e.g., other livestock, arable, horticulture, scrub).

Figure 17 shows the simple correlation between long term median *E. coli* concentrations in surface waters and land use area of different types for the various WRC sites (median across survey years). Similarly to Figure 15, median *E. coli* concentrations generally increase with area of dairy or sheep-beef (sb) or urban, but generally *decrease* with area in forest (either native or plantation). It is noteworthy that fully native catchments (median *E. coli* about 30 CFU/100 mL as area fraction approaches 1) have less than approximately 1/10th the average *E. coli* concentrations of mostly dairy catchments (about 500 CFU/100 mL as the dairy fraction approaches 1).

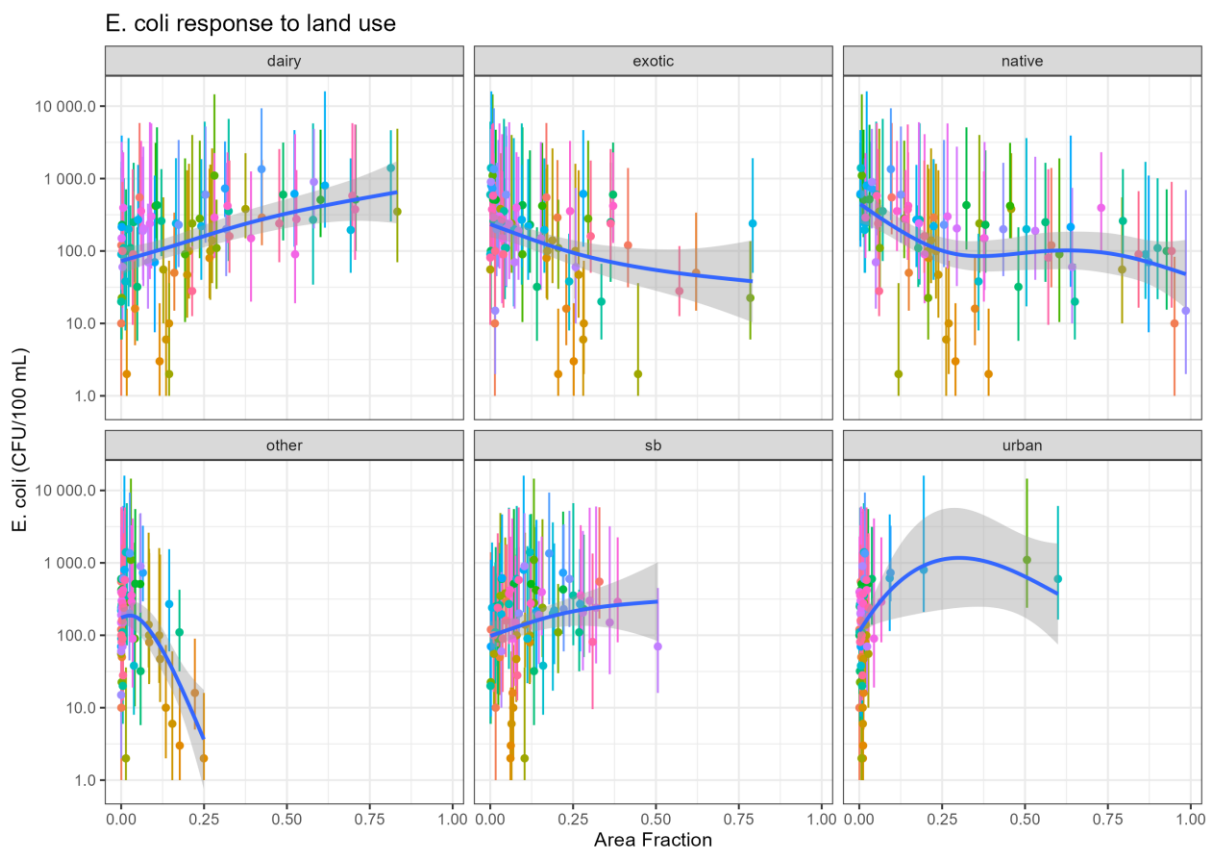


Figure 17: Correlation between *E. coli* and CLUES (AgriBase/LCDB3) land use area. Points are coloured by site, and median *E. coli* points and 5-95% quantile ranges are plotted for each site and a smoothed response curve is shown (sb = sheep and beef).

7.5 Fencing

WRC surveyed fencing of streams adjacent to dairy and drystock pasture across all stream orders and subregions in 2002, 2007, 2012 and 2017 (Norris et al. 2020). Stratified sampling was used to achieve similar numbers of survey locations in each subregion × land use × stream order category. Drains were differentiated from other waterways for the purposes of the survey by using a stream order designation of 0. In each survey year, most survey sites were retained from the previous survey year, and additional sites were added. Survey sites initially consisted of both banks of a 1 km stretch of waterway; however, this was reduced to 500 m in 2017.

The proportion of fenced stream bank is summarised in Figure 18 and Figure 19. Dairy pasture streams are generally fenced more than drystock pasture streams, but proportions of fenced stream bank have been increasing across the Waikato under both land uses.

7.6 Point source discharges

Major point source wastewater discharges occur into several Waikato streams, generally associated with town sewage or agricultural processing facilities such as dairy factories (see Vant, 2014). Annual average *E. coli* loads for the 2006-2015 period (expressed as 10⁹ CFU per year) were available or estimated for 24 point source discharges, representing the major point source discharges in the region. The locations of these point source discharges are shown on Figure 3. From these data, the total upstream point source yield (i.e., total load divided by catchment area) was determined for each of the *E. coli* monitoring sites in our study.

While we do not have information about changes in point source discharge loads over time, we can assess to what extent point sources yields determine *E. coli* concentrations measured in-stream. For each stream monitoring site, *E. coli* median and range for the 2006-2015 period was plotted against total upstream point source yield for the same period (Figure 20). The lack of correlation suggests that the contribution of point source loads to *E. coli* concentration in surface waters is relatively small compared with diffuse sources. That is, diffuse sources mask point source impacts on *E. coli*.

7.7 Flow

Streamflow data (m³/s) were available at 38 WRC flow sites (see time series of mean annual flow by site in Figure 21). The median annual flow has tended to decrease in the last few years (since approximately 2017), associated with the low rainfall (Figure 13).

Each *E. coli* monitoring site (Table 2) was associated with either: (1) the flow site at the same location, (2) the flow site recommended by Vant (2018) as a flow indicator, or (3) the closest flow site on the same river, in that order of preference. This resulted in 56 WRC *E. coli* sites with an index of flow, leaving 26/82 WRC sites without flows (Table 2). Correlations between mean daily flow and *E. coli* concentrations are shown in Figure 22. Associations with mean daily flow were typically definite, but generally weak.

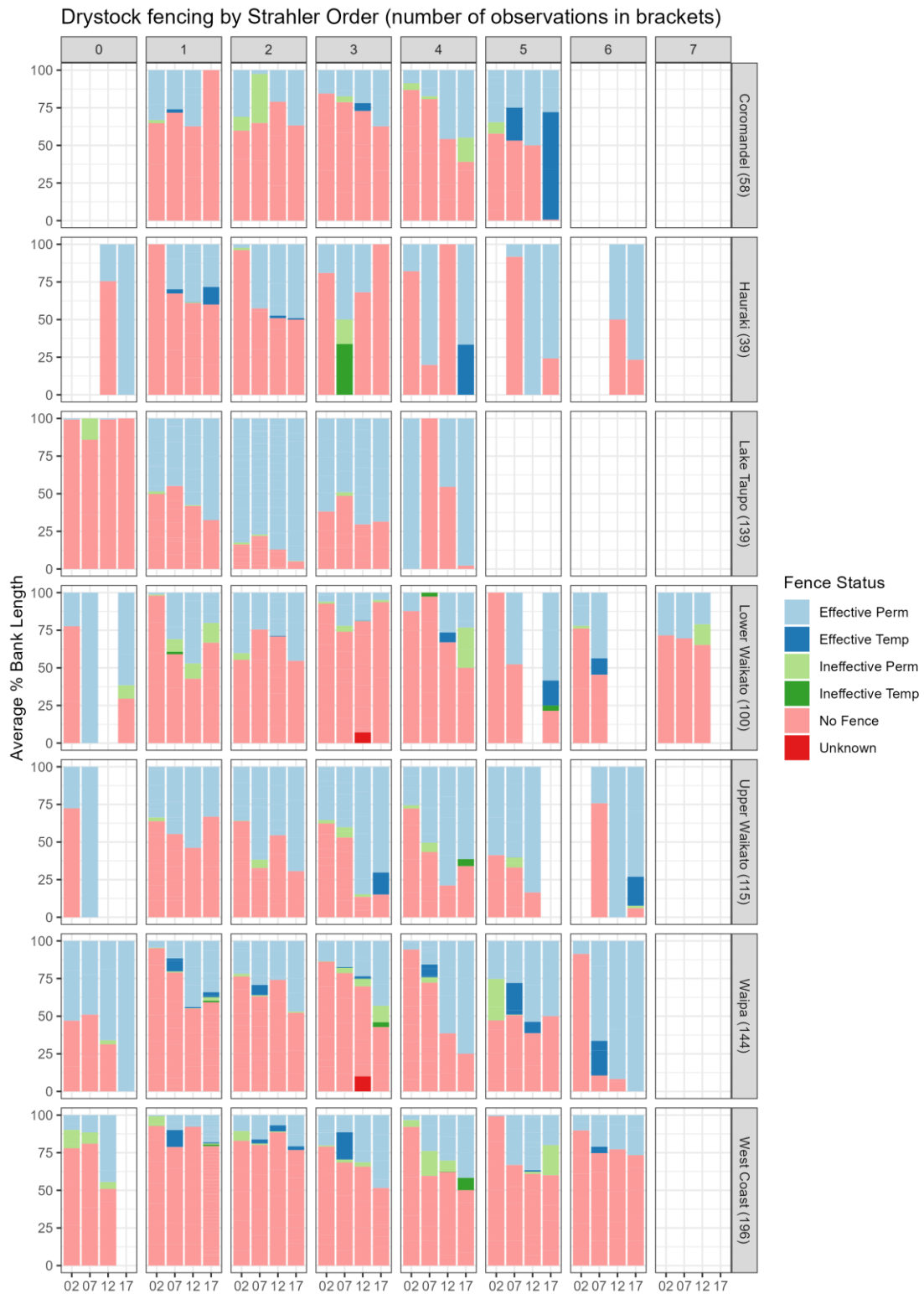


Figure 18: Changes in proportions of fenced streambank adjacent to drystock (sheep-beef) pastures, across subregions and stream orders. Order 0 refers to drains. The x-axis shows the survey year.

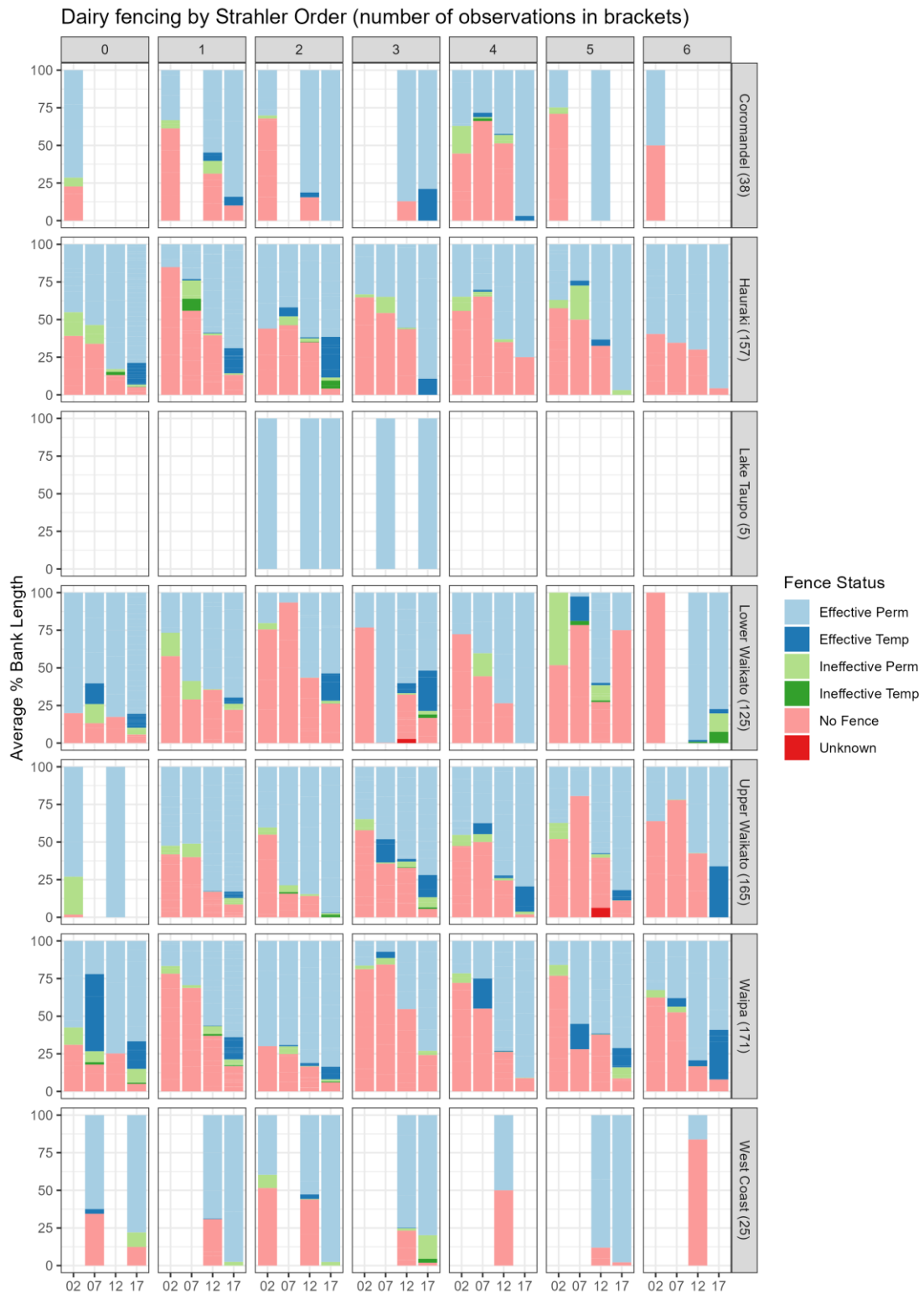


Figure 19: Changes in proportions of fenced streambank adjacent to dairy pastures, across subregions and stream orders. Order 0 refers to drains. The x-axis shows the survey year.

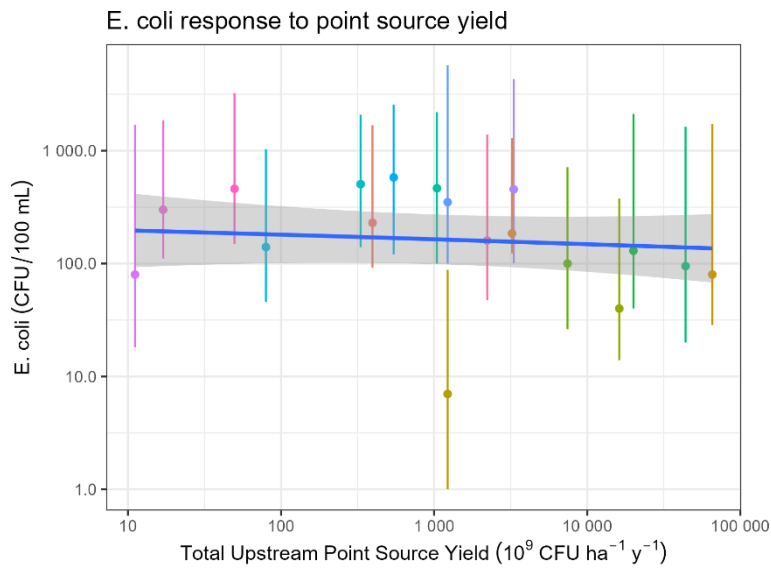


Figure 20: Correlation between *E. coli* concentrations at stream monitoring sites and total upstream point source yield. Points are coloured by site; median *E. coli* concentration and 5-95% quantile ranges were calculated for the 2006-2015 period (to match the point source estimate period). A smoothed response curve (calculated using a simple GAM) is also shown. The Total Upstream Point Source Yield for a monitoring site is the sum of annual loading over all point sources upstream of the monitoring site divided by the area of the catchment associated with the monitoring site.

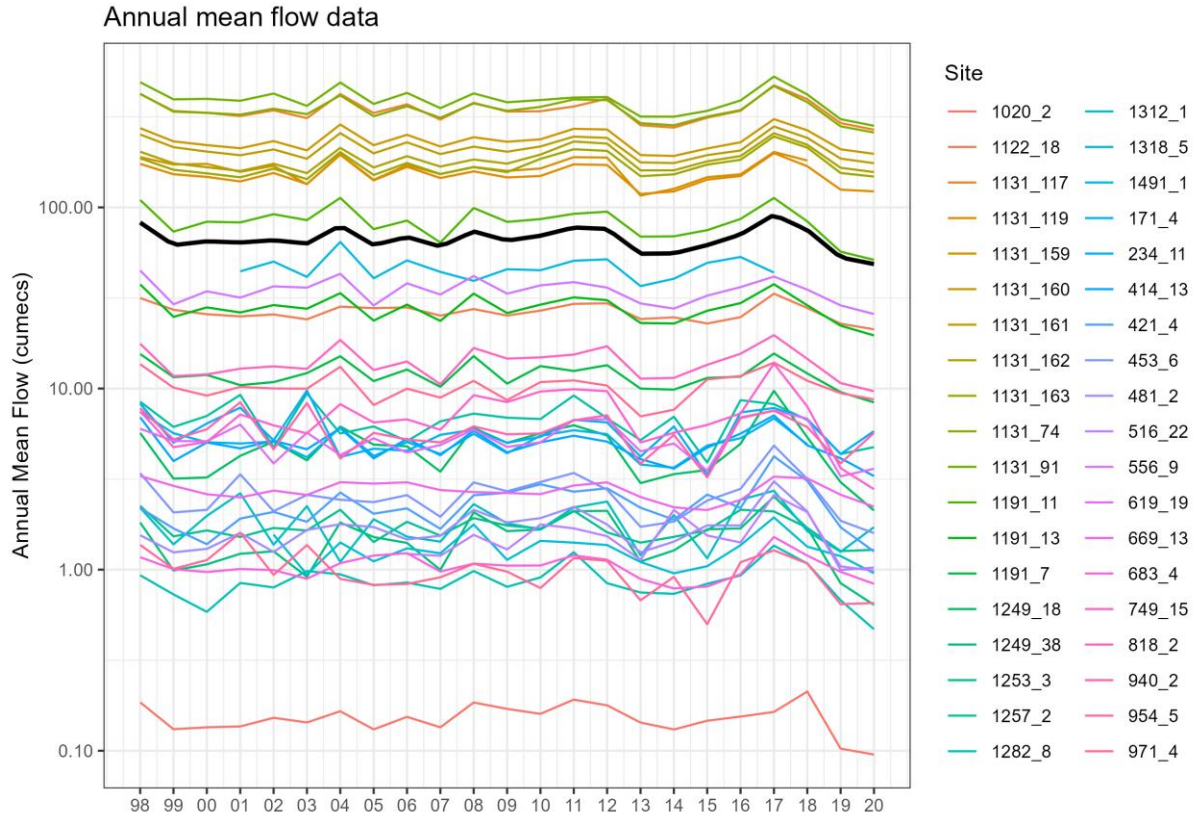


Figure 21: Annual average flow (m³/s) at 38 WRC flow sites. The black curve plots the annual median across all sites (based on scaled data so that each site has the same mean).

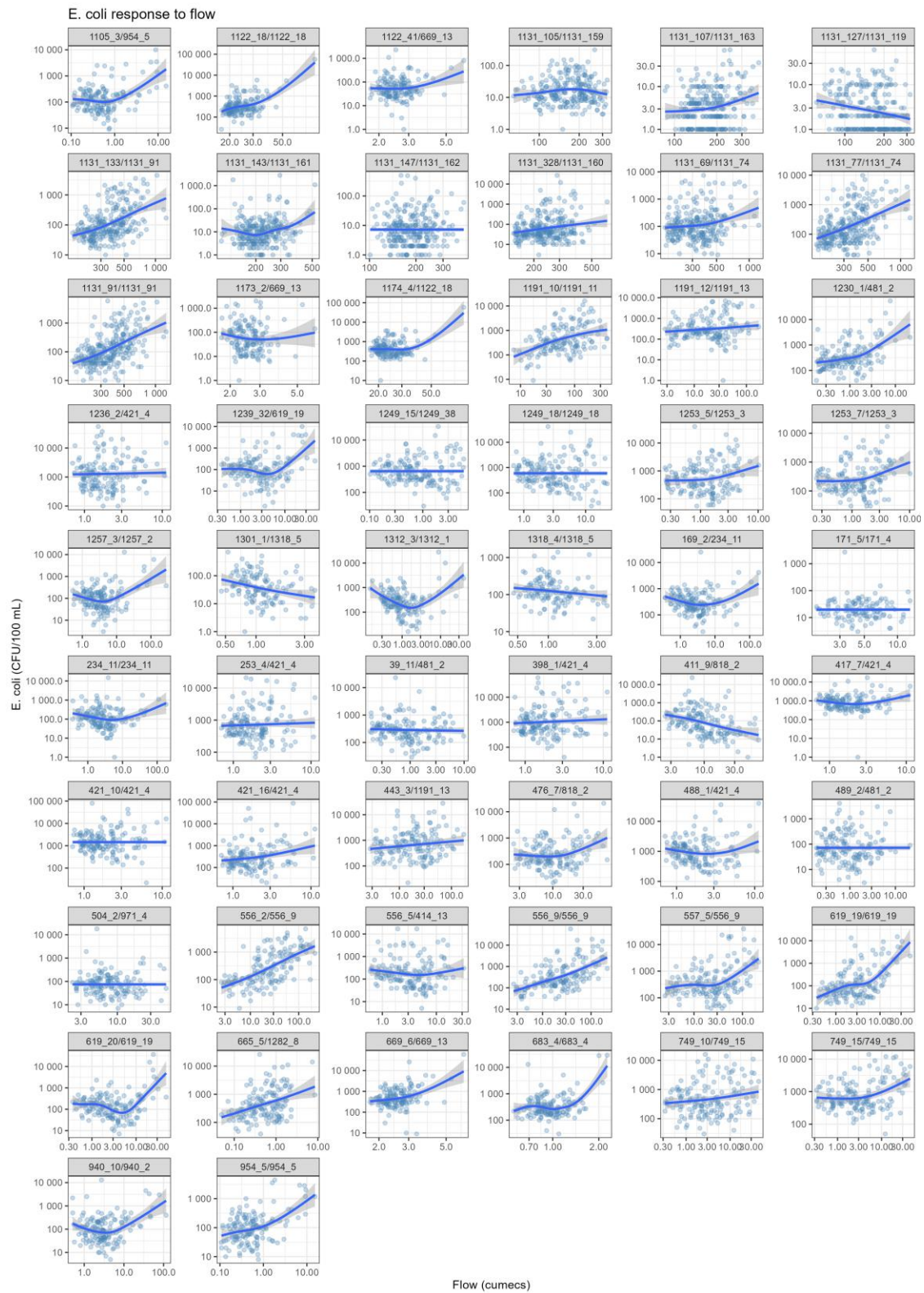


Figure 22: Correlation between *E. coli* and flow (m^3/s) at a nearby flow gauge. A smoothed response curve (calculated using a simple GAM) is also shown. Site code/flow site code pairs are described in Table 2.

8 Estimation of *E. coli* trends

8.1 Time window selection

The purpose of trend detection is to identify a change in a quantity over time. The two main issues that arise are:

1. What is the time scale of the trend we wish to detect?
2. Are the data being affected by processes whose influence we wish to ignore? For example, we might wish to filter out the effect of streamflow on the trend to highlight the effect of land use change.

Regarding the first issue, traditional trend detection methods (Thiel-Sen slope estimator) attempt to detect the presence of a *linear* trend, either using all available data, or data within a specified time window. In order to detect *non-linear* trends, these methods must be applied to multiple, shorter time windows of the data. However, a shorter time window may contain too few observations to detect a statistically significant trend. Traditional trend detection methods therefore require the modeller to choose between:

- using a short time window that can identify short term changes, but with greater uncertainty, or
- a long time window to estimate a linear trend with greater reliability, but which may hide non-linear patterns in the data.

In response to this forced choice, analysts have recently tended to restrict themselves to inferring linear trends from datasets of at least 10 years in length (Snelder et al. 2018; Fraser et al. in prep.). This reduces the incidence of false-positive trends that may occur with shorter data series but probably preclude detection of non-linear trends, which may only become apparent over longer time periods.

In the current study, overlapping time windows were initially tested, matching the approach used by LAWA (2021a). These windows were 2000-2019, 2005-2019, 2010-2019, and 2015-2019. However, using this approach, comparison and interpretation of the trend results was difficult. Longer time windows contained more data points and therefore the trend slopes were estimated with apparently lower uncertainty. On the other hand, longer windows also tended to have flatter trend slopes, due to the linear trend assumption. Furthermore, comparison of trend slopes between different time windows was confounded because the periods overlapped, shared data, and had different uncertainties.

To avoid these problems, the trend analysis periods were subsequently changed to 5-year periods for this study: 2000-2004, 2005-2009, 2010-2014, and 2015-2019. Although 5-years may be considered too short for application of the traditional trend analysis methods, particularly since the regional streams only had quarterly *E. coli* data prior to 2013, it allowed direct comparison between periods and focus on the 2010-2014 and 2015-2019 periods of particular interest in which *E. coli* concentrations have fallen and then risen again. However, we expect the Thiel-Sen slope estimates for these short time periods to be appreciably variable and uncertain.

Specification of the time window is only necessary for the traditional trend detection approach, as the alternative method used (i.e., GAMs, Section 4.2) allows non-linear trends to be automatically identified when these are supported by the data, so avoiding the issue of time window selection by treating the dataset as a whole. In order to make comparisons between the results from the two methods, linear approximations of the 5-year sections of the non-linear GAM trends were calculated as described in Section 8.3.

8.2 Traditional methods (based on Sen slope)

The traditional method of identifying and quantifying linear trends uses the Mann-Kendall Slope Test and the Theil-Sen Slope Estimator. This method may also assume seasonal data (Hirsch et al. 1982) and/or may be applied to flow-adjusted data.

For each site, the *E. coli* data were first transformed using the optimal Box-Cox transformation (described in Section 6.4) and censored values were then imputed to avoid inducing artefactual trends (as described in Section 6.3). Potential extreme outliers were then counted but not removed (as described in Section 6.4). Observations with missing covariate data (e.g., flow data at the time of sampling) were counted and removed.

Four variants of Mann-Kendall/Theil-Sen trend analysis were then carried out for the data in each 5-year period separately, optionally including “seasonal” analysis and/or flow-adjustment.

For the flow adjusted analyses, a concentration-flow relationship (e.g., Figure 22) was first fitted to the (Box-Cox transformed) *E. coli* data at each site (Smith et al. 1996) using a simple GAM model. The (Box-Cox transformed) *E. coli* data were then adjusted by subtracting this flow relationship, and trend analysis was carried out on the adjusted data.

For the “seasonal” analyses, blocking was done by month, so that trend analysis and slope estimation only compare observations taken in the same month of the year.

The four traditional approaches are therefore (terms in parentheses):

1. Sen slope (“none”).
2. Seasonal Sen slope (“seas”).
3. Sen slope of flow-adjusted data (“flow”).
4. Seasonal Sen slope of flow-adjusted data (“flowseas”).

8.3 Alternative methods (based on GAM)

The alternative approach to inferring trends in the data used the Generalised Additive Model (GAM) approach, with six different sets of covariates (c.f., Yang and Moyer, 2020). As explained in Section 4.2, GAM models are regression models constructed by adding curvilinear terms and offer many advantages over the traditional approach.

The first four GAM models were constructed using covariates corresponding to those used in the traditional approach. The simplest GAM trend model (“none”) has a single curvilinear term representing the response (of *E. coli*) to year (similar to the curves in Figure 4, but fitted to the Box-Cox transformed data). GAM models with a seasonal term (“seas”, “flowseas”) add a curvilinear term representing the response to time of the calendar year (i.e., “month”), and GAM models with a flow

response term (“flow”, “flowseas”) add a curvilinear term representing the response to flow (similar to the curves in Figure 22, but fitted to the Box-Cox transformed data). In this way, a GAM model is the sum of non-linear terms representing different covariates of interest.

The four GAM models constructed to match the traditional models were therefore:

1. $y \sim f_1(\text{year})$ (“none”),
2. $y \sim f_1(\text{year}) + f_2(\text{month})$ (“seas”),
3. $y \sim f_1(\text{year}) + f_3(\text{flow})$ (“flow”), and
4. $y \sim f_1(\text{year}) + f_2(\text{month}) + f_3(\text{flow})$ (“flowseas”),

where y is the Box-Cox transformed *E. coli* data. Interaction terms (e.g., $f_i(\text{year}, \text{month})$) were not included in our GAM models. Although these can explain more of the variation and result in a better fit, they also make interpretation more difficult.

Two additional GAM models were also tested. One used rain and temperature data as additional covariates. Since rain and temperature data are widely available through NIWA’s VCSN, this approach may be particularly useful for sites without a nearby flow recorder. The other approach used all available covariates.

5. $y \sim f_1(\text{year}) + f_2(\text{month}) + f_4(\text{rain}) + f_5(\text{air_temp}) + f_6(\text{water_temp})$ (“raingam”), and
6. $y \sim f_1(\text{year}) + f_2(\text{month}) + f_3(\text{flow}) + f_4(\text{rain}) + f_5(\text{air_temp}) + f_6(\text{water_temp})$ (“allgam”).

Although seasonal patterns of *E. coli* concentration are mainly responses to changing rainfall, flow and temperature which are included as covariates (Section 3), the month term was retained in these models to account for other seasonal factors such as solar radiation and land management actions that are not included explicitly as covariates (e.g., calving, livestock wintering, crop harvesting). The GAM fitting algorithm automatically assesses the evidence for each model term in order to avoid overfitting, and p-values are estimated for each term of the fitted model. Variable selection may also be done (Marra and Wood, 2011), but was not done here in order to apply the same models to all sites.

All GAM models that used rain and/or flow as covariates also included rain and/or flow data from the previous 3 days (defined as midnight-midnight periods) as additional covariates; i.e., $\text{rain}(t)$, $\text{rain}(t-1)$, $\text{rain}(t-2)$, $\text{rain}(t-3)$, $\text{flow}(t)$, $\text{flow}(t-1)$, $\text{flow}(t-2)$, $\text{flow}(t-3)$. This allows the time for *E. coli* entering the stream to travel to the monitoring site to be considered, especially useful for larger catchments. In addition, *E. coli* concentrations may be sampled *prior to*, and therefore not be highly correlated with, rain or flow events on the same day. Correlations with earlier days’ rain or flow might be more consistent.

In R code, the “allgam” model (for example) was written as:

```
y ~ ti(year, k = 9) + ti(month, bs = 'cc', k = 6) + ti(flow0) + ti(flow1) + ti(flow2) + ti(flow3) + ti(rain0) +
ti(rain1) + ti(rain2) + ti(rain3) + ti(air_temp) + ti(water_temp)
```

The mgcv package in R offers three types of smooth terms for a GAM model: $s()$ which are spline smooths, $te()$ which are full tensor product smooths, and $ti()$ which are tensor product interaction smooths. Use of $ti()$ terms is appropriate when interaction terms and main effects occur

simultaneously, or when the interactions are on difference scales. The basis dimension (k) of each term has a default value of 5, which gives a curve with a maximum of $k - 1 = 4$ degrees of freedom. Model fitting returns the “reference degrees of freedom” of each term. If this is near k , k may be increased, and the model refitted to allow greater flexibility. Based on early model fits, k was increased to 9 for the year (trend) term and 6 for the month (seasonal) term.

The default smoothing basis function is $bs = 'cr'$ which is a cubic regression spline. The $bs = 'cc'$ option gives a periodic/cyclic cubic regression spline, which is suitable for periodic covariates such as month (seasonal).

By default, GAM uses a maximum likelihood approach to automatically determine the optimal smoothness of the model. This can result in curvilinear terms being reduced to linear terms. Terms can optionally be removed completely if they are not significantly different to zero (using the $select = TRUE$ option in *mgcv*). However, since forcing terms to zero may exaggerate the importance of the remaining terms, this option was not used in the current study.

The result of fitting a GAM is the best-fit smooth function for each term. The GAM algorithm uses maximum likelihood to trade-off between model smoothness and goodness-of-fit to the data. Each term and its uncertainty can be plotted, and their magnitudes compared. This includes the trend term (e.g., $f_i(\text{time})$) which estimates the remaining trend in the data after the effects of the covariates have been accounted for.

The statistical significance of each term in the GAM is assessed using an F test (and associated p-value), which tests the null hypothesis that the term is everywhere zero. If the covariates explain the changes in the data such that the trend term is not needed, the trend term will not be statistically significant (i.e., not statistically different from zero). If the trend term is statistically significant, on the other hand, this indicates that the covariates do not fully explain the changes in the data and an unexplained trend is still present.

Statistical significance does not test whether the model is a good model of the data; this is done by examining the model residuals. The distribution of model residuals can be plotted to check that the regression assumptions have been met (e.g., independent, normally distributed residuals). If the residuals are not normally distributed this can indicate that model is not flexible enough to represent the data. The residuals are also used to assess the model's goodness-of-fit, for example to calculate the Nash-Sutcliffe Model Efficiency (NSE = the proportion of the variance in the data that is explained by the model). NSE should be high relative to 0 to indicate that the model is a good representation of the data. Very high values of NSE (approaching 1) can indicate overfitting, but this was avoided in the current study by using the $method = "REML"$ option in *mgcv*.

In order to compare the GAM trend results with the Thiel-Sen results, a linear slope was calculated from the GAM curve for each 5-year period (see Section 8.1). As in Yang and Moyer (2020), this was done by connecting the two endpoints of the GAM curve for each 5-year period (taken as the observation times of the first and last data point in that time period) with a straight line. The slope of this line segment was interpreted as the slope of the GAM for this period. Treating the two endpoints as being independent also allowed us to calculate confidence intervals for these slopes (Yang and Moyer, 2020).

The reported trends estimate the rate of increase of *E. coli* once the effects of the covariates have been accounted for. For example, flow-adjustment attempts to remove the effects of flow, and so

any trend in the flow-adjusted data represents *E. coli* increases for the hypothetical case where flow has remained constant over time, and any flow-driven increases in *E. coli* have been filtered out.

8.4 Uncertainty, significance and strength of evidence

The uncertainty of and strength of evidence for the Thiel-Sen and GAM slope estimates in this study were expressed as credible intervals (CrI) and significance levels (α -values). Traditional significance tests and p-values were not used for assessing the slope estimates. The 90% credible interval reported for each slope estimate is an interval that has a 90% probability of containing the true slope. The strength of evidence is an alternative to the traditional “p-value” (McBride et al. 2014; McBride, 2019), and gives the probability that trend estimate has the correct sign (positive or negative). The strength of evidence probability can be reported using category labels such as “virtually certain” (99–100%), “extremely likely” (95–99%), “very likely” (90–95%) and “likely” (66–90%) (Table 3).

The GAM approach (as implemented in the *mgcv* package in R) also reports the goodness of fit of the fitted model, and the effective degrees of freedom (edf), F-statistic, and p-value for each term in the model (Table 4). The effective degrees of freedom (edf) describes the curvature of the fitted model term; for example, edf = 1 means that the fitted term was linear, edf > 1 means that the fitted term was curvilinear, and edf = 0 means that the fitted term has been dropped from the model. The F-statistic and corresponding p-value for each term indicate the overall statistical significance of the term, i.e., whether there is sufficient evidence that the term is not zero. However, it does not tell us whether the term is *important*, i.e., whether it explains much of the variation in the data. This can be assessed by comparing the Nash-Sutcliffe Model Efficiency (NSE) and Akaike Information Criterion (AIC) of alternative models; the former describes the proportion of variance in the data that is explained by the model, and the latter supplements this by adjusting for model complexity—a lower AIC value indicates a better fit to the data, but if two models have AIC values that differ by less than 2 then the simpler model is preferred.

In the following sections we apply these models and assessment process in two test case catchments, where we identify the relative strengths and weaknesses of the approaches. We then apply the most useful approaches more generally to all sites across the region that satisfy data adequacy requirements.

Table 3: Intergovernmental Panel on Climate Change likelihood categories (from McBride, 2019).

Term	Likelihood of outcome
Virtually certain	99–100%
Extremely likely	95–99%
Very likely	90–95%
Likely	66–90%
About as likely as not	33–66%
Unlikely	10–33%
Very unlikely	5–10%
Extremely unlikely	1–5%
Exceptionally unlikely	0–1%

8.5 Example 1 (Waihou River at Whites Road, no flow data)

Figure 23 shows an example of how Sen slope trends are estimated with no covariates (“none”) for the periods 2000-2004, 2005-2009, 2010-2014, and 2015-2019, as well as the associated GAM model with no covariates (“none”). These data are for the Waihou River at Whites Road site, just downstream from the Blue Spring. No flow information was available at this site, although flow from a different river (Oraka Stream at Lake Road) was used for flow adjustment later.

Figure 23 and subsequent figures show the following information:

- The title shows the name of the water quality monitoring site (e.g., stream name and road name), along with its WRC code (Section 6.1) and the code of the flow site used for flow-adjustment (Section 7.7).
- The *E. coli* measurement data used for trend analysis are shown as dark orange points.
- Extreme outliers are circled in light orange (there is one above the statistics table and one at (2004, 1)).
- Censored values are shown as dark green circles (there are none in this data set). The imputed value is shown as a dark orange point (see Section 6.3).
- Points that were dropped from the analysis due to missing covariates are shown as a blue circle (there were none in this data set).
- The thin horizontal dotted (or solid) lines show the concentrations delimiting state attribute bands in the the National Policy Statement for Freshwater Management 2020 (New Zealand Government, 2020). The overall attribute band for *E. coli* is calculated from four separate metrics including the median and 95th percentile concentrations. For median concentrations, 130 CFU/100 mL separates the A/B/C bands from the D band, while 260 CFU/100 mL separates D from E. For 95th percentile concentrations, 540 (solid), 1000, or 1200 CFU/100 mL lines separate A from B, B from C, and C from D/E bands respectively.
- The Sen slopes for each 5-year period are shown as brown line segments. In addition, the total change in each 5-year period is indicated by a vertical brown arrow, to facilitate comparison with the GAM model change for the same period (vertical green arrows). The transparency of the lines and arrows indicates the statistical strength of evidence that the trend is increasing or decreasing in that period, e.g., virtually certain, very likely, likely, etc., (see Section 8.4, Table 3).
- The GAM model trend (i.e., year term) is shown as a thick green line with a 95% confidence interval band. Vertical green arrows show the change over the 5-year period. The transparency of the arrows indicates the statistical strength of evidence that the trend is increasing or decreasing in each period.
- The GAM model fit to the data (including the covariate terms) is shown as a thin pink line (see Figure 24 and Figure 25). For GAM models that do not include covariates (e.g., Figure 23), this is equal to (and occluded by) the GAM model trend (thick green line).

The table of statistics describes the fit for each term of the GAM model on the left-hand side, and summary statistics for the data set and the GAM model fit in the right-hand column. Details are provided in Table 4.

Correcting for season (“seas”, Figure 24) makes little difference to the trend analysis at this site. The model fit (NSE, Nash-Sutcliffe Model Efficiency) of the GAM model increased slightly from 14.8% to 20.7%, indicating that the seasonal model explains a slightly greater proportion of the variation in the data (the thin pink curve in Figure 24). The Akaike Information Criterion (AIC) decreases from 356.8 to 351.2; the difference is greater than 2 which indicates that the additional model complexity is justified by the data.

Adding rain and temperature covariates (“raingam”, Figure 25) improved the model fit NSE considerably, to 41.9% (the thin pink curve in Figure 25), and the AIC dropped to 315.7. The estimated trend (the thick green curve and confidence band in Figure 25) remained similar. Based on its high F statistic in the GAM table (Figure 25), rain1 (i.e., catchment average daily rainfall (mm) on the previous day) was an effective predictor in the improved model fit. Interestingly the GAM fitting procedure reduced the rain0, rain1, rain2, rain3, at (air temperature) and wt (water temperature) response terms to linear responses (see Section 8.3), indicated by their effective degrees of freedom (edf) being equal to 1.

This probably means that the data contained insufficient information to determine any non-linear component in the responses. Note also that the month, rain2 and rain3 terms were not significant (ns) in this model, which indicates that there was insufficient information to be 95% confident in the reported sign of these terms.

For each GAM model fit, model residuals and model terms were checked. The model residual and model term analysis for Figure 25 is shown in Figure 26. The *E. coli* data and model predictions in these plots are all given in Box-Cox transformed coordinates (Section 6.4). The top four subplots explore the distribution of the residuals, which are assumed to be independent and identically and symmetrically distributed around zero. The quantile-quantile subplot (“QQ plot of residuals”) compares the distribution of the residuals to a normal distribution; the deviation in this example shows that the residuals have “fat” tails compared with a normal distribution, which is common with real world data. The “Residuals vs linear predictor” subplot shows the independence and changing variance of the model residuals against the GAM model prediction (of *E. coli* concentration in Box-Cox transformed coordinates), and the “Histogram of residuals” subplot shows the same data plotted as a histogram. The “Observed vs fitted values” subplot shows the model prediction (“Response”) directly against the data (“Fitted values”); these should lie along the 1:1 line.

The bottom half of Figure 26 shows the individual terms of the GAM model, one for each covariate. The x-axis shows the covariate values, and the y-axis shows the term’s corresponding contribution to the GAM model (in Box-Cox transformed *E. coli* units). The uncertainty band around each generalised term indicates whether the term is credibly different from zero. In this example, the $ti(\text{year})$ term is the trend shown in green in Figure 25, the $ti(\text{month})$ term is the seasonal cycle (after accounting for rain and temperature), and the remaining terms in this case show a linear response to rain0, rain1, rain2, rain3, at (air temperature) and wt (water temperature). The uncertainty envelopes for month, rain1 and rain2 are wide enough to encompass the x-axis, which corresponds to their lack of statistical significance as reported in Figure 25. The importance of $ti(\text{rain1})$ relative to $ti(\text{rain0})$ is reflected in its larger range of y-values.

Table 4: Explanation of statistics included in the trend plots.

Statistic	Description
term	GAM term
edf	Effective degrees of freedom of the model term (e.g., 1 = linear, 2 = quadratic)
Ref.df	Reference degrees of freedom (not used)
F	F statistic for the term (weighted proportion of variance explained)
p-value	Probability that the F value this large is by chance
sig	Statistical significance of the term
misc	Miscellaneous statistics
ncens	Number of censored values (circled in dark green)
ndrop	Number of dropped rows due to missing covariates (blue circles)
noutlier	Number of extreme outliers (circled in light orange)
ny	Total number of data values (y)
ncomplete	Number of data rows used for trend estimation
lambda	Box-Cox transformation lambda
sd y	Standard deviation of y (rmse should be smaller than this)
shap y	p-value in Shapiro-Wilks test of normality on data (y). Small values warn that the data may not be sufficiently normal.
aic	Akaike Information Criterion of model. Used for comparing models.
shap res	p-value in Shapiro-Wilks test of normality on the residuals. Small values warn that the data may not be sufficiently normal.
rmse	Root mean squared error of prediction (standard deviation of the residuals). This should be smaller than sd y.
nse	Nash-Sutcliffe Model Efficiency (proportion of variance in y explained by the model). $nse = 1 - (rmse / sd y)^2$

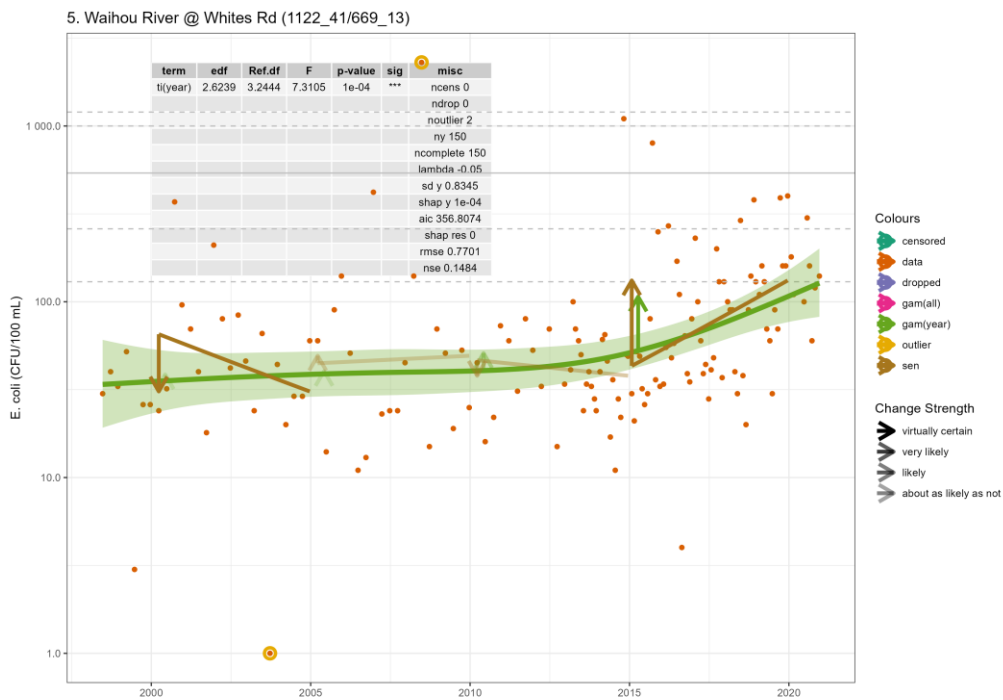


Figure 23: Trends and 5-year changes in *E. coli* concentrations for the Waihou River at Whites Road (no adjustment). Sen slope (brown line segments and arrows) and GAM (green curve and arrows) without covariates (“none”). Full plot details are explained in Section 8.5 and Table 4.

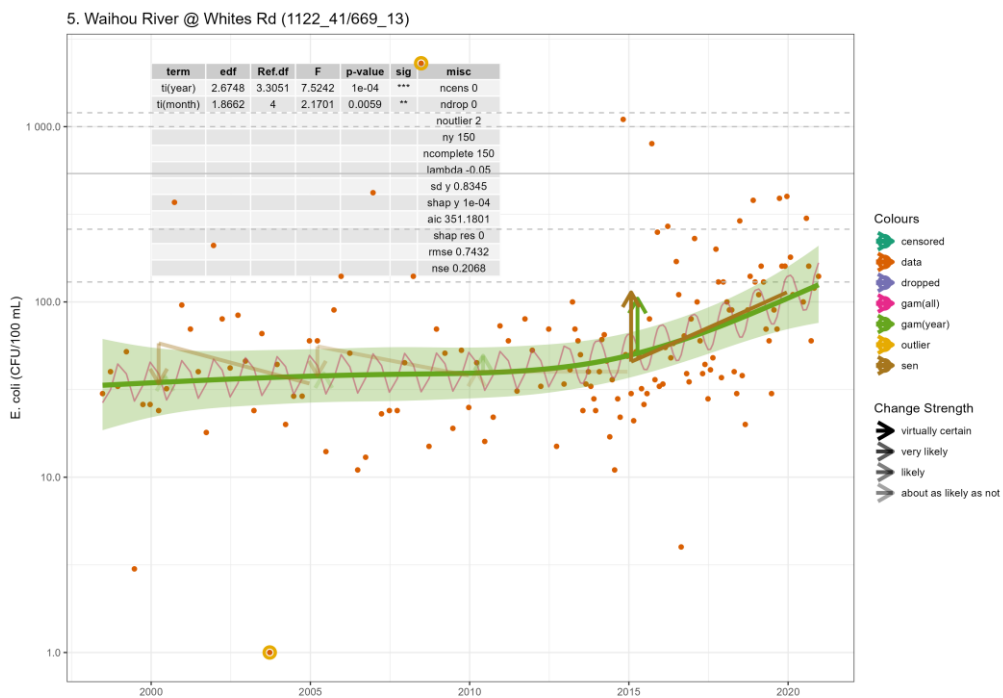


Figure 24: Trends and 5-year changes in *E. coli* concentrations from the Waihou River at Whites Road (seasonal adjustment). Seasonal Sen slope (brown line segments and arrows) and GAM (green curve and arrows, no covariate), and with a seasonal covariate (thin pink line “seas”). Full plot details are explained in Section 8.5 and Table 4.

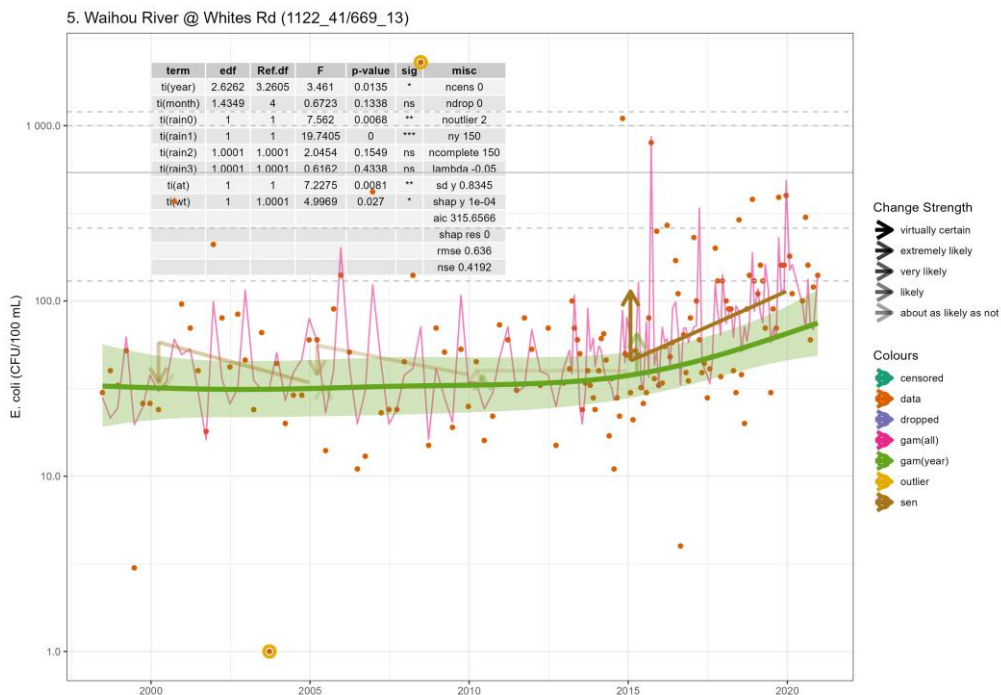


Figure 25: Trends and 5-year changes in *E. coli* concentrations from the Waihou River at Whites Road (seasonal, rain and temperature adjustment). Seasonal Sen slope (brown line segments and arrows) and GAM (green curve and arrows – no covariates), and with seasonal, rainfall, air temperature (at) and water temperature (wt) covariates (“raingam”) – pink line. Full plot details are explained in Section 8.5 and Table 4.

8.6 Example 2 (Waitoa River at Landsdowne Road, flow data)

A second example is given in Figure 27 for a site which has index-of-flow data (from a nearby flow recorder on the same stream). This data set had two censored values which are shown as dark green circles, their imputed values are shown as dark orange points (Section 6.3).

The Sen slope estimates in Figure 27 (based on the raw data without covariate adjustment, “none”) identified decreasing *E. coli* concentrations during the 2010-2014 period followed by increasing concentrations during the 2015-2019 period. The Sen slope estimates for the 2000-2004 and 2005-2009 periods were quite sensitive to the small number of data points collected during this time. The fitted GAM curve followed an S-shape, similar to the direction of the Sen slope estimates but far less steep.

When adjusting for flow (“flow”, Figure 28) two data points (indicated by blue circles) had to be dropped due to missing flow data at that time. Flow-adjustment made little difference to the Sen slope estimates. This is not surprising since the *E. coli* concentration-flow relationship is very flat, showing weak flow-dependence for this site (Figure 22). Including flow as a covariate in the GAM model, however, made a substantial difference to the goodness-of-fit, with NSE increasing markedly from 8.0% to 48.4%, and the AIC decreasing from 156.8 to 74.4. This was unexpected, given the weak flow-dependence. Analysis of the model residuals and model terms (Figure 29) shows that this increase in predictive power was achieved by combining the information in flow0 (mean daily flow on the day of sampling) and flow3 (mean daily flow three days prior to sampling)—both the ti(flow0)

and $ti(flow3)$ terms have significant and opposite slopes. So, *E. coli* is highest on days when it rained but did not rain 3 days previously, whereas *E. coli* is lowest on days when it didn't rain but it rained 3 days previously. This could be interpreted as *E. coli* accumulating when it doesn't rain, and then becoming mobilised during rain events. However, caution should be exercised when interpreting regression models; compared with process-based models, regression models are good for making accurate predictions rather than providing meaningful interpretations of the underlying processes. This example does however demonstrate that inclusion of lagged flow in the model improved prediction of *E. coli* dynamics at this site and suggests that lagged drivers should be examined more thoroughly in future work.

Including seasonal Sen analysis of the flow adjusted data (Figure 30) did not change the Sen slope estimates. However, the strength of evidence for trends in the data was reduced, since seasonal Sen analysis only compares data from the same month of the year, resulting in less comparisons overall and lower statistical power. Similarly, including season as an additional covariate in the GAM model ("flowseas") had little effect on the estimated trend, and only gave a small additional improvement to the goodness-of-fit, with NSE increasing to 53.5% and AIC dropping to 65.1.

Including the remaining covariates (i.e., rainfall, water temperature and air temperature; "allgam", Figure 31) allowed a non-linear trend to be identified, although less steep than the trend inferred from the raw data (Figure 27). The additional covariates improved model fit NSE to 64.7% and dropped AIC to 43.9, indicating a more explanatory model where additional complexity was justified by the data. In this model the seasonal ("month") term was eliminated from the model (effective degrees of freedom (edf) = 0), indicating that this covariate provided no additional information beyond what was provided by the other covariates.

A subsequent GAM model fit without flow data ("raingam", Figure 32) resulted in a NSE of 59.2% and the AIC of 57.3—only slightly less favourable than the model with flow included. Since flow data are not available at many sites, this outcome suggests that rainfall may be a useful alternative covariate to flow. This has widespread potential application because NIWA's VCSN interpolated weather data set is able to generate historical daily rainfall estimates for the whole of New Zealand.

In all of these models, the inclusion of covariates explained a considerable proportion of the variance in the *E. coli* data. The covariates could not, however, fully account for trends in *E. coli* through time. This suggests that additional, currently unidentified factors contribute substantially to the observed trend, and further investigation will be required to identify these covariates .

5. Waihou River @ Whites Rd (1122_41/669_13)

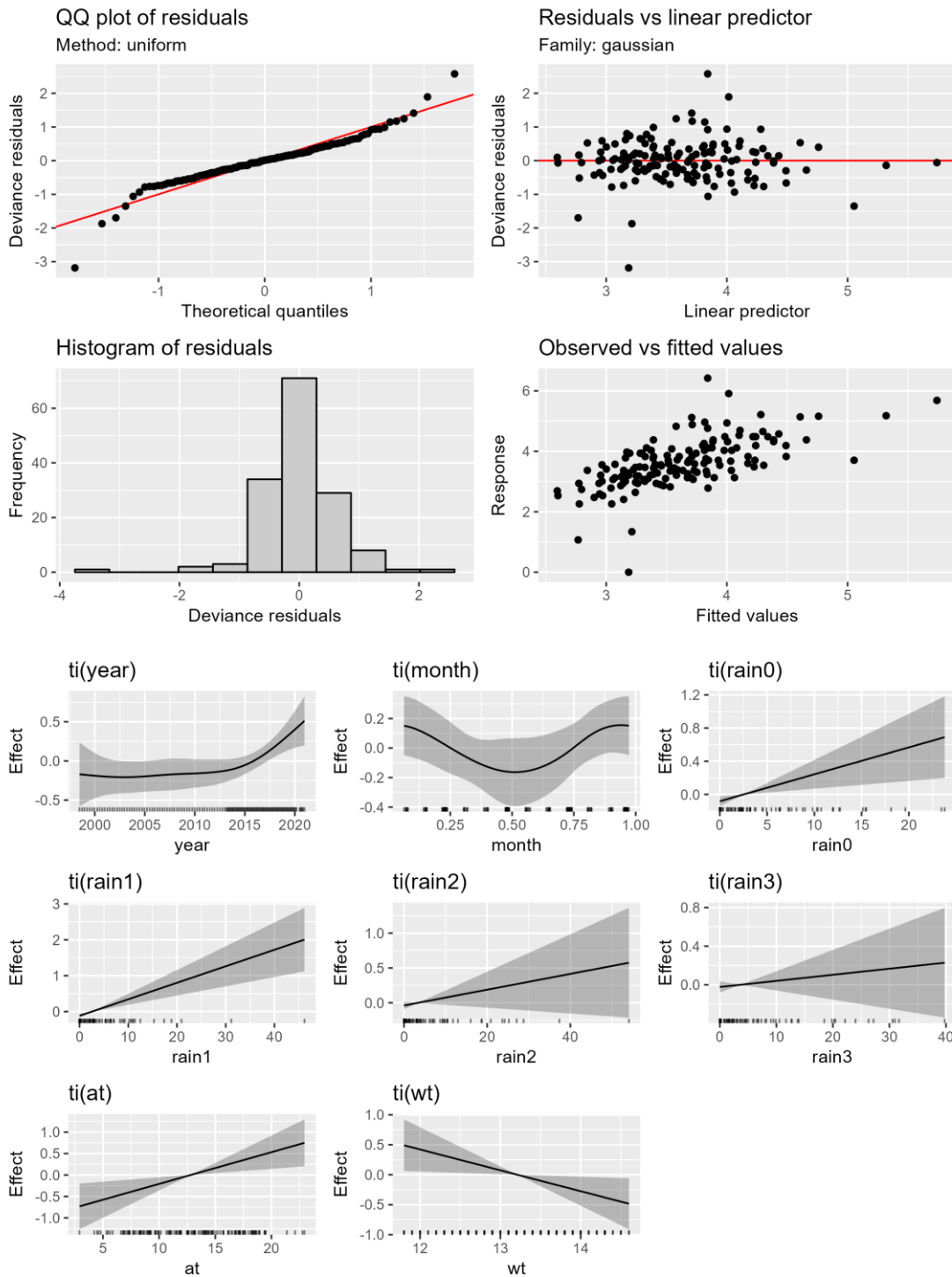


Figure 26: GAM residuals and model terms for *E. coli* at Waihou River at White’s Road (seasonal, rain and temperature adjustment). This is an analysis of the GAM model fit shown in Figure 25.

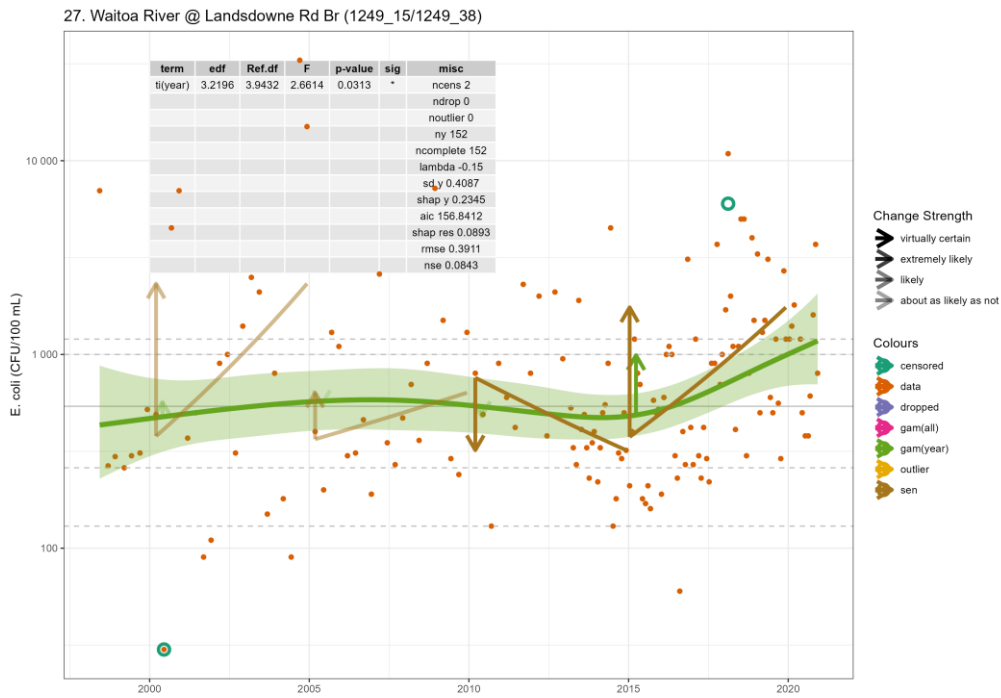


Figure 27: Trends and 5-year changes in *E. coli* concentrations from the Waitoa River at Landsdowne Road (no adjustment). Sen slope (brown line segments and arrows) and GAM (green curve and arrows) without covariates (“none”). Full plot details are explained in Section 8.5 and Table 4.

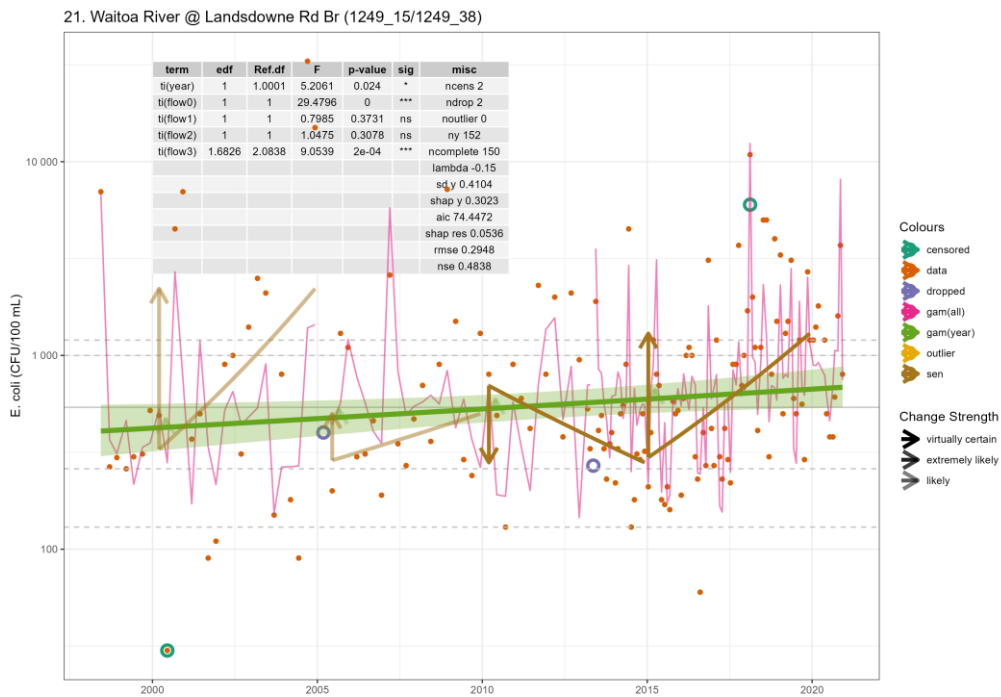


Figure 28: Trends and 5-year changes in *E. coli* concentrations from the Waitoa River at Landsdowne Road (flow adjustment). Flow-adjusted Sen slope (brown line segments and arrows) and GAM (green curve and arrows) with a flow covariate (“flow”). Full plot details are explained in Section 8.5 and Table 4.

21. Waitoa River @ Landsdowne Rd Br (1249_15/1249_38)

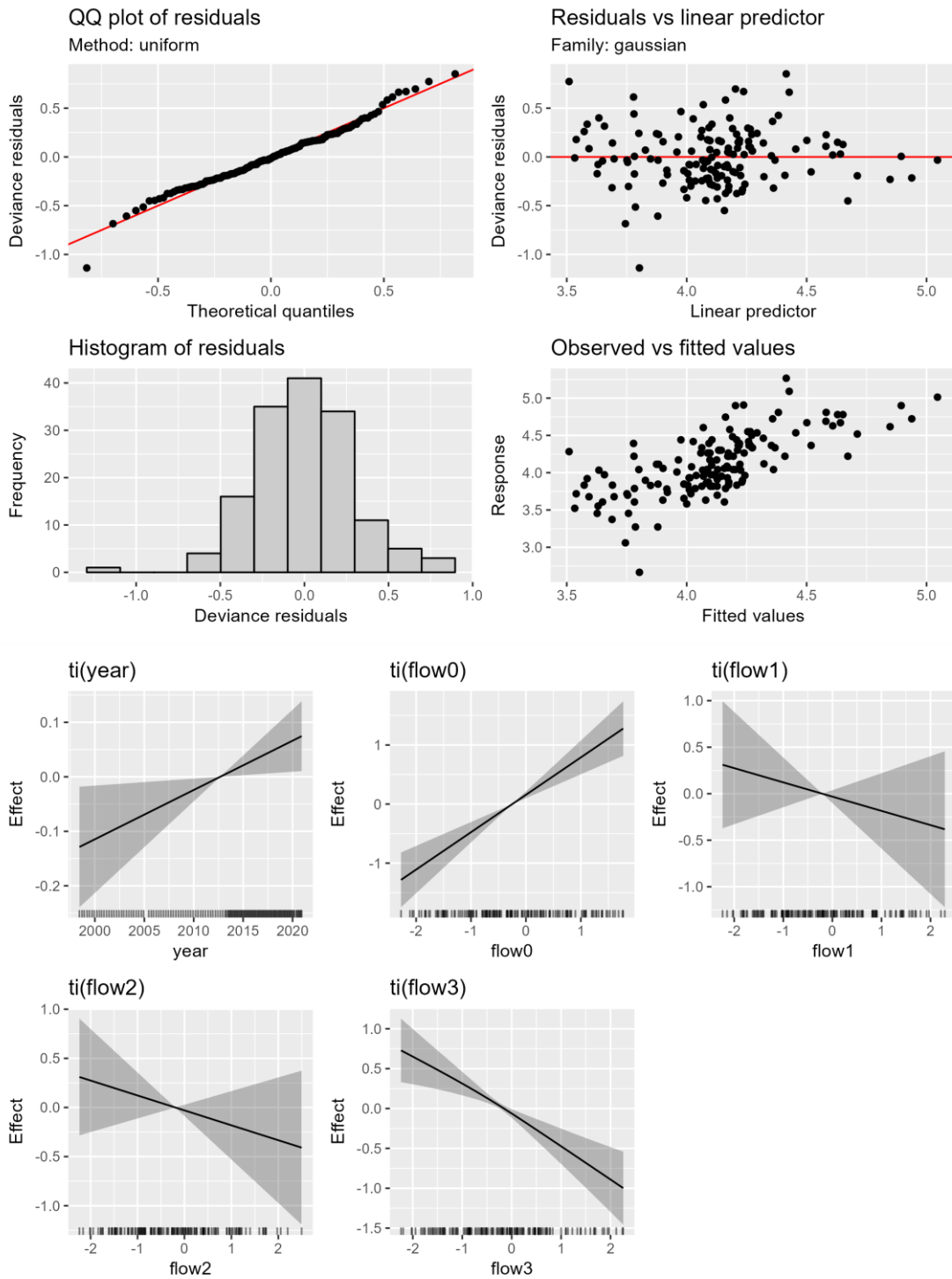


Figure 29: GAM residuals and model terms for *E. coli* at Waitoa River at Landsdowne Road (flow adjustment). This is an analysis of the GAM model fit shown in Figure 28.

21. Waitoa River @ Landsdowne Rd Br (1249_15/1249_38)

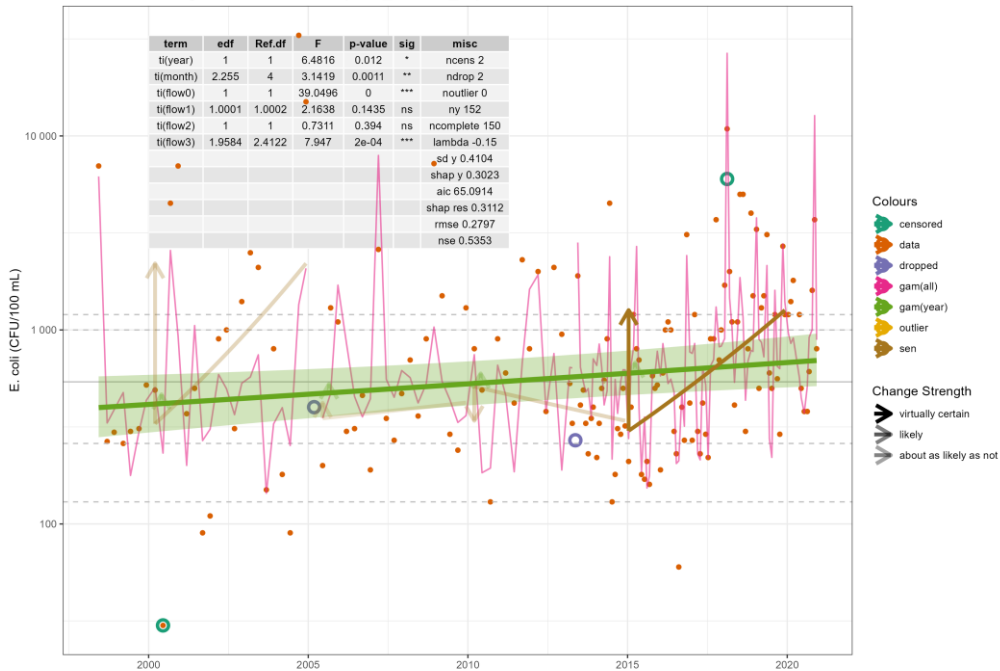


Figure 30: Trends and 5-year changes in *E. coli* concentrations from the Waitoa River at Landsdowne Road (seasonal and flow adjustment). Flow-adjusted seasonal Sen slope (brown line segments and arrows) and GAM (green curve and arrows) with seasonal and flow covariates (“flowseas”). Full plot details are explained in Section 8.5 and Table 4.

21. Waitoa River @ Landsdowne Rd Br (1249_15/1249_38)

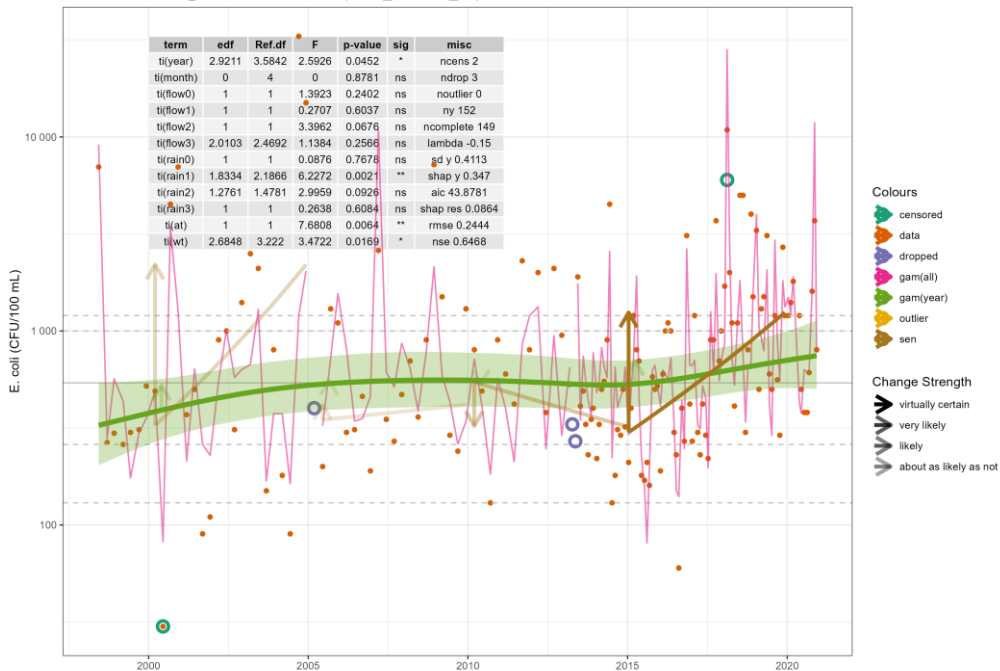


Figure 31: Trends and 5-year changes in *E. coli* concentrations from the Waitoa River at Landsdowne Road (seasonal, flow, rain and temperature adjustment). Flow-adjusted seasonal Sen slope (brown line segments and arrows) and GAM (green curve and arrows) with seasonal, flow, rain, air temperature (at) and water temperature (wt) covariates (“allgam”). Full plot details are explained in Section 8.5 and Table 4.

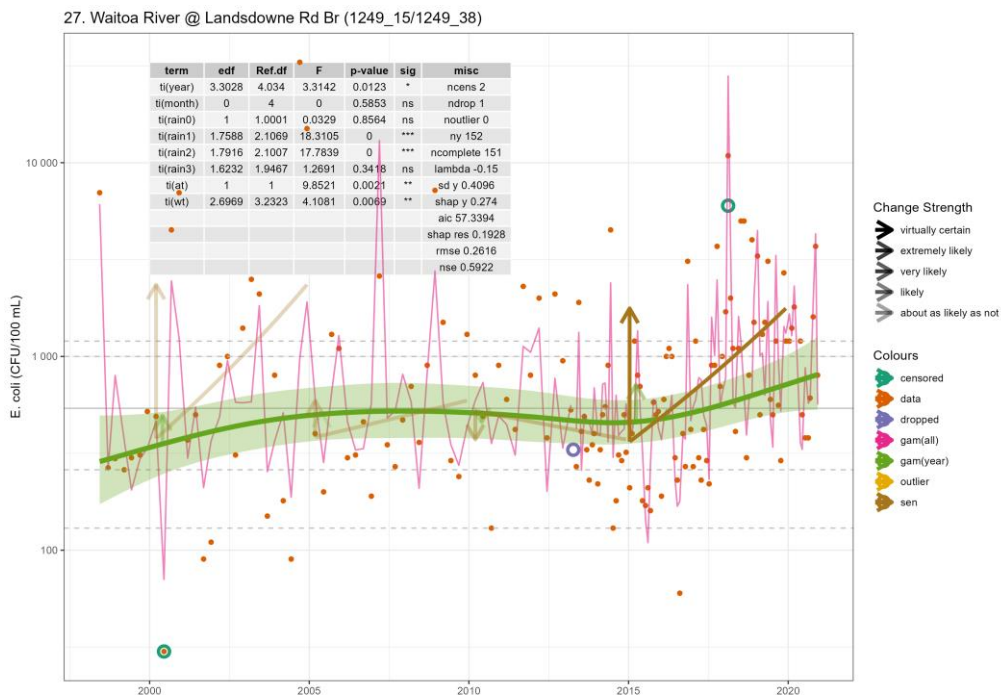


Figure 32: Trends and 5-year changes in *E. coli* concentrations from the Waitoa River at Landsdowne Road (seasonal, rain and temperature adjustment). Seasonal Sen slope (brown line segments and arrows) and GAM (green curve and arrows) with seasonal, rain, air temperature (at) and water temperature (wt) covariates (“raingam”). Full plot details are explained in Section 8.5 and Table 4.

8.7 *E. coli* trends for all sites

Sen slope and GAM trend analysis was carried out for all 82 catchments for the “none”, “seas” and “raingam” methods, and for the 56 catchments with index-of-flow data for the “flow”, “flowseas” and “all gam” methods (Sections 8.1 to 8.6). The analysis was carried out on the Box-Cox transformed data (Section 6.4), and the Sen slope and GAM trend estimates were then back-transformed and expressed in relative change units (percentage increase per year across each 5-year period).

Collecting the trend estimates from the Sen slope and GAM approaches for the Waikato River and for each subregion of the Waikato region, we can see the differences between methods and time periods at each site.

These results are summarised in Figure 33A-H (consisting of 8 sets of plots) for:

- The main Waikato River sites (ordered from south to north along the river).
- Tributaries to the lower Waikato River.
- Tributaries to the upper Waikato River.
- Inflows to Lake Taupo.
- Waipa River and tributaries.

- F. Hauraki.
- G. Coromandel.
- H. West Coast.

In each set of plots the Sen slope and GAM trend estimates at each site are plotted for each period (2000-2004, 2005-2009, 2010-2014, 2015-2019) and each covariate model (“none”, “seas”, “raingam”, “flow”, “flowseas”, “allgam”).

Within each subplot:

- The GAM trend estimates for each covariate model (“none”, “seas”, “raingam”, “flow”, “flowseas”, “allgam”) are shown as filled circles. The y-axis position of the centre of this circle is the estimated *E. coli* trend for that period (% increase in *E. coli* concentration per year).
- The corresponding Sen slope trend estimates (“none”, “seas”, “flow”, “flowseas”) are shown as open squares (i.e., the middle/largest of the three squares). The y-axis position of the centre of this square is the estimated *E. coli* trend for that period (% increase in *E. coli* concentration per year).
- The size of these symbols (the central symbol in the case of the Sen slope markers) shows the Strength of Evidence that the estimated trend is positive or negative as shown (McBride, 2019); e.g., “virtually certain to be positive”.
- The 90% credible interval for each GAM trend estimate is shown by a vertical line segment (these tend to be very short when the trend estimate has a high strength of evidence). These represent the range of trend slopes that is supported by the data (with the top and bottom 5% removed).
- The 90% credible interval for each Sen slope trend estimate is shown by two small squares (truncated to the plot window if necessary). These represent the range of trend slopes that is supported by the data (with the top and bottom 5% removed).
- The horizontal dotted line marks the x-axis.

These plots make it easy to compare trend estimates (and uncertainty) between time periods, between covariate models, and between GAM and Sen slope approaches.

Several general results are apparent from these plots:

1. Overall, GAM gives similar direction of trend to Sen Slope.
2. GAM trend estimates were generally very similar across the 6 covariate models. Although including covariates increased model fit substantially (i.e., explained short term variation in the data, Section 8.10), **the long-term trend was not accounted for by the covariates. Additional covariates need to be identified for inclusion in the model to fully explain the observed trend.**

3. Sen slope estimates (squares) tend to exaggerate the trend compared with GAM models (circles). This is partly because we are using Sen slope analysis with less than the recommended amount of data (Section 8.1), and partly because the GAM models, by taking into account the entire data set simultaneously, are less prone to “end effects” in each 5-year window.
4. Seasonal Sen slope analysis tends to have greater uncertainty than non-seasonal Sen slope analysis. This is because of the smaller number of slopes compared in seasonal Sen analysis.
5. Sen slope and GAM analysis both indicated that most sites have increasing/accelerating trends for *E. coli* concentrations (even after covariate adjustment), particularly in the 2015-2019 period. This is still the case in the models which have adjusted for season, rain, flow and other covariates. **That is, the increasing trend in *E. coli* from about 2015 is not explained by the covariates we have considered here.**
6. The rain + temperature models (“raingam”) give similar results to the rain + flow + temperature models (“allgam”) but do not require flow data (which is not always available). This suggests that rain is a useful proxy for flow.

Figure 34 summarises the statistical significance of the different terms in the different GAM models. These indicate the probability that the term is not zero. They do not however directly indicate the importance of the term (e.g., the proportion of the model variance explained by each term). The following general observations can be made:

1. The “month” term, accounting for seasonality, was generally only significant in the “seas” and “flowseas” models. Inclusion of temperature and rainfall, both of which (particularly the former) are strongly seasonal, tended to reduce the significance of month *per se*.
2. Flow0 (i.e., flow(t-0)) was usually a significant covariate in the “flow” and “flowseas” models, but lagged flow (flow1, flow2, flow3) were usually *not* significant. The addition of rain in the “allgam” models reduced the significance of flow0, which suggests that flow and rain provide similar information.
3. The air temperature terms (in the “raingam” and “allgam” models) were rarely statistically significant. The water temperature terms (in the “raingam” and “allgam” models) were also generally not statistically significant—suggesting that air and water temperature at time of (or up to 3 days prior to) sampling are not important explanatory variables. **Air and water temperatures in a longer time window might be important in explaining *E. coli* measurements however and should be explored in future work.**
4. Rain1 (i.e., rain(t-1)) was the most significant rain term in the “raingam” and “allgam” models. Rain on the day of sampling (rain0) was not usually significant. Rain2 was also significant in some catchments. That is, lagged rain is a useful predictor, and can substitute for flow where this is not readily available.

Figure 33A

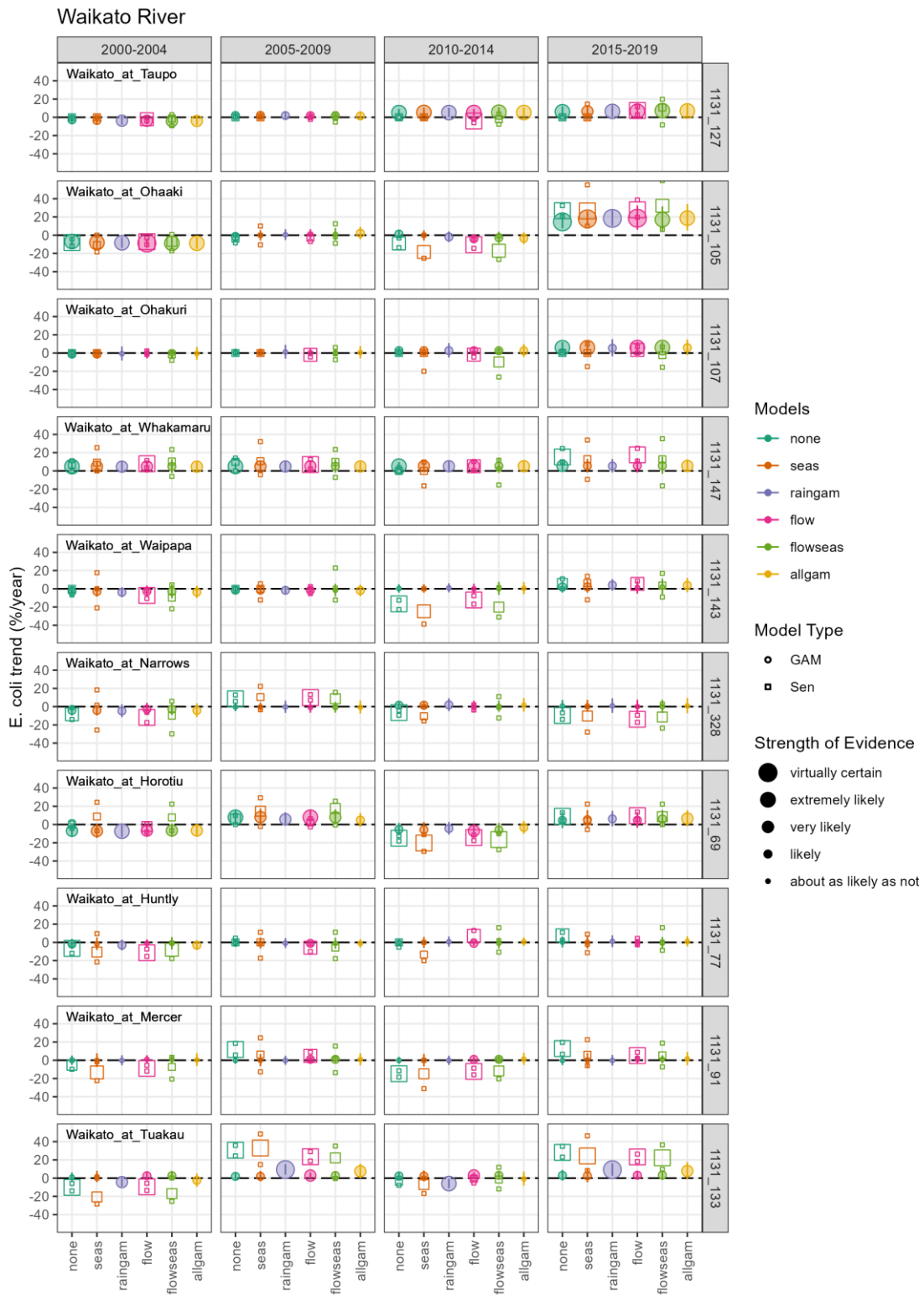


Figure 33B

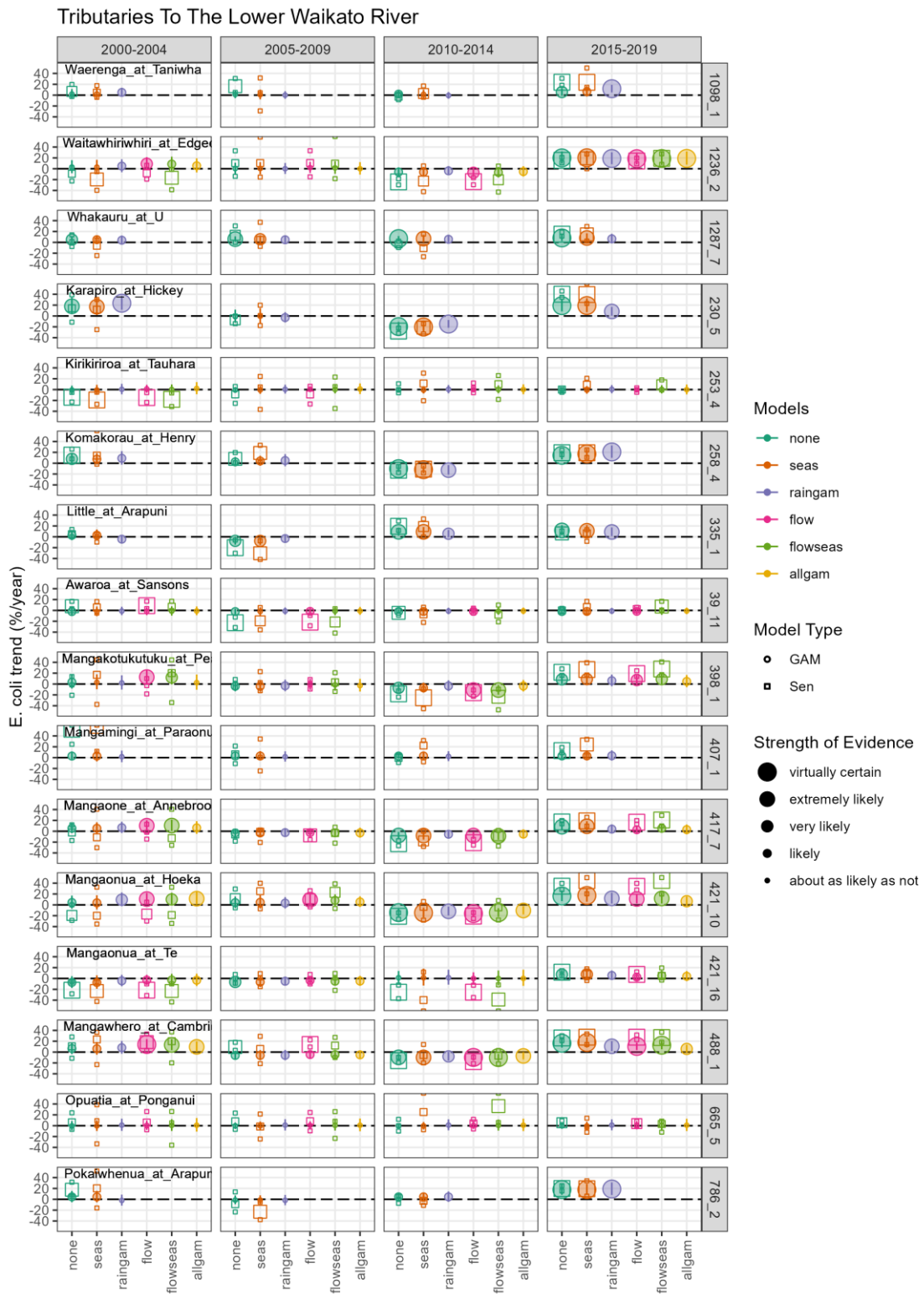


Figure 33C

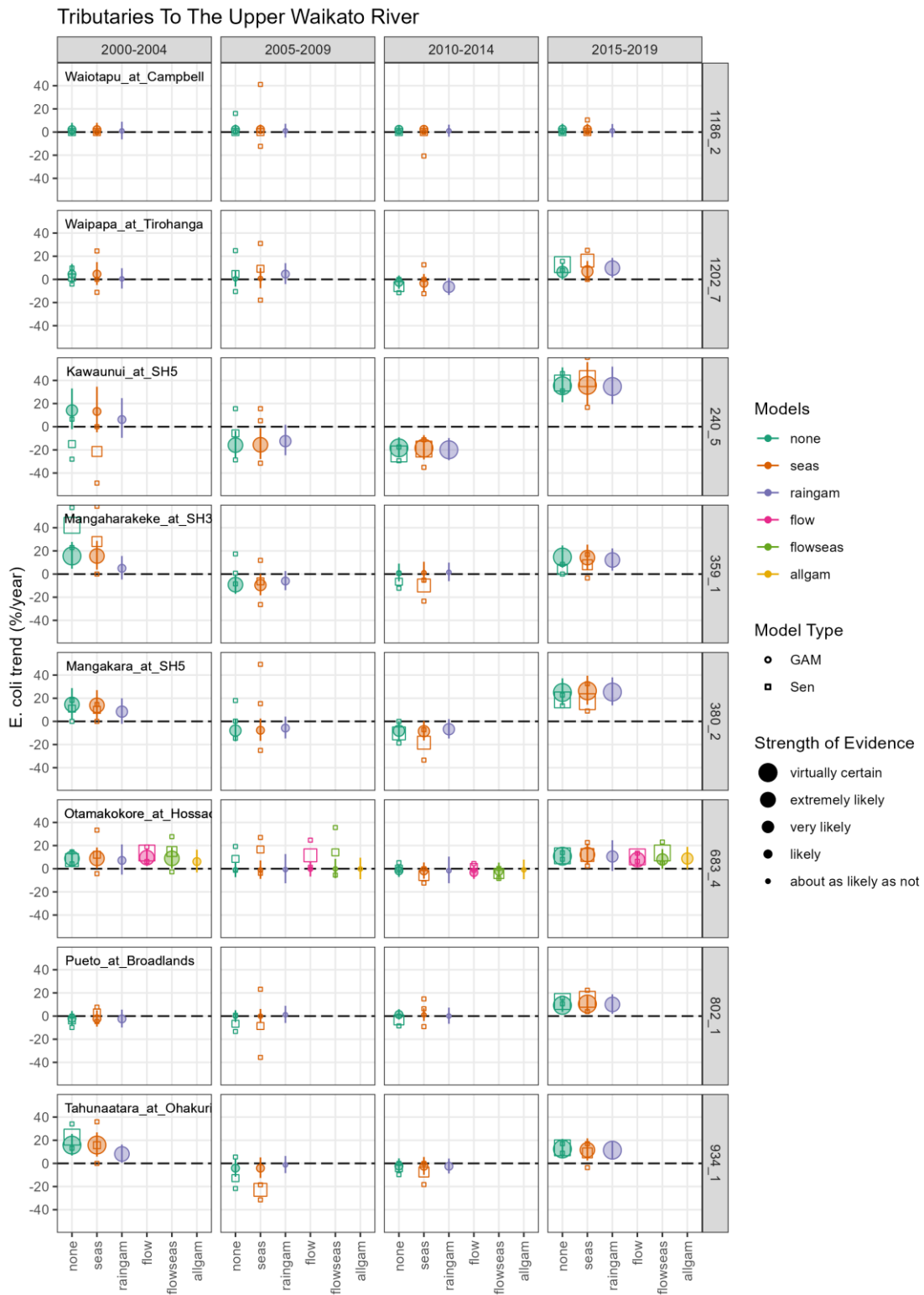


Figure 33D

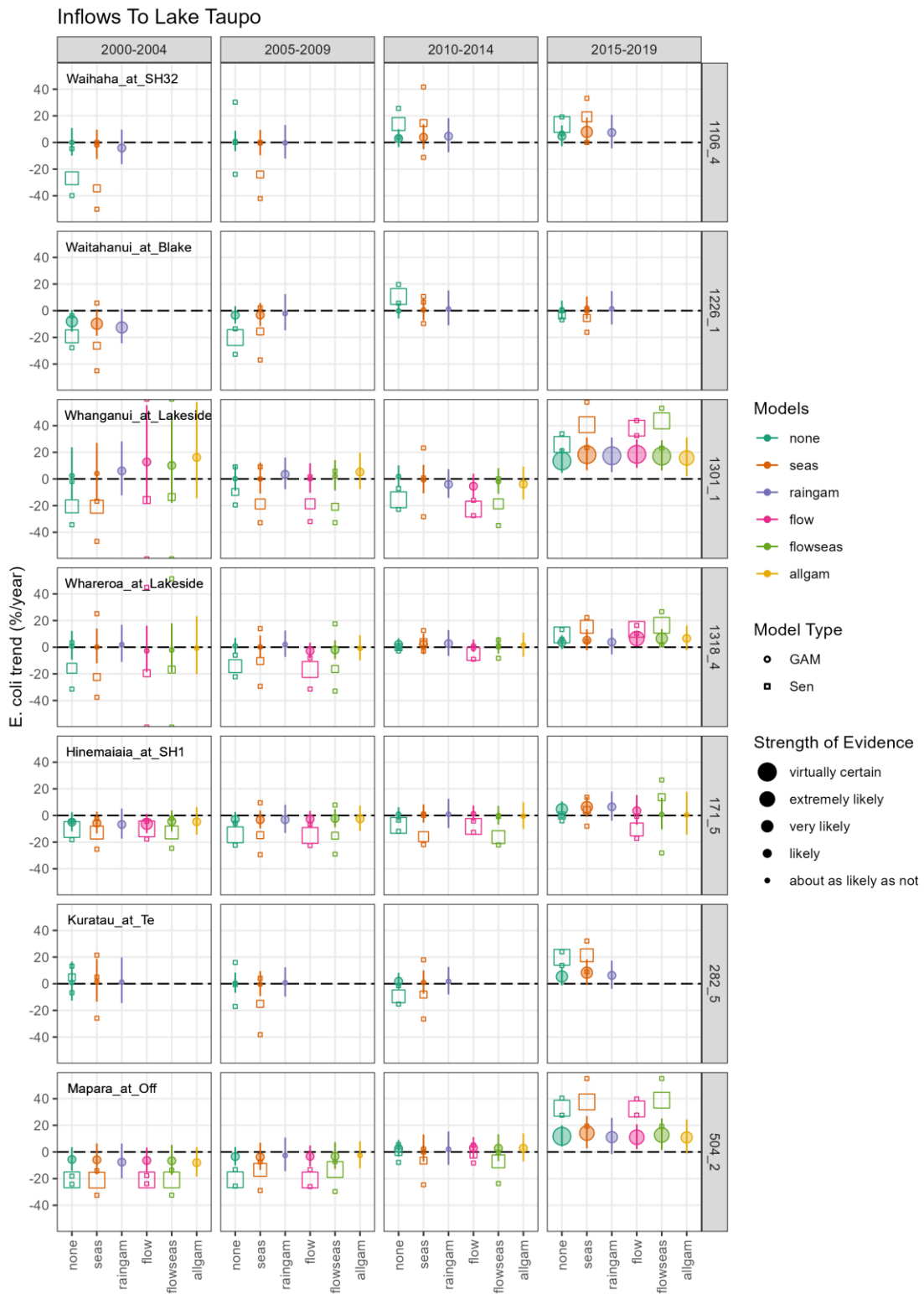


Figure 33E

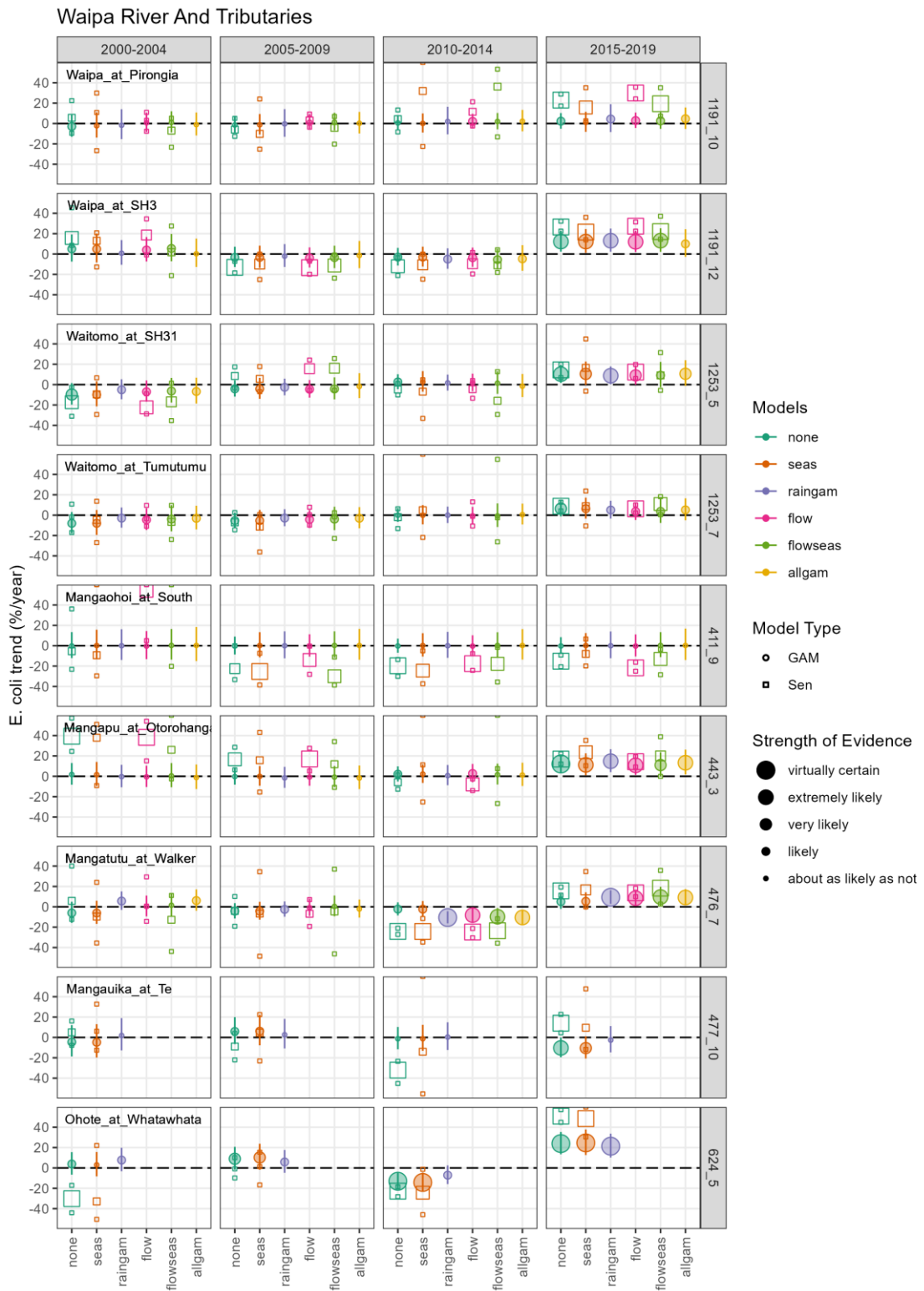


Figure 33F

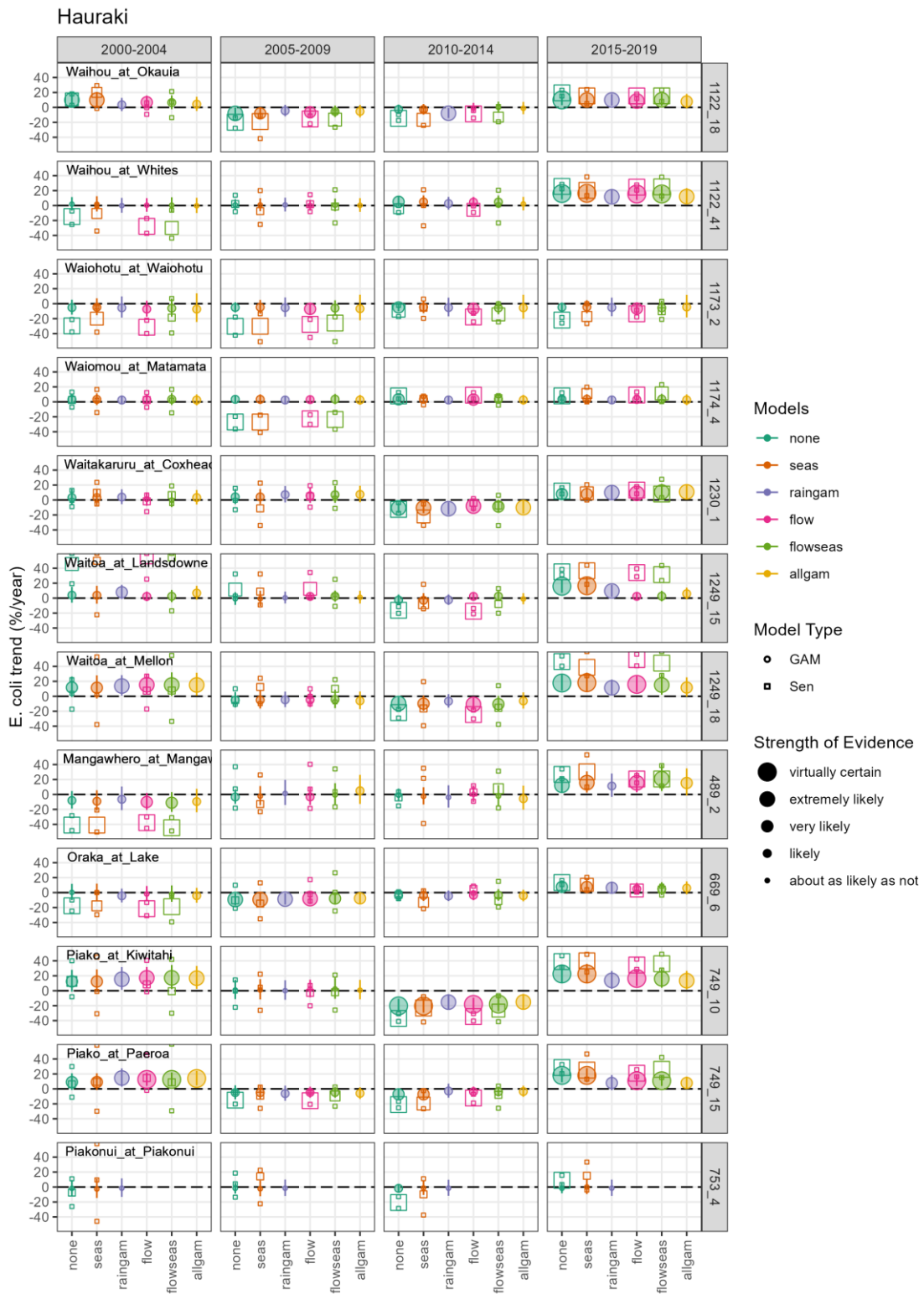


Figure 33G

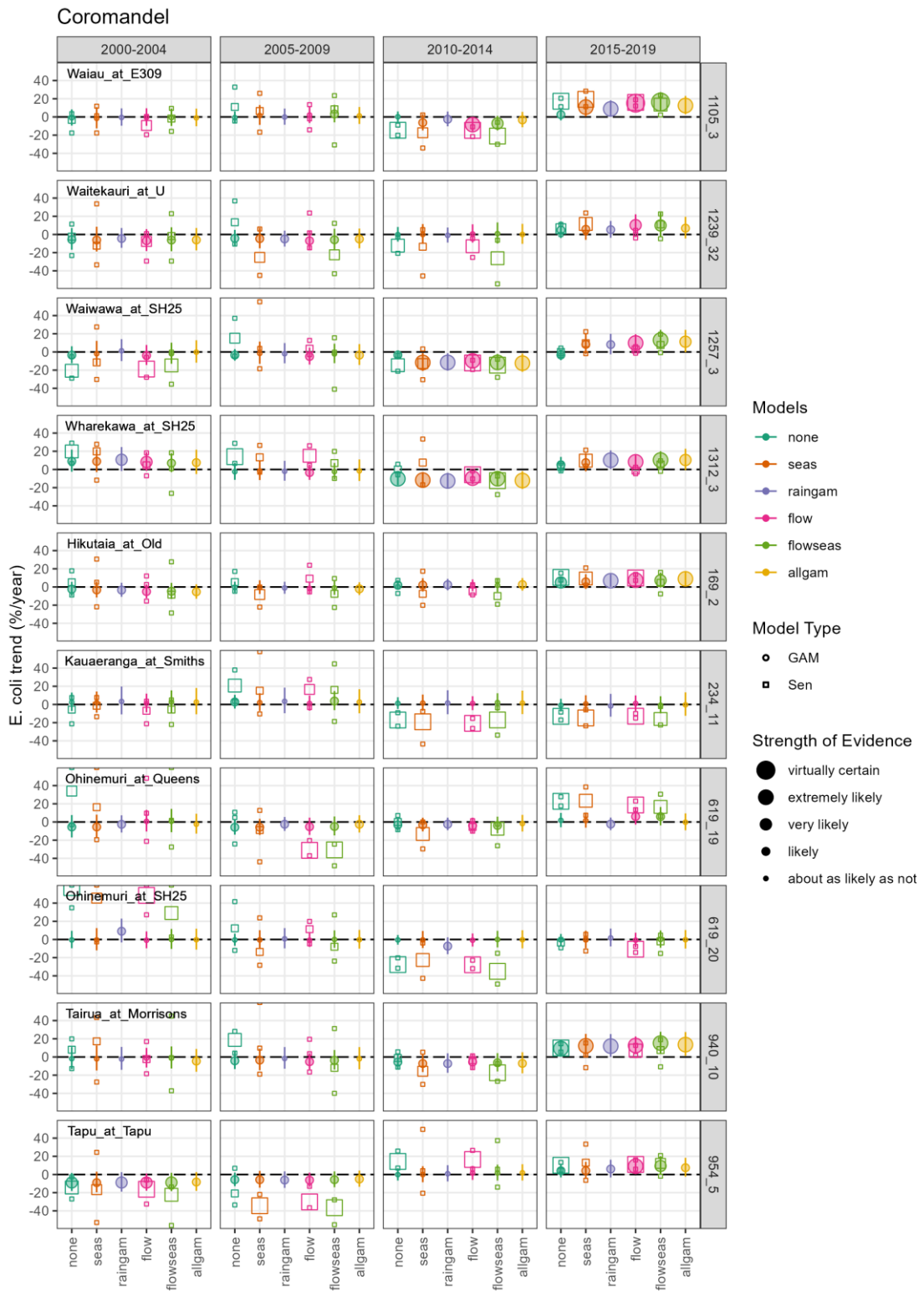


Figure 33H

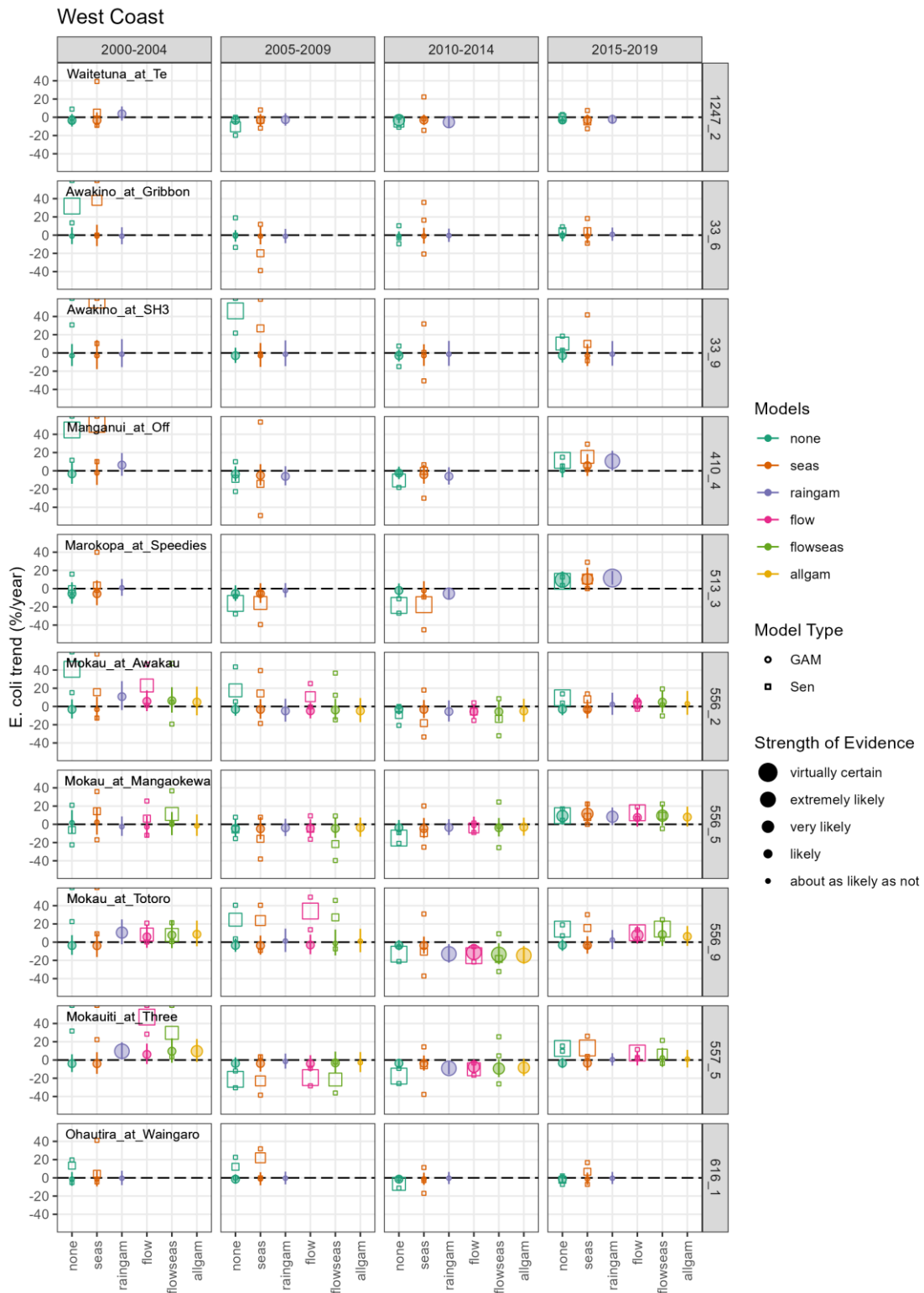


Figure 33: Five-year trends in *E. coli* concentration (% increase/year) in the Waikato River and regional streams according to subcatchment groupings. Groups A-H are defined on page 63. Trends estimated using Sen slope (squares) and GAM (circles) methods with different covariate corrections. Strength of evidence for trend sign is indicated by the size of the symbols, and uncertainty (90% credible intervals) by the small squares/vertical lines respectively. Further details are given in Section 8.7 (page 63).

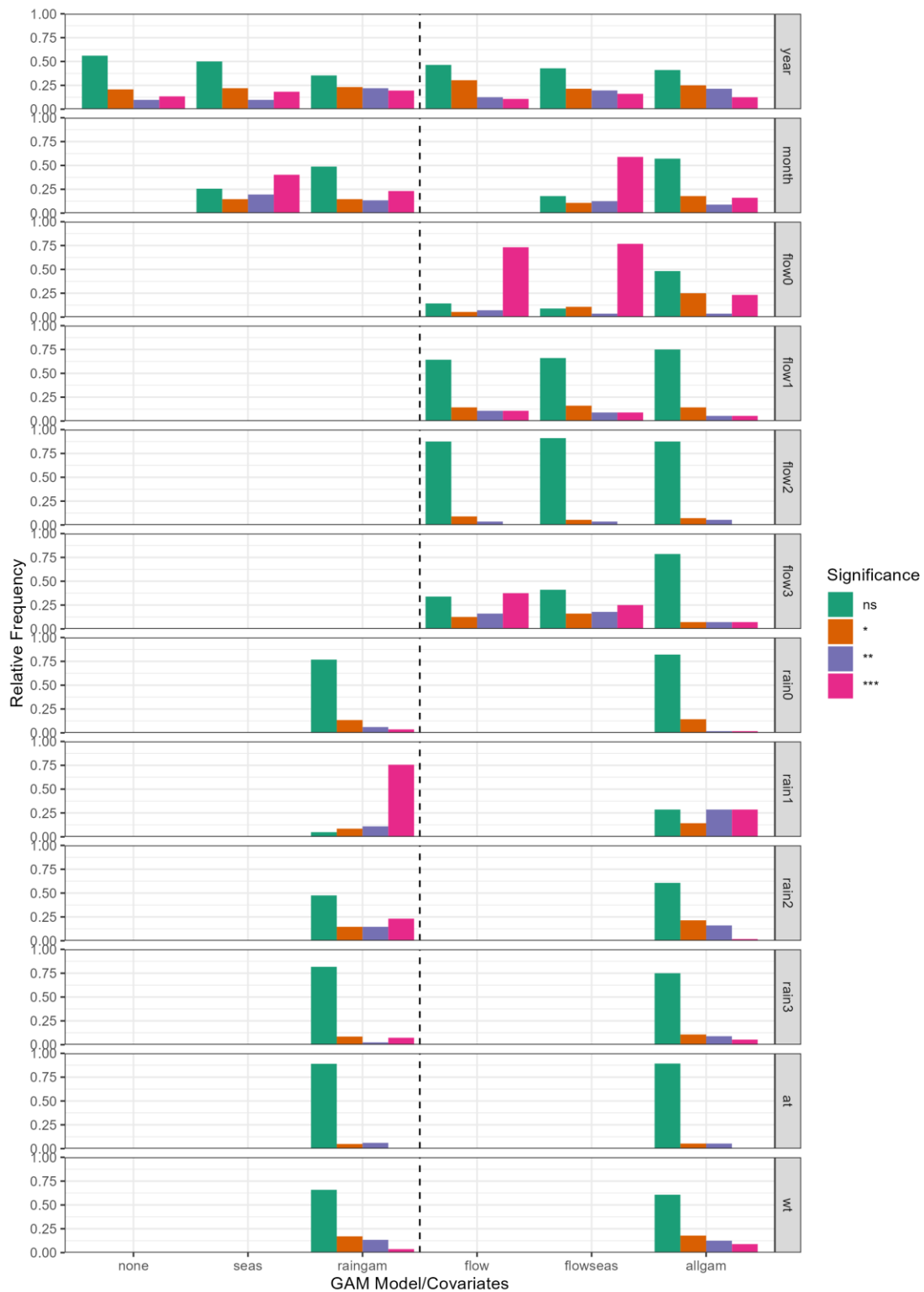


Figure 34: Summary of statistical significance of GAM covariate terms.

8.8 *E. coli* trends by subregion

The Sen slope and GAM trend estimates from Figure 33 are summarised in Figure 35 and Figure 36, respectively, for each of the 8 subregions. Results for “none”, “seas” and “raingam” are available for all 82 sites, but results for “flow”, “flowseas” and “allgam” are only available for the 56 sites with index-of-flow data available at nearby sites.

Figure 35 shows that the Sen slope estimates may have large magnitude, low strength of evidence, and considerable variability within a subregion, especially in the 2000-2004 and 2005-2009 periods. This is partly a consequence of the Thiel-Sen approach not being well-suited to use with less than 5 years of monthly data. Nevertheless, the general pattern of downward trends in *E. coli* (improving water quality) in 2010-2014 followed by upward trends in *E. coli* (deteriorating water quality) in 2015-2019 is apparent. For example, Seasonal Sen slopes (“seas” model) were negative (improving) in 2010-2014 at 59 of 82 (72%) of sites, with a median trend of -9% per year, but positive (deteriorating) in 2015-2019 at 69 of 82 (84%) of sites, with a median trend of +13% per year.

The GAM trend estimates in Figure 36 gave similar but more consistent results. For example, GAM slopes (“raingam” model) were negative (improving) in 2010-2014 at 39 of 82 (48%) of sites, with a median trend of -2% per year, but positive (deteriorating) in 2015-2019 at 60 of 82 (73%) of sites, with a median trend of +7% per year. The following general observations can be made:

- The six GAM models all gave similar trend estimates, regardless of which covariates were accounted for.
- There is strong evidence for a region-wide ‘up-swing’ in stream *E. coli* concentrations in the 2015-2019 period, even after accounting for covariates. This includes the Lake Taupo streams, which generally did not show strong trends in the earlier time periods.
- This was preceded by a period of generally decreasing trends in the period 2010-2014, although this had a smaller magnitude than the increase in 2015-2019.
- In earlier periods there were less pronounced and more variable trends.

8.9 *E. coli* trends overall summary

The *E. coli* trends for the Waikato region are summarised in Table 5 and Table 6 for the Thiel-Sen and GAM methods respectively (as shown in Figure 35 and Figure 36). For each five-year period and each set of covariate adjustments, the number of sites classified as having likely negative, indeterminate, or likely positive trends is shown. A likely trend was defined as one having a 66% or greater Strength of Evidence. The overall median trend slope (%/year) is given, as well as the median slope for each classification.

The number and magnitude of negative and positive trends were roughly equal in 2000-2004, according to both analysis methods. Water quality began to improve in 2005-2009 (predominance of negative trends). This was less marked in the Thiel-Sen results compared with the GAM results, possibly due to the low frequency of water quality samples at this time (prior to 2013, *E. coli* measurements were only taken four times a year). Negative trends (improving water quality) continued to dominate in 2010-2014, while positive trends (deteriorating water quality) dominated in 2015-2019, as previously noted.

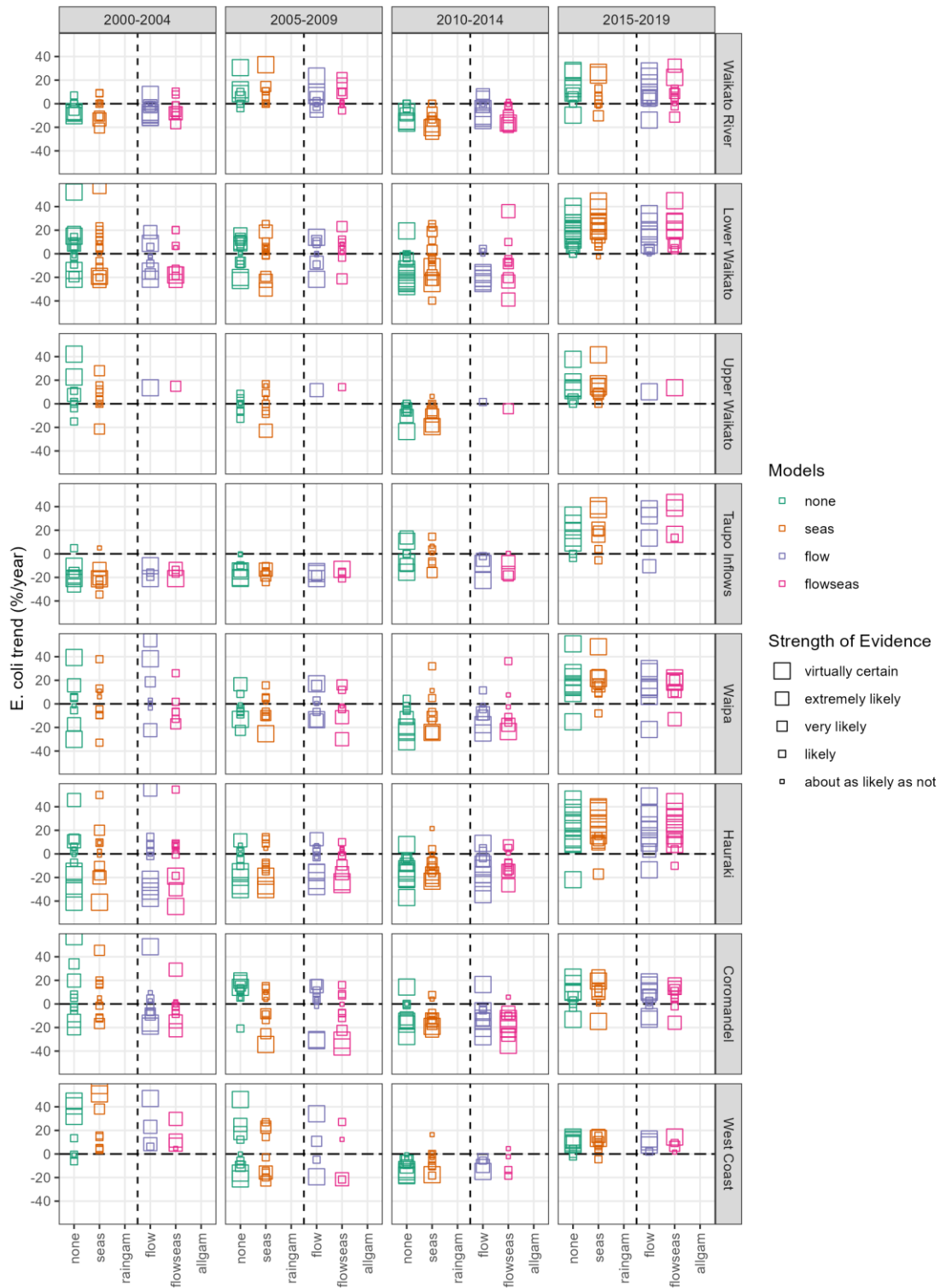


Figure 35: Summary of 5-year trends in *E. coli* concentration (% increase/year) by subregion (Thiel-Sen Slope Estimator). Estimated using the Thiel-Sen Slope Estimator with or without seasonal and/or flow adjustment. Strength of evidence for trend sign is indicated by the size of the symbols. Further details are given in Section 8.7.

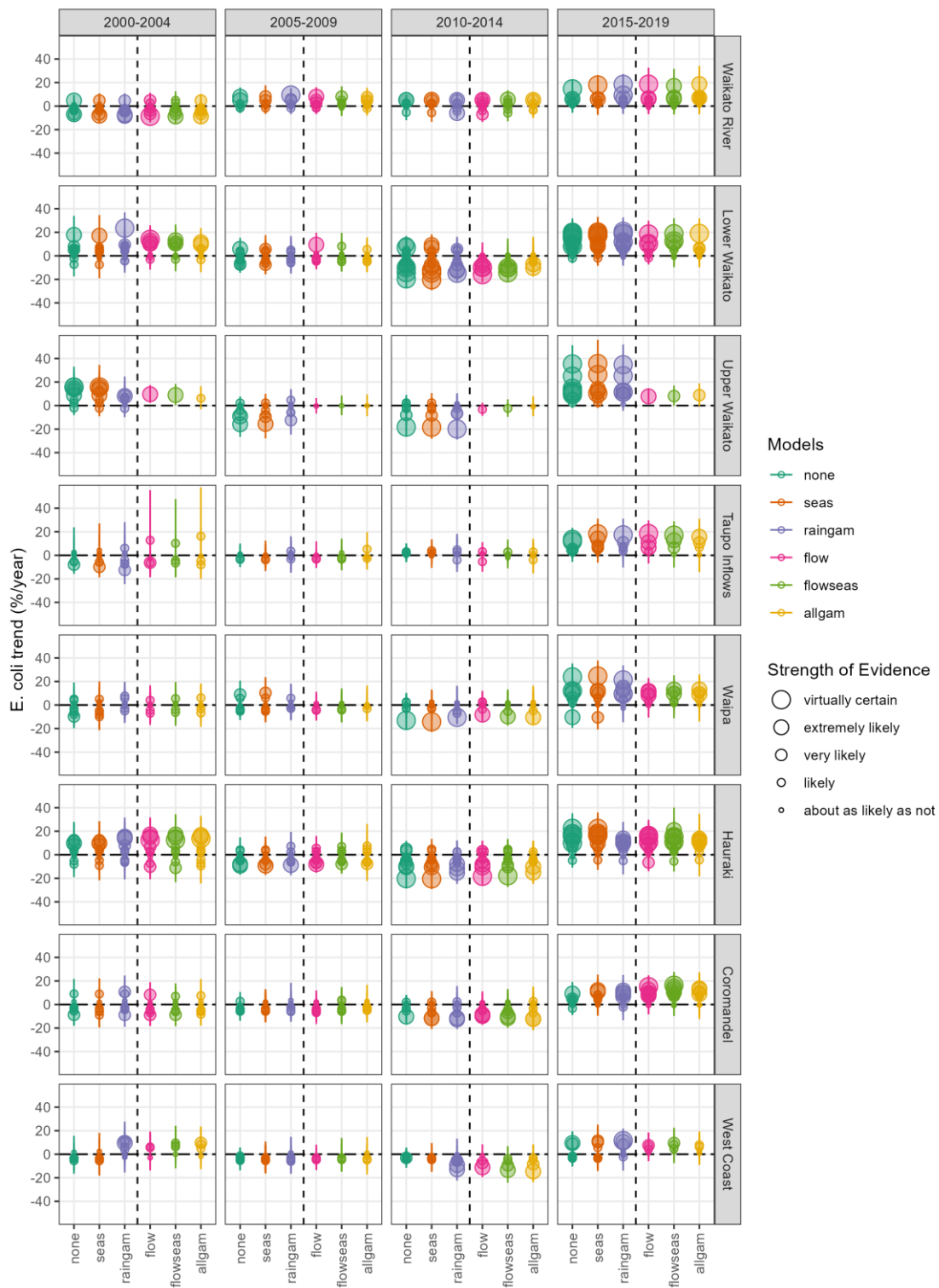


Figure 36: Summary of 5-year trends in *E. coli* concentration (% increase/year) by subregion (GAM). Strength of evidence for trend sign is indicated by the size of the symbols, and uncertainty (90% credible intervals) by the vertical lines. Further details are given in Section 8.7.

Figure 37 and Figure 38 map the distribution of upward *E. coli* trends across the Waikato region for the 2015-2019 period using Seasonal Sen (“seas”) and rainfall-adjusted GAM (“raingam”) models respectively. These correspond to the “seas” values from Figure 35 and the “raingam” values from Figure 36 for 2015-2019. The predominance and strength of increasing *E. coli* (red) trends is clear in both analyses, in all subregions across the Waikato. There is no obvious spatial pattern, indicating that the increasing trends of interest are found in all subregions. Since land use varies considerably between subregions, this means that the observed trends are unlikely to be linked to land use. Instead the cause must be one that affects all subregions, such as climate or microbial measurement methodology.

Table 5: Summary of Waikato *E. coli* trends (%/year) assessed using Thiel-Sen analysis. N = total number of sites, N>0, N=0, N<0 = number of sites with likely positive, indeterminate and likely negative trends respectively. Med = median trend (%/year), Med<0, Med = 0, Med >0 = median trend (%/year) of sites with likely positive, indeterminate and likely negative trends respectively. Individual values are plotted in Figure 35.

Period	Adjust	N	N<0	N=0	N>0	Med	Med<0	Med=0	Med>0
2000-2004	none	82	33	6	38	0	-0.142	-0.008	0.130
	seas	82	30	14	35	0.027	-0.172	0.023	0.157
	flow	56	28	9	19	-0.022	-0.116	0.003	0.136
	flowseas	56	32	7	17	-0.018	-0.127	0.024	0.113
2005-2009	none	82	33	13	31	0	-0.105	0	0.115
	seas	82	39	13	25	0	-0.147	0.039	0.134
	flow	56	22	11	23	0.002	-0.152	0	0.107
	flowseas	56	25	15	16	-0.010	-0.152	0.010	0.119
2010-2014	none	82	60	6	6	-0.070	-0.131	0	0.122
	seas	82	54	12	11	-0.078	-0.138	0.025	0.113
	flow	56	43	4	9	-0.081	-0.122	-0.005	0.051
	flowseas	56	41	10	5	-0.099	-0.143	0.013	0.100
2015-2019	none	82	7	0	67	0.127	-0.097	-	0.143
	seas	82	6	4	69	0.131	-0.092	-0.011	0.154
	flow	56	7	3	46	0.107	-0.129	0	0.136
	flowseas	56	6	2	48	0.117	-0.107	0.009	0.137

E. coli Sen Trend 2015-2019

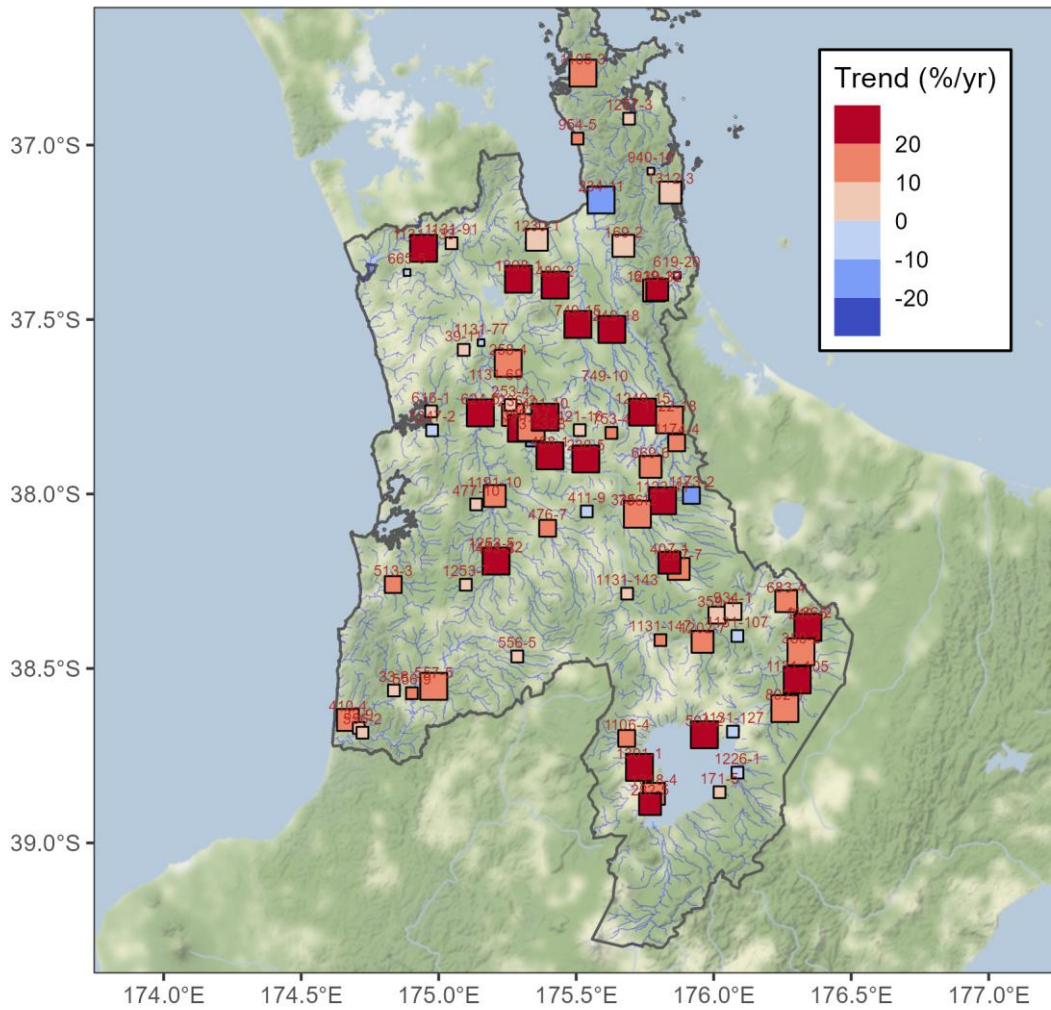


Figure 37: Map of 2015-2019 *E. coli* trends (%/year) assessed using Thiel-Sen analysis (with seasonal adjustment). Values shown are the 2015-2019 “seas” trends from Figure 35. Increasing trends are coloured red and decreasing trends are coloured blue. Symbol size indicates statistical Strength of Evidence, matching Figure 35. Note predominance of red (increasing trends).

Table 6: Summary of Waikato *E. coli* trends (%/year) assessed using GAM analysis. N = total number of sites, N>0, N=0, N<0 = number of sites with likely positive, indeterminate and likely negative trends respectively. Med = median trend (%/year), Med<0, Med = 0, Med >0 = median trend (%/year) of sites with likely positive, indeterminate and likely negative trends respectively. Individual values are plotted in Figure 36.

Period	Adjust	N	N<0	N=0	N>0	Med	Med<0	Med=0	Med>0
2000-2004	none	82	31	23	28	-0.002	-0.046	0	0.053
	seas	82	25	31	26	-0.002	-0.056	-0.004	0.059
	raingam	82	23	28	31	0.009	-0.044	-0.001	0.077
	flow	56	16	20	20	0.004	-0.063	-0.005	0.087
	flowseas	56	15	21	20	0.003	-0.061	0	0.088
	allgam	56	19	18	19	-0.003	-0.047	-0.003	0.068
2005-2009	none	82	39	29	14	-0.014	-0.042	-0.003	0.037
	seas	82	33	36	13	-0.013	-0.047	-0.004	0.041
	raingam	82	26	44	12	-0.012	-0.046	-0.002	0.048
	flow	56	28	19	9	-0.013	-0.043	0.001	0.030
	flowseas	56	21	24	11	-0.010	-0.043	-0.001	0.035
	allgam	56	18	28	10	-0.011	-0.048	-0.002	0.049
2010-2014	none	82	39	21	22	-0.010	-0.037	-0.001	0.026
	seas	82	36	31	15	-0.013	-0.059	-0.001	0.034
	raingam	82	39	31	12	-0.016	-0.060	0.007	0.036
	flow	56	27	18	11	-0.009	-0.073	0.003	0.030
	flowseas	56	25	22	9	-0.011	-0.072	0.002	0.031
	allgam	56	25	25	6	-0.011	-0.055	0.002	0.028
2015-2019	none	82	10	13	59	0.056	-0.032	-0.002	0.091
	seas	82	7	15	60	0.072	-0.035	0.001	0.101
	raingam	82	3	19	60	0.067	-0.023	0.005	0.095
	flow	56	2	10	44	0.070	-0.041	0.003	0.084
	flowseas	56	1	12	43	0.073	-0.056	0.002	0.095
	allgam	56	1	13	42	0.066	-0.044	0.004	0.079

E. coli GAM Trend 2015-2019

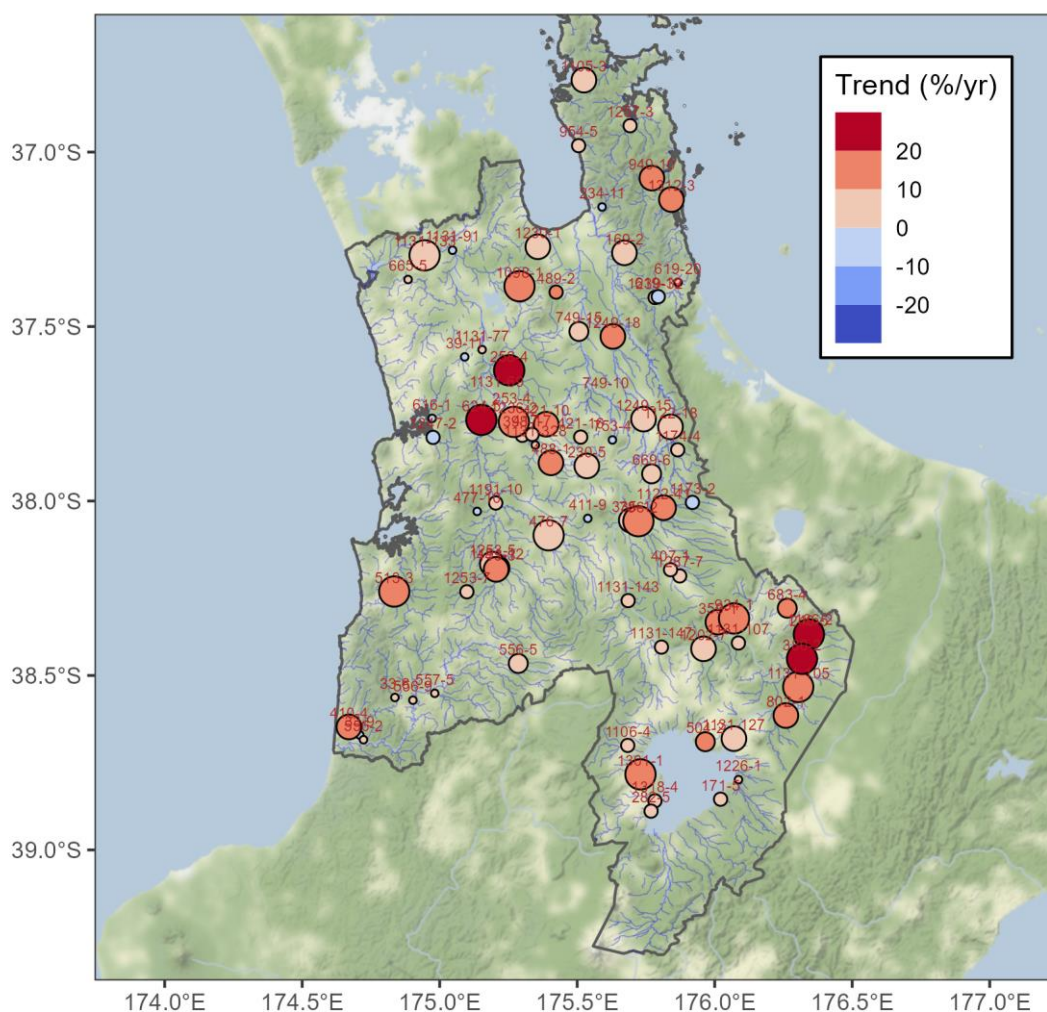


Figure 38: Map of 2015-2019 *E. coli* trends (%/year) assessed using a GAM model (seasonal, rain and temperature adjustment). Values shown are the 2015-2019 “raingam” trends from Figure 36. Increasing trends are coloured red and decreasing trends are coloured blue. Symbol size indicates statistical Strength of Evidence, matching Figure 36. Note predominance of red (increasing) trends.

8.10 Comparison of GAM Models

Performance statistics were collected for each GAM model (defined on page 49) as described in Table 4. The NSE statistic indicates the proportion of variance in the data that is explained by the model. Models with high NSE are desirable, since they more successfully explain the data in terms of covariates and any remaining trend (i.e., the “year” term). The unexplained portion of the variance ($1 - \text{NSE}$) is due to model inadequacy (e.g., missing covariates or interactions) plus measurement error (typically $\pm 33\%$ error or more for *E. coli* grab samples, Harmel et al. 2016). The trend represents slow changes with time due to anthropogenic or environmental processes that are not included in the model (e.g., land use, land or effluent management practices, wild mammal and bird populations).

Figure 39 summarises the goodness of fit (NSE) of the GAM models. GAM models using no covariates (i.e., only year), or only season and year (violin plots on the left hand side of Figure 39), did not

explain much of the variation in the data. Including rain and/or flow improved model explanatory power considerably. Interestingly, including rain and temperature (“raingam”, purple violin plot in Figure 39) gave very good explanatory power (median NSE around 50%)—second only to the all-inclusive GAM (“allgam”, yellow violin plot in Figure 39).

These results make the case for using a model such as “raingam” in the future, due its good explanatory power and because it reduces dependency on flow data.

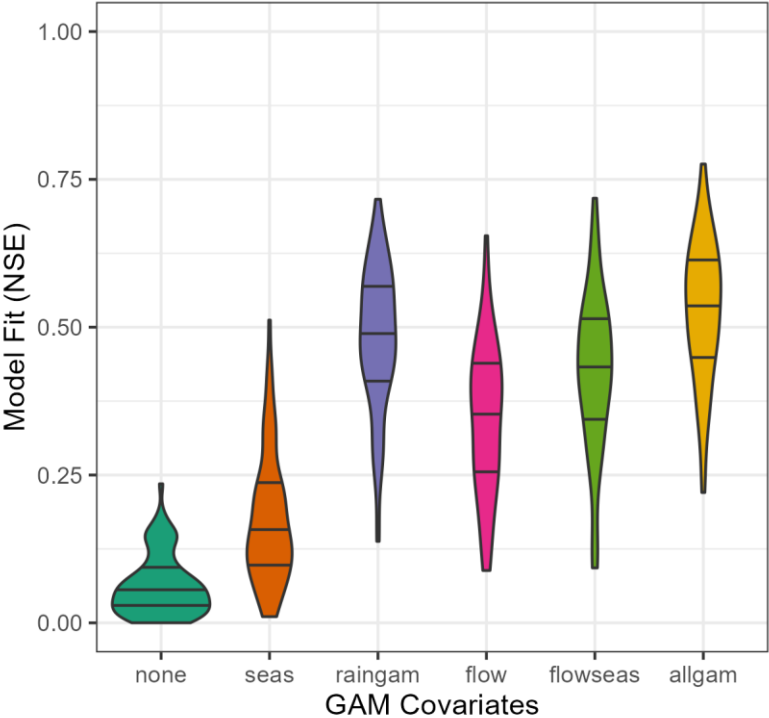


Figure 39: Comparison of model fit to *E. coli* data (NSE) for the GAM models with different covariates. This violin plot shows the range and distribution of NSE values, and the horizontal lines show the quartiles, for each model across all 82 sites (56 sites for the “flow”, “flowseas” and “allgam” models).

9 Turbidity and visual clarity trends in relation to *E. coli* trends

This section examines *E. coli* trends in relation to visual clarity and turbidity trends, to investigate whether these covariates might provide additional insight into *E. coli* trends and drivers.

Since *E. coli* measurement currently requires laboratory incubation and is relatively expensive, there is interest in finding proxy measurements that may be able to give rapid and potentially cheaper (although less accurate) estimates of faecal pollution in a water body. Two potential proxies are turbidity and visual clarity. Both of these water quality variables were measured alongside *E. coli* at the WRC sites.

Turbidity is often proposed as a possible proxy for *E. coli*, since mobilization of fine sediment and faecal bacteria are driven by similar processes (“co-mobilized”, Davies-Colley et al. 2018). Correlations between turbidity and *E. coli* at the WRC sites were shown in Figure 9.

Visual clarity may be an even better indicator for *E. coli* for various reasons including better reproducibility (Davies-Colley et al. 2018). Visual clarity measurements also have the advantage of being a ‘proper’ scientific quantity (measured in SI units) and relatively independent of the instrument used (e.g., black disk) (Davies-Colley et al. 2018). Correlations between visual clarity and *E. coli* at the WRC sites were shown in Figure 10. Unlike turbidity, visual clarity is negatively correlated with *E. coli*, with high values of clarity representing good water quality.

9.1 Waihou and Waitoa examples

Trends in turbidity and visual clarity trends, were analysed using the same methods as used for *E. coli*. For example, Figure 40 and Figure 41 show the estimated turbidity and visual clarity trends using the “raingam” GAM model and the seasonally corrected Sen slope analysis for the Waihou River at Whites Road, corresponding to the *E. coli* trends in Figure 25.

After taking season, rain and temperature into account, the temporal patterns in turbidity and visual clarity are quite different to the *E. coli* patterns over time (again, after taking season, rain and temperature into account). In Figure 25, *E. coli* remained fairly stable from 2000-2014 and then increased (deteriorated) from 2015-2019. Turbidity, in contrast (Figure 40), appears to have decreased (improved) from 2000-2004, increased (deteriorated) from 2005-2014, and then remained fairly stable from 2015-2019. Visual clarity patterns show a deterioration from 2005-2009 with fairly stable conditions in other periods, including 2015-2019. Neither turbidity nor visual clarity show strong deterioration in water quality in the 2015-2019 period (according to the GAM model, after taking season, rain and temperature into account) whereas *E. coli* deteriorated.

Similarly, Figure 42 and Figure 43 show the estimated turbidity and visual clarity trends (using the “raingam” GAM model) corresponding to the *E. coli* trends in Figure 32 for the Waitoa River at Landsdowne Road (site 1249_15 with associated flow site 1249_38). Again, turbidity and visual clarity patterns over time for the Waitoa River at Landsdowne Road are different to the *E. coli* patterns over time, after accounting for effects of rain, season and temperature. The temporal trend of *E. coli* (Figure 32), has weak evidence of changes from 2000-2014 and then deterioration from 2015-2019, whereas turbidity and clarity did not change over 2015-2019 after correction.

This suggests that *E. coli* have responded to a different set of drivers compared with turbidity and visual clarity over the 2015-2019 period. While *E. coli* and the optical variables are generally correlated (Section 7.1), due to the similar influence of factors such as rainfall, additional drivers appear to be having an influence in the more recent results.

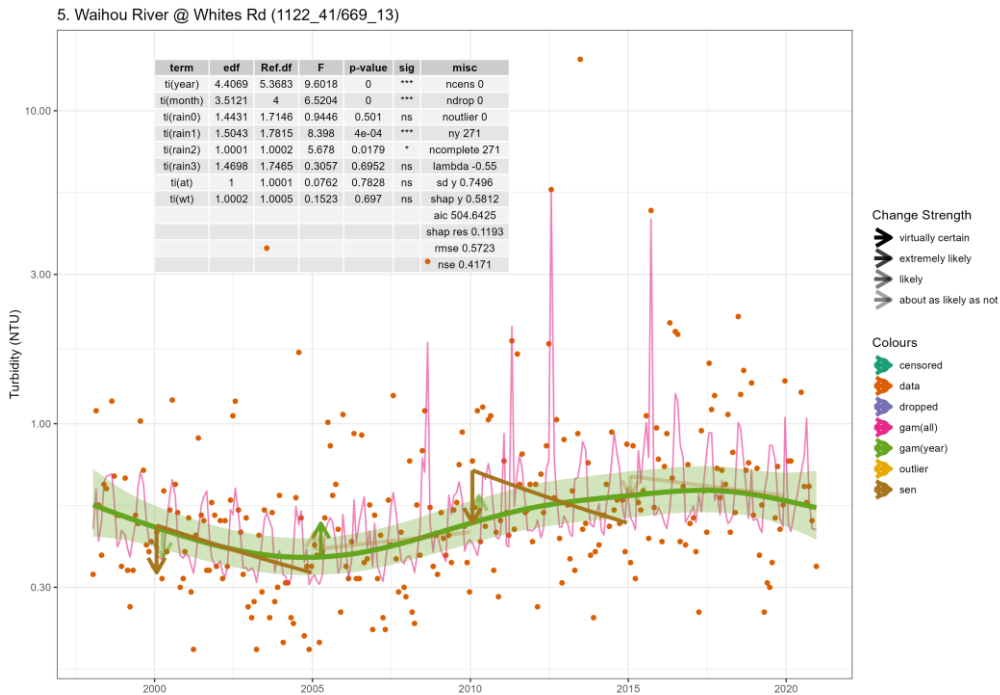


Figure 40: Trends and 5-year changes in Turbidity from the Waihou River at Whites Road (seasonal, rain and temperature adjustment). Seasonal Sen slope (brown line segments and arrows) and GAM (orange curve and arrows) with seasonal, rainfall, air temperature (at) and water temperature (wt) covariates (“raingam”). Full plot details are explained in Section 8.5 and Table 4.

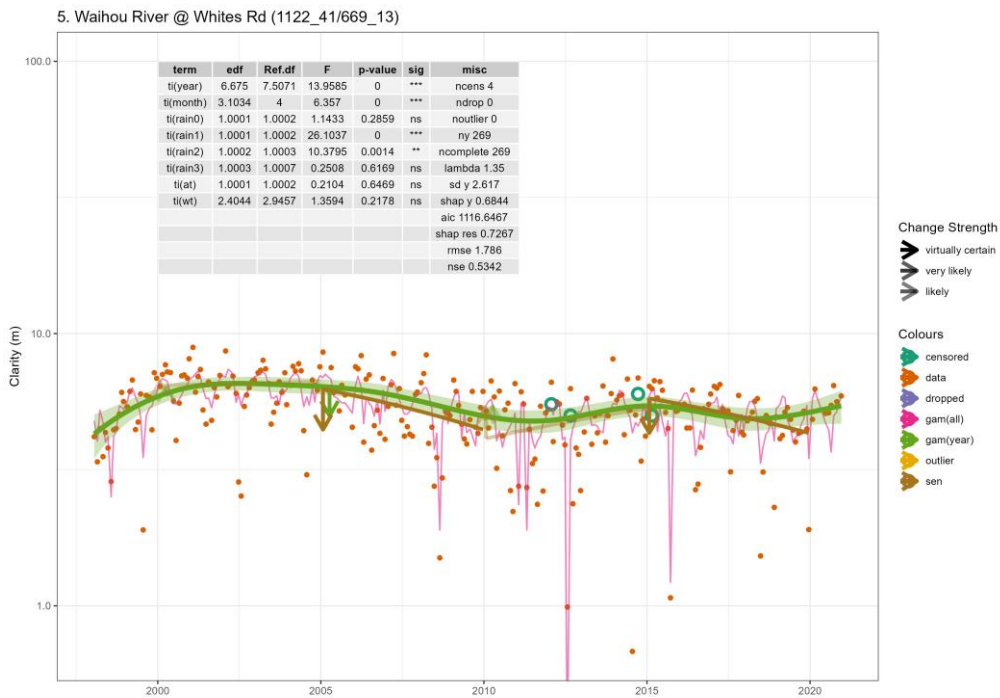


Figure 41: Trends and 5-year changes in visual clarity from the Waihou River at Whites Road (seasonal, rain and temperature adjustment). Seasonal Sen slope (orange line segments and arrows) and GAM (pink curve and arrows) with seasonal, rainfall, air temperature (at) and water temperature (wt) covariates (“raingam”). Full plot details are explained in Section 8.5 and Table 4.

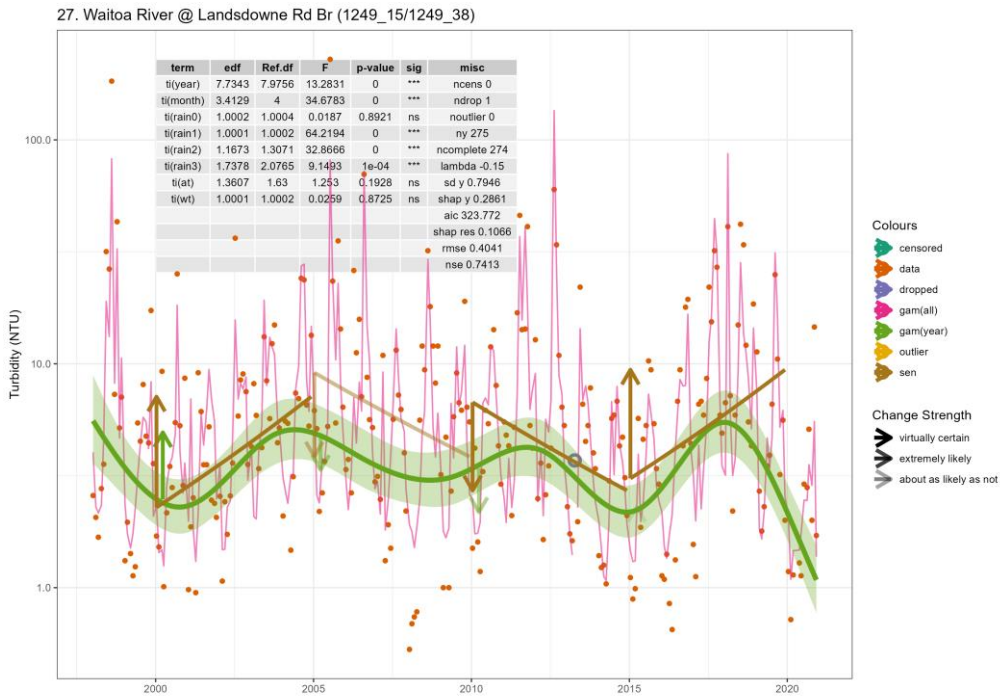


Figure 42: Trends and 5-year changes in Turbidity from the Waitoa River at Landsdowne Road (seasonal, rain and temperature adjustment). Seasonal Sen slope (brown line segments and arrows) and GAM (orange curve and arrows) with seasonal, rainfall, air temperature (at) and water temperature (wt) covariates (“raingam”). Full plot details are explained in Section 8.5 and Table 4.

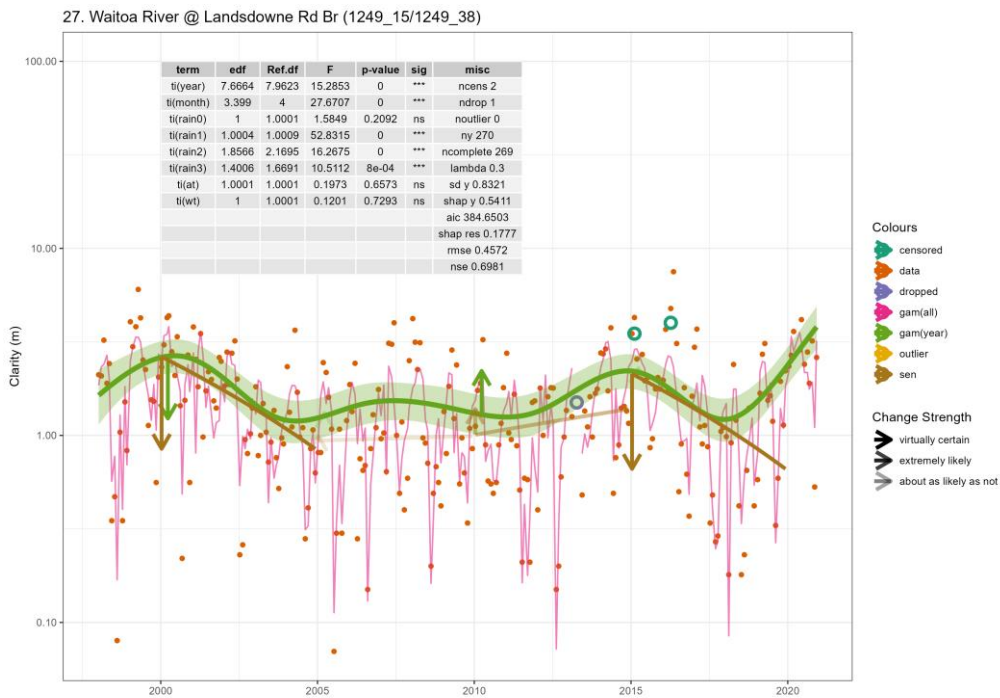


Figure 43: Trends and 5-year changes in Visual Clarity from the Waitoa River at Landsdowne Road (seasonal, rain and temperature adjustment). Seasonal Sen slope (orange line segments and arrows) and GAM (pink curve and arrows) with seasonal, rainfall, air temperature (at) and water temperature (wt) covariates (“raingam”). Full plot details are explained in Section 8.5 and Table 4.

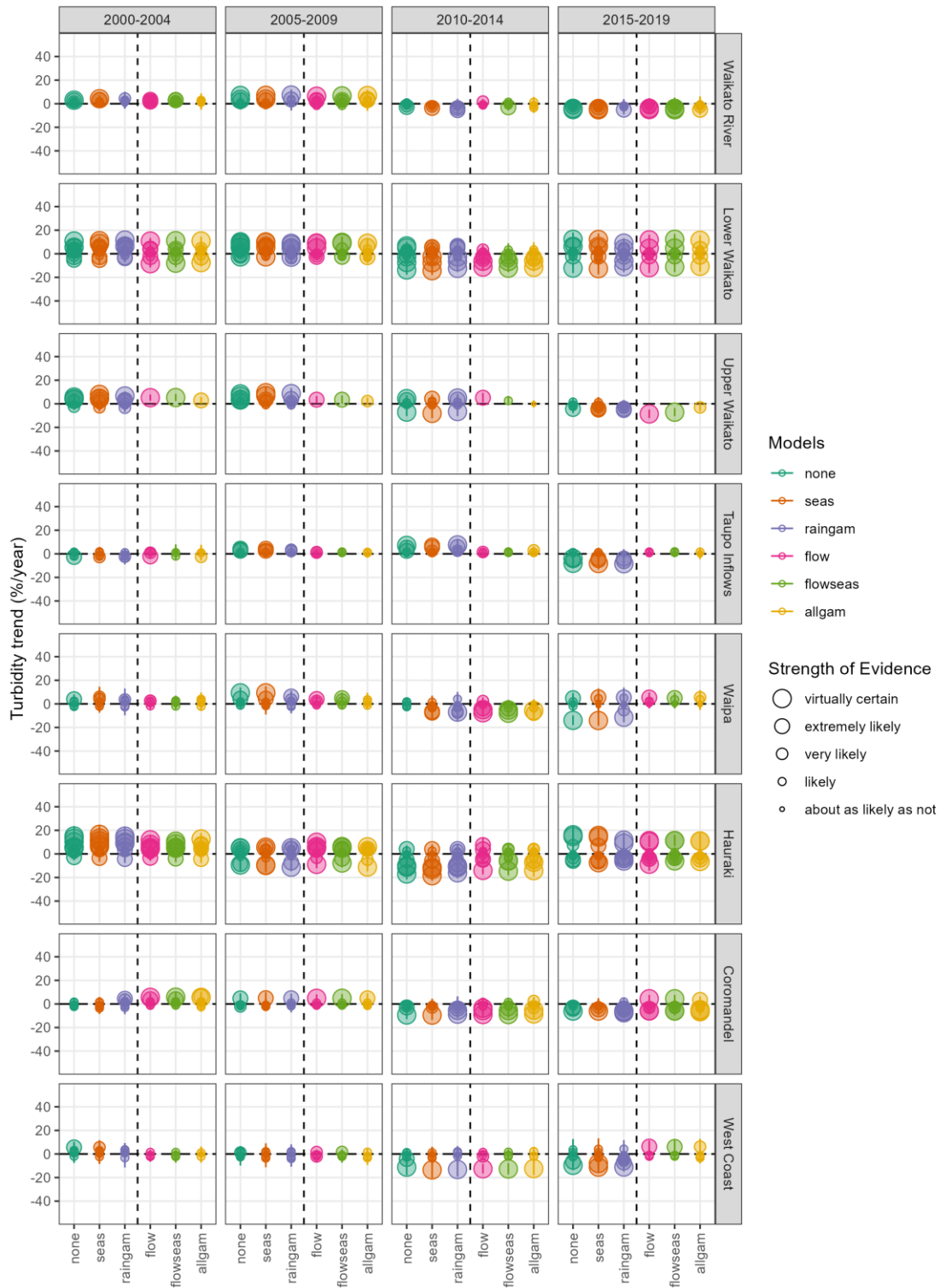


Figure 44: Summary of 5-year trends in Turbidity (% increase/year) by subregion (GAM). Strength of evidence for trend sign is indicated by the size of the symbols, and uncertainty (90% credible intervals) by the vertical lines. Further details are given in Section 8.7.

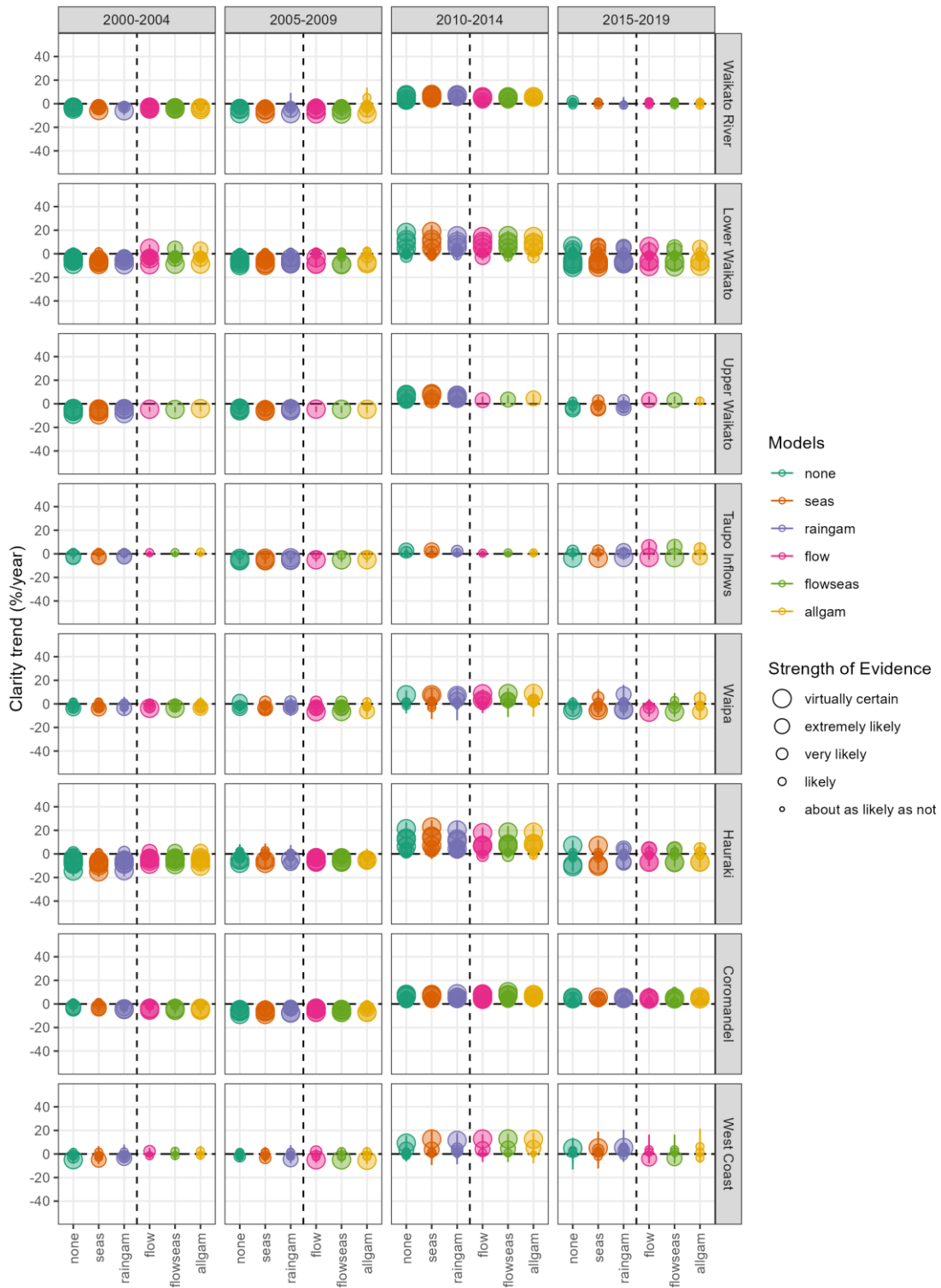


Figure 45: Summary of 5-year trends in Visual Clarity (%/year) by subregion (GAM). Strength of evidence for trend sign is indicated by the size of the symbols, and uncertainty (90% credible intervals) by the vertical lines. Further details are given in Section 8.7.

9.2 Trends for all sites and summary

The trend results from the GAM model for all sites are summarised in Figure 44 for turbidity and Figure 45 for visual clarity (analogous to Figure 36). It is apparent that overall, turbidity and visual clarity do not exhibit a notable deterioration in the 2015-2019; in contrast to *E. coli* which deteriorated over that period (after accounting for the covariates in the GAM models). However there does appear to be a widespread improvement in optical water quality in the 2010-2014 period, as previously noted for *E. coli*.

Maps of the 2015-2019 trend of turbidity and visual clarity are provided in Figure 46 and Figure 47 respectively, for comparison with Figure 38 for *E. coli*.

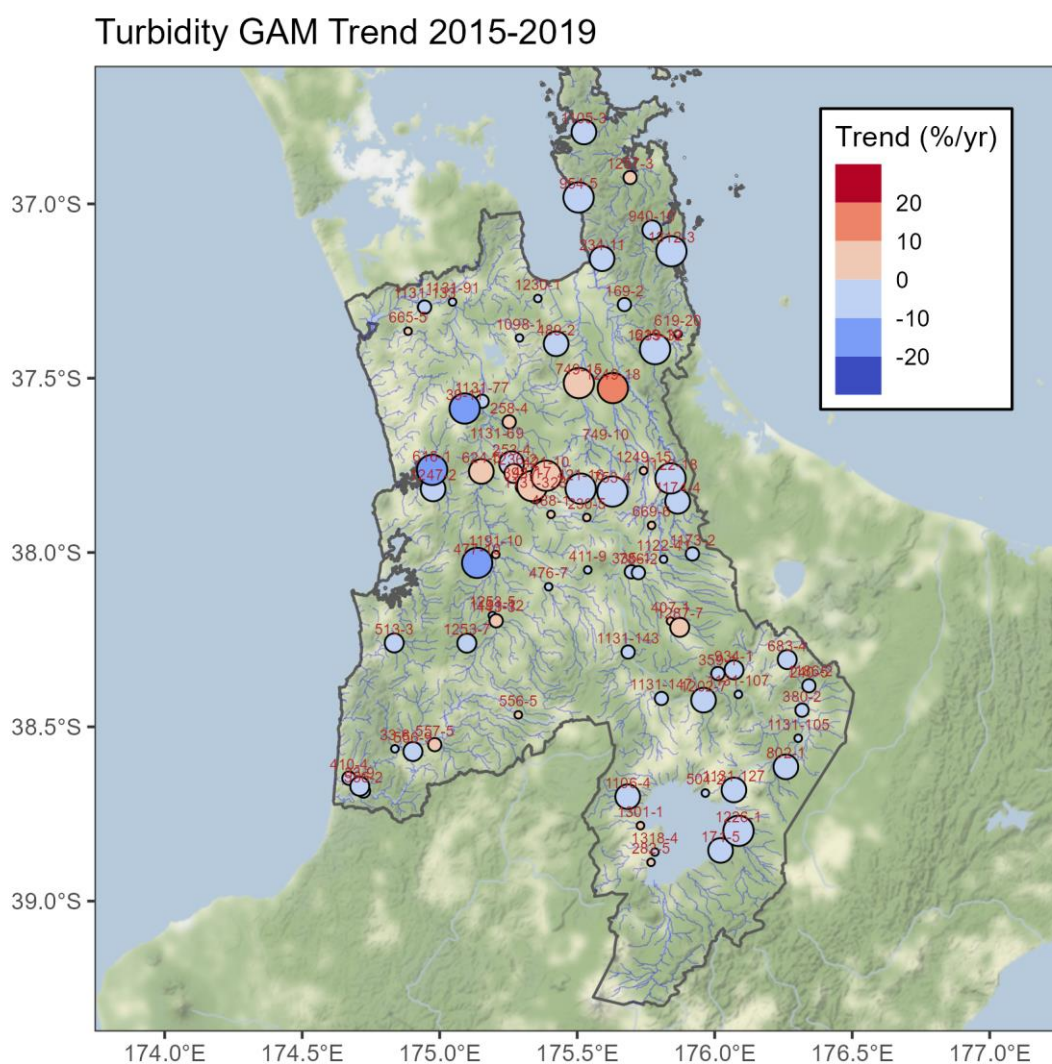


Figure 46: Map of 2015-2019 Turbidity trends (%/year) assessed using a GAM model (seasonal, rain and temperature adjustment). Values shown are the 2015-2019 “rainam” trends from Figure 44. Increasing trends are coloured red and decreasing trends are coloured blue. Circle size indicates statistical Strength of Evidence, matching Figure 44.

10 Interpretation of *E. coli* trends

Our application of both the traditional Mann-Kendall/Thiel-Sen trend detection method and the alternative GAM regression method showed that *E. coli* concentrations generally declined during the 2010-2014 period but have increased during the 2015-2019 period in most (73% of) catchments in the Waikato region (Figure 35 and Figure 36). These results agree with recent assessments by WRC (unpublished).

A key objective of this study was to identify potential drivers responsible for this increase, whether natural (e.g., rainfall, temperature) or human induced (e.g., land use, fencing). In the preceding analysis, effects of environmental drivers at the time of sampling (water temperature at time of sampling, mean daily air temperature, mean daily rainfall, mean daily streamflow) on *E. coli* concentrations were accounted for by incorporating them as explanatory covariates in the fitted GAM models. The covariate effects were then removed from the data and the remaining trend was reported. Although including water temperature, air temperature, rainfall and streamflow at the time of sampling explains a large proportion of the variation in the *E. coli* measurements at each site (Figure 39), they did *not* explain (account for) the trend in most cases, and the widespread upswing in *E. coli* concentrations over the period 2015-2019 remains unexplained by variations in temperature, rain and flow in most catchments. The upswing does not seem to be related to immediate changes in the environmental covariates.

Other explanatory factors were not included in the trend modelling. This is particularly the case for data representing human activities intended (in part) to reduce the loss of faecal contaminants to water (e.g., changes in livestock density, land use, point source discharges, and fencing); these data were not available at sufficiently high temporal resolution to include in the GAM models. In order to evaluate whether these factors may be responsible for the observed trends, we looked for correlations between the data representing these factors and the 2015-2019 trends estimated using the “raingam” model.

10.1 Livestock density

Livestock are a major source of faecal contamination, and clearly have an impact on *E. coli* concentrations in Waikato streams (e.g., Figure 15), but livestock densities change relatively slowly (Figure 14).

Median livestock density of each type was calculated from the 2008, 2012, 2019, and 2021 surveys. Plotting *E. coli* trend magnitude against the type and median density of livestock did not reveal any correlation (Figure 48); *E. coli* trends were similar across a wide range of livestock types and densities. The *E. coli* upswing in 2015-20 is not correlated to livestock density.

Changes in livestock density between the 2008, 2012, 2019, and 2021 surveys were assumed to adequately represent the 2005-2009, 2010-2014 and 2015-2019 periods respectively. Plotting *E. coli* trend magnitude against the estimated annual percent *change* in livestock density did not reveal any correlation (Figure 49); *E. coli* trends are not correlated to changes in livestock density.

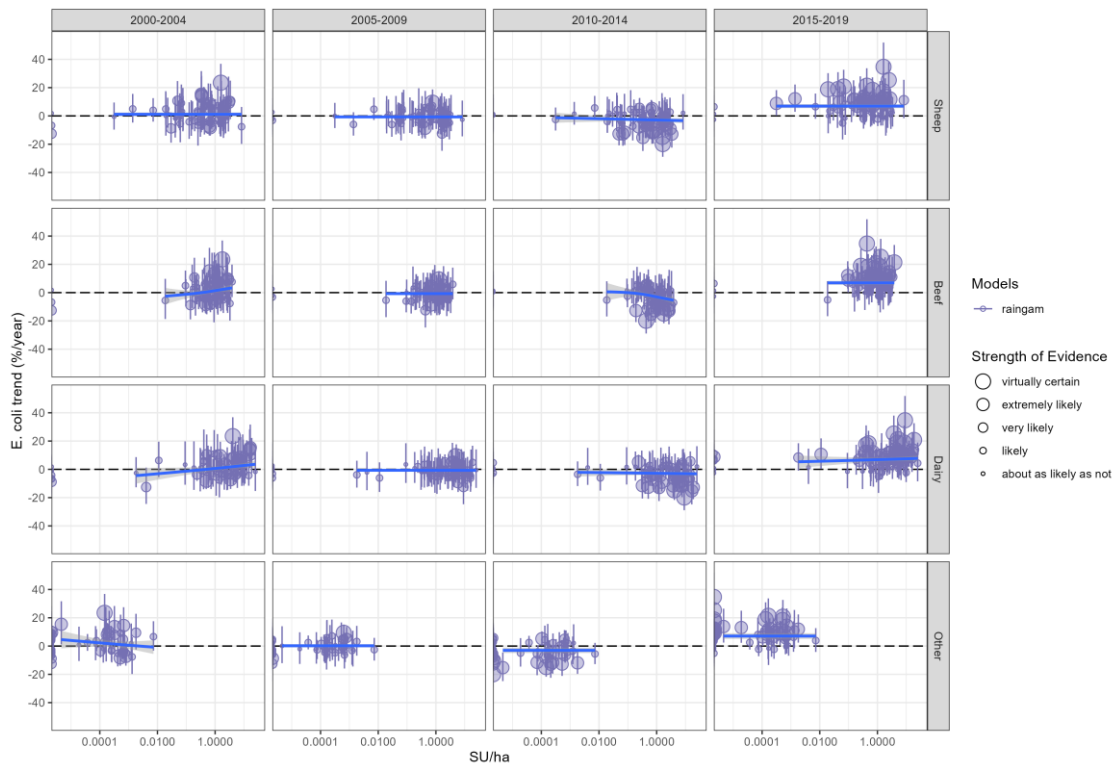


Figure 48: *E. coli* “raingam” trend estimates from Figure 36 against median livestock density (stock units per hectare).

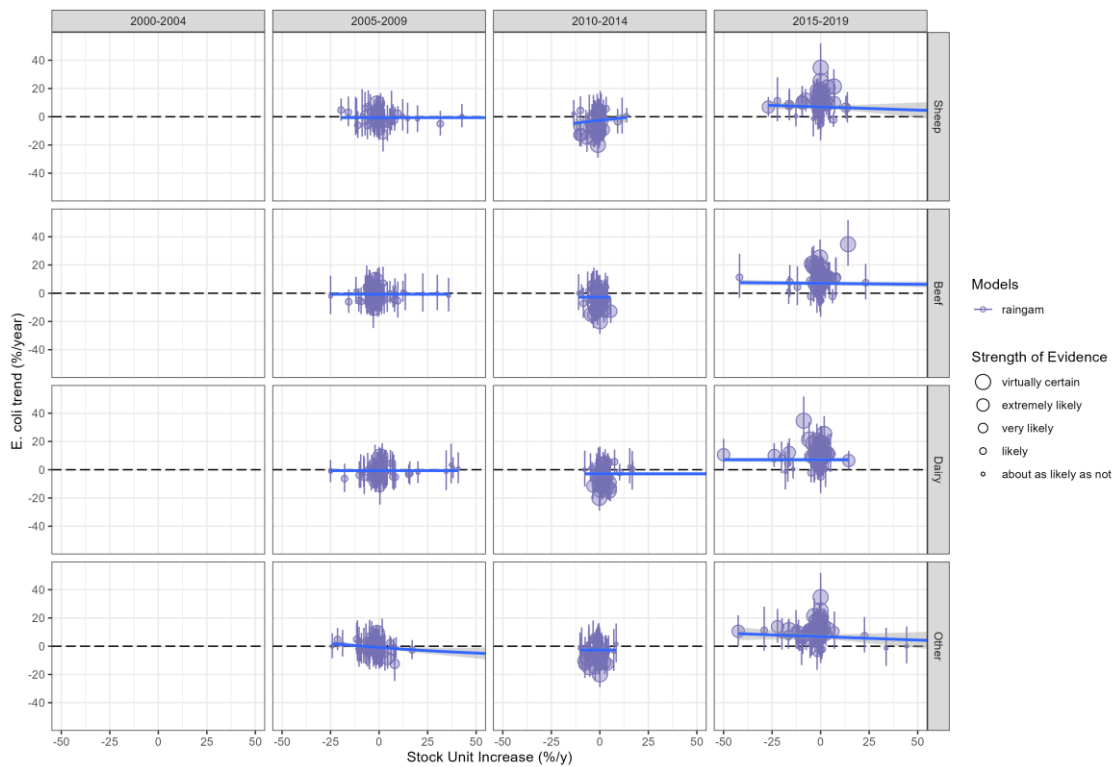


Figure 49: *E. coli* “raingam” trend estimates from Figure 36 against 5-year percent change in livestock density (stock units per hectare).

10.2 Land use and regional variations

Increases in *E. coli* concentration might plausibly be associated with land use or changes in land use (Sections 3.1 and 7.3). Plotting *E. coli* trend estimates from the “raingam” GAM model for the 2005-2009 and 2015-2019 periods against CLUES land use areas for 2008 and 2018 does not reveal any correlation however (Figure 50). Also, the upswing in *E. coli* occurs with very similar relative magnitude (about +7% per year) in almost all Waikato catchments regardless of dominant land use (Figure 48). There is a slight increase in trend magnitude with increased proportion of dairy in the catchment, but that is weak, and given the small changes in dairy proportion over time, this would not explain the widespread increasing concentrations that have occurred recently. We conclude that there is no evidence that land use changes are responsible for the recent trends in *E. coli* concentrations.

The analysis of Section 8.8 indicated that there are not significant variations in recent trends between sub-regions. This finding, as well as the lack of sensitivity to land use or stock unit trends, suggests that the upswing in *E. coli* in 2015-2019 is the result of a driver that occurs across the region, but that has not been accounted for in the corrections for factors such as rain, temperature, and flow.

10.3 Point sources

Although we do not have comprehensive information on changes in point sources over time, limited information is available that allows commentary on the role of point sources.

As noted in Section 7.6, there is little relationship between *E. coli* concentrations at monitoring sites and *E. coli* discharged from point sources in the upstream catchment. This suggests that changes in point sources are unlikely to be responsible for recent trends in *E. coli*.

We also discussed with Dr Bill Vant from WRC whether there were any recent changes in point sources, from his knowledge. From that discussion:

- As documented in a report on nutrients in the Hauraki basin (Vant, 2016), improvements in Tirau wastewater may have given rise to improvements in *E. coli* concentrations in the Oraka Stream (site 669_6) from 1991-2015 (8.2% per annum reduction). That finding is supported by our GAM analysis (see supplementary materials provided to WRC). However, those improvements in monitored water quality have since stopped or reversed.
- Treatment of Waihi township wastewater improved around 2005 (to tertiary treatment with UV disinfection), which could affect water quality in the Ohinemuri River at Queens Head (site 619_19). There does seem to have been a slight long-term decrease in concentration at that site (Figure 4), however the Seasonal Sen slope model detected a recent increase while the raingam GAM model inferred no recent trend. We have examined NIWA’s model of *E. coli* in the Hauraki catchment (Semadeni-Davies et al. 2016), and determined that the treatment plant made less than 0.02% contribution to the load at the monitoring site; on that basis, changes in treatment of the Waihi discharge are unlikely to be responsible for recent trends at the monitoring site. Although recent discharges are not compliant with the consent conditions and *E. coli* concentrations have increased over time (Fiona Forrest, WRC, personal communication), even a ten-fold increase in discharge concentrations would

not account for much of an increase in stream concentrations, based on the catchment model and also on simple dilution calculations.

- Cambridge introduced UV disinfection in 2020, but that is unlikely to show in the trend analysis due to the timing of the reduction.
- There were some issues with the Hautapu dairy factory discharging non-faecal *E. coli* in the past due to bacterial growth in a discharge pipe which resulted in a measured spike in concentrations at the lower Waikato at Narrows sites around 2002. That source has been addressed and would not be associated with recent trends. However, it does highlight the potential importance of non-faecal sources of *E. coli*.
- Consent monitoring of the Te Kuiti wastewater discharge showed that introduction of UV disinfection in about 2013 resulted in a two orders of magnitude decrease in *E. coli* concentrations in the discharge (see also Semadeni-Davies et al. 2015). However, the stream monitoring site is upstream of the discharge and would not reflect the reduction in *E. coli* in the discharge.

Our interrogation of a previous budget-based model of the Hauraki catchment (Semadeni-Davies et al. 2016) shows that point sources made <1% contribution to non-storm *E. coli* load at monitoring sites. The Waitoa River at Mellon Rd Recorder and Waihou River at Te Aroha had 5.5% and 3.4% contribution from point sources, respectively. Similarly, modelling of the Waikato and Waipa rivers (Semadeni-Davies et al. 2015) showed a small contribution to *E. coli* loads from point sources, with the largest fraction at Mangamingi (8.6%), near Tokoroa, and about 5% at Horotiu. This suggests that point sources make a small contribution to the total *E. coli* load at most sites, and therefore recent wide scale increases in concentrations at monitoring sites are unlikely to be related to changes in point sources. A further note in this regard is that changes in point sources are likely to be in the direction of reductions in sources due to improved treatment, rather than increases.

Direct discharges of dairy shed wastewater to streams can affect microbial water quality locally. In early catchment modelling of the Waikato River (Alexander et al. 2002), there were about 1800 dairy discharges to streams in 1998 based on WRC consents. More recent catchment modelling of the Waikato/Waipā (Semadeni-Davies et al. 2015) it was noted that there were 97 discharges directly to streams, based on information provided by the WRC, mainly in the Waipa and lower Waikato River. The large reduction in the number of discharges direct to streams between 2002 and 2015 (down to 97), which is likely to have contributed to historical reductions in stream *E. coli* concentrations. We expect that there will have been further reductions in discharges since 2015. However, further reduction in the number of these sources is unlikely to have influenced water quality on a widespread basis, due to the relatively small number of remaining discharges. From our modelling for the Waikato/Waipā from 2015, removing all dairy shed direct discharges would have resulted in a mean reduction of 0.8% in *E. coli* load at monitoring sites, with the largest being 9.8% reduction for Kirikiriroa. Similarly, for the Hauraki subregion, the mean reduction would be 1.4%, with the largest being 7.6% for the Piako at Kiwitahi. There were about 40 discharges to Hauraki streams at that time. Further reductions in discharges since 2015-16 could have resulted in reductions in stream water concentrations, however recent trends indicate increasing concentrations. We conclude that recent changes in dairy shed discharges are not responsible for recent increasing stream concentrations.

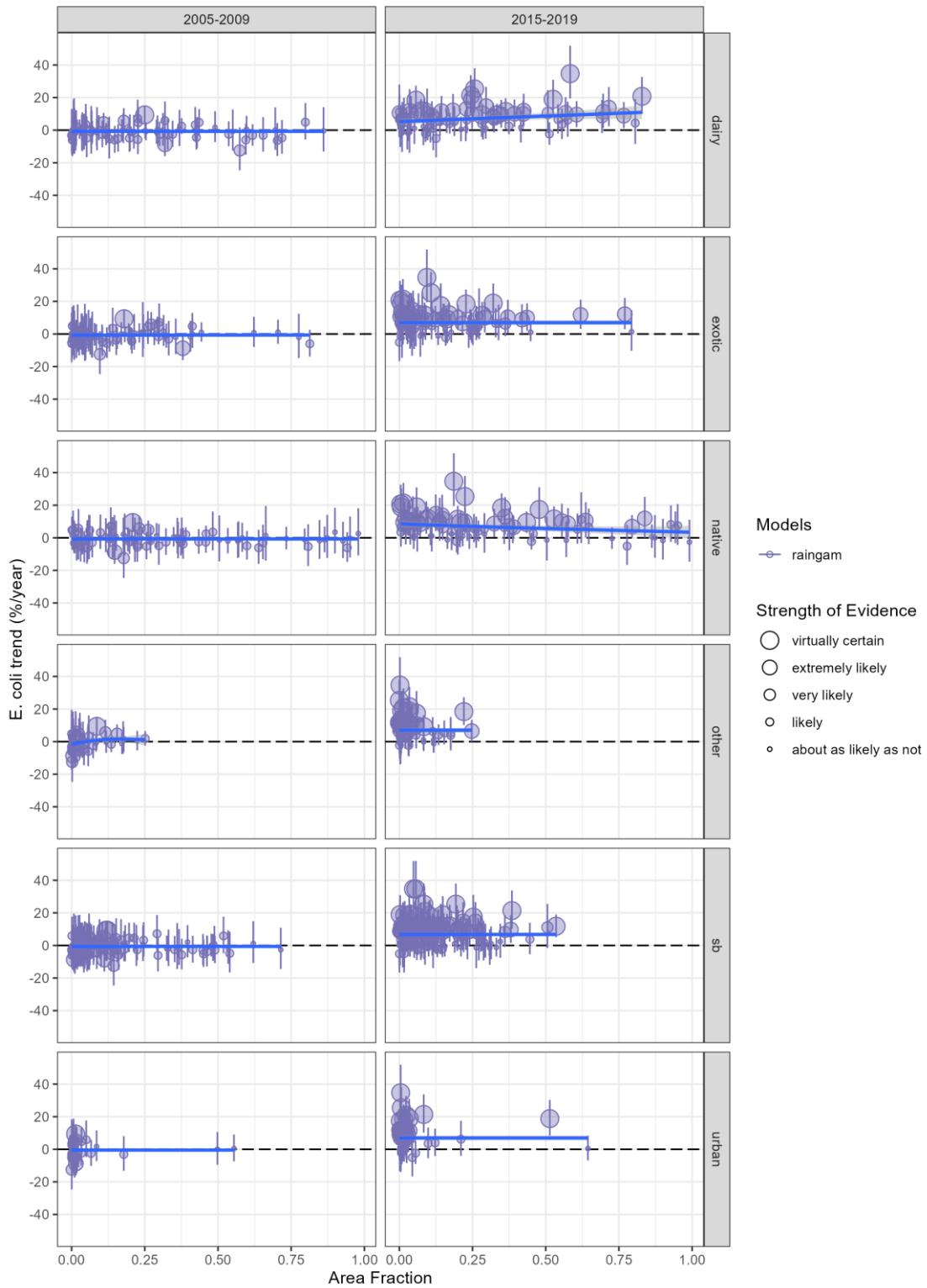


Figure 50: *E. coli* “rangam” trend estimates from Figure 36 against land use type and fraction of catchment area.

10.4 Fencing

As noted in Section 3.1, access of livestock to streams has been shown internationally to increase concentrations of faecal indicators in stream water (e.g., Kay et al. 2018). Hence, we would expect an increase in fencing to reduce stream concentrations. As noted in Section 7.5, 5-yearly surveys indicate an increase in fencing over time. Most dairy streams are now fenced, although there are some variations with stream size and region. Dairy streams are generally fenced more than drystock streams. We would expect the increased fencing to improve water quality, and it is possible fencing contributed to water quality improvement (decreased *E. coli* concentrations) in the 2010-2014 period (Figure 36). However, we would expect the extent of fencing to have remained the same or to have increased over the period 2015-2019, with an associated neutral or improving effect on water quality, yet water quality generally deteriorated over this period.

Attempts to demonstrate a link between the fence survey data and *E. coli* concentrations in the current study were hampered by the nature of the data. Ideally, we would like to determine the change in the proportion of river upstream of each sampling site that has been fenced, but the available fencing data is not well suited for that purpose. These data are also spatially sparse, making a full spatial analysis difficult and subject to considerable uncertainty.

Overall, we tentatively conclude that recent increases in concentration are unlikely to be related to changes in stock access to streams.

The increased shading of streams from riparian vegetation and potential reduction in bacterial disinfection was discussed in Section 3.3. Riparian vegetation surveys (Norris et al. 2020) found no significant change in the proportion of woody vegetation in riparian areas between 2002 and 2017, or between 2012 and 2017. We therefore consider that increases in riparian vegetation are unlikely to have caused the increase in stream concentrations.

11 Discussion

Water temperature, air temperature, rainfall and streamflow helped explain the month to month variability in *E. coli* measurements but did not account for the long-term trends of *E. coli* concentrations. After taking these natural factors into account, recent increasing trends in concentration did not seem to be related to changes in stock density, land use, point sources, or fencing.

The results suggest that the observed increasing trend in *E. coli* in 2015-2019 (approximately +7% per year) are likely to be due to factors not included in this study, but are present across pastoral, forested and urban land uses (Figure 50). Here we discuss some other potential factors or further analysis that might shed further light.

One possibility is that increases in concentration are an artefact of sampling, handling, or laboratory analysis methods. By design, these remain the same over time, but subtle changes can sometimes occur. Also, the samples are collected and handled by experienced staff, and the samples are analysed in a professional accredited laboratory with standard methods, so the likelihood of errors or changes are small. Nonetheless, it is prudent to check for inadvertent changes, especially when unexplained trends are evident. To check this, field staff could be interviewed to determine whether there have been any recent changes. Another approach would be to compare our results with trends from other nearby regions which might use different methods yet have similar land use and drivers of water quality.

Refinements to the GAM analysis might help discriminate between short-term environmental influences and longer-term variations that might be more relevant to long-term trends. For example, there is considerable seasonal and short-term fluctuation in temperature, which might cloud any signal from longer-term, more persistent effects. The GAM procedure assumes that the temperature sensitivity established largely on the basis of short-term variations would capture the effects of any longer-term components, however longer-term temperature changes may have a different mechanism of influence. It may therefore be of value to extract longer-term signals from the environmental signal (by digital filtering, for example) as a separate covariate.

The recent increases may be related to naturalised forms of *E. coli* that respond to environmental conditions such as temperature in unusual ways (see Section 3.2 for discussion). If environmental conditions are becoming more conducive to survival of such naturalised populations, then measured concentrations of *E. coli* could increase. For example, increased temperature could favour the growth of environmental strains. This is a somewhat tentative explanation for the recent trends, and it is not clear why the naturalised populations would have increased recently. However, the influence of naturalised population is potentially important. We therefore recommend further literature review on this topic, especially the role of environmental drivers such as temperature on the survival of naturalised populations. Depending on the findings, the literature review could be followed with (a) field measurements to detect naturalised populations and environmental clades at key sites, and (b) follow-up experiments on factors affecting the survival and growth of naturalised populations.

An environmental driver that was not included in the analysis was solar radiation, which is known to kill in-stream *E. coli* when high. It would be possible to include this covariate (e.g., obtained from the VCSN) in the GAM model approach in future work.

There may be additional drivers of *E. coli* increases that we have not yet considered, such as changes in bird or pest animal populations. These drivers would be difficult to quantify. Repeated source-tracking might assist to some degree, but source tracking studies have not been widely conducted to date. In addition, current methods provide indicators of source types rather than highly accurate estimates of abundance. Considering the limitations of the tracking methods, we recommend that this work have a lower priority.

We also consider that it would be appropriate to compare recent trends in the Waikato to trends in neighbouring regions. It would be valuable to know if other regions of NZ, and temperate regions overseas, are also experiencing similar recent increases in *E. coli* concentrations in streams that are not explainable by land management changes, but might, plausibly, reflect common factors such as global warming. This could also help identify possible influences of changes in sampling and analysis methodologies, and also shed light on drivers (for example, if trends are not the same in other regions, then there is a suggestion that the causes of trends are Waikato-specific, which will help narrow the search for causes).

12 Conclusion

This study used traditional non-parametric (Sen slope) and alternative GAM trend estimation methods to quantify and explain trends in *E. coli* concentrations in Waikato streams in terms of a range of drivers.

In relation to the statistical methods for trend detection and corrections for natural drivers such as temperature, rain and flow:

- Sen slope estimates adjusted for season and flow were similar to unadjusted slope estimates.
- Sen slope estimates based on 5-year data periods were often much larger than slope estimates inferred from GAM models fitted to the entire 20-year series. In many cases non-zero Sen slopes were predicted where the GAM estimate was not different from zero.
- Trend estimates based on GAM models were consistent in terms of magnitude and likelihood, regardless of which covariates were included. Including covariates helped explain the month-to-month variation in *E. coli* measurements but did not change the long-term trend estimates.
- GAM models that included rain and/or flow were much better at explaining month-to-month *E. coli* concentrations than those that excluded these variables. Rain may be preferable to flow for trend estimation purposes, because estimates are available throughout New Zealand from the NIWA VCSN network, whereas measured flow is currently only available at limited sites (virtual flow estimates will become available in the future via the NIWA New Zealand Water Model (NZWaM) project).

Our trend assessment confirms widespread decrease in *E. coli* concentrations (improvement in microbial water quality) in the 2010-2014 period, followed by widespread, strongly increasing *E. coli* concentrations (deterioration in microbial water quality) in the 2015-2019 period (Figure 36).

Measured *E. coli* concentrations were shown to be influenced by environmental drivers of flow, temperature, and rain; this observation is consistent with how these factors mobilise and transport particulates, such as *E. coli*. The GAM models made corrections for effects from these factors by including them as covariates in the statistical model, but even after these corrections for effects were made, an increasing trend in concentrations in the 2015-2019 period persisted.

Analysis of the data and knowledge of contaminant mobilisation and transport processes confirms that land use and stock numbers affect microbial concentrations in streams. However, changes in stocking rates and land use in the 2015-2019 period have been small and are unlikely to explain the recent increasing concentration trend.

Recent increases in *E. coli* are unlikely to be related to increases in fencing, because fencing has been increasing over time whereas concentrations have been increasing recently.

Recent increases in *E. coli* are also unlikely to be related to changes in point sources, because discharges from wastewater treatment plants have generally decreased over time, and they typically make a small contribution to stream microbial contamination at the monitoring sites. Similarly, the

number of dairy shed effluent discharges to streams have steadily decreased over time, and their impact of stream microbial water quality is expected to be decreasing rather than increasing.

E. coli concentrations are generally correlated with optical water quality variables such as turbidity and clarity. However, recent trends in turbidity and clarity differed from those of *E. coli*, suggesting that recent increases in *E. coli* concentration over time are due to factors that are not influencing either turbidity or visual clarity.

The recent trend did not seem to be associated with any particular land use, or with stocking density. Recent increases occurred even in catchments dominated by native and exotic land use.

We did not detect systematic sub-regional variations in the recent trends.

Overall, the causes of recent increases remain unknown. The observed trends could be due to processes and drivers that were not included in the current study, limitations of the statistical models, or artefacts of sample handling, storage and analysis methods. The cause would seem to operate across the region.

Several factors have been identified for further investigation (with a view to explaining the cause of the trend of increasing *E. coli* concentrations), including:

- Undertaking a similar exercise using data from other regions to see whether this is a Waikato-specific or national phenomenon.
- Refining the statistical models to address long-term, gradual variations in temperature as a specific covariate.
- Adding solar radiation to the models.
- Reviewing the literature to identify whether naturalised populations or other strains of microbe that are not of faecal origin but are counted in the *E. coli* analysis could have an effect on recently observed trends.
- Reviewing the literature to identify whether temperature changes (related to climate change) may have an effect on growth of organisms in faecal matter in pastures and in riparian areas, as well as in naturalised populations.
- Undertaking a brief review of sample collection, storage and analysis to identify factors that might have changed recently and could have resulted in apparent trends in microbial concentrations. While the sampling and storage is undertaken by experienced teams, and sample analysis is conducted by a high-quality accredited laboratory with standard methods, it would be prudent to eliminate changes in sample collection, storage or analysis as factors contributing to unexpected trends.

13 Supplementary material

The full set of trend analysis plots for the 82 sites and 6 GAM methods (e.g., Figure 23—Figure 32) for *E. coli*, turbidity and visual clarity have been provided to Waikato Regional Council, include the associated Sen slope trend estimates. For each trend analysis a GAM diagnostic and residual plot is also available.

14 Acknowledgements

We wish to thank Waikato Regional Council staff, including:

- Eloise Ryan for ongoing discussions, guidance and liaison.
- Thomas Wilding for discussions and suggestions for analysis.
- Bill Vant for early discussions on microbial trends, and for providing point source data.
- Matt Norris for providing fencing data and interpretations.
- Debbie Eastwood for providing flow data.
- Dan Borman for providing land use and stocking rate data.
- Aroha Salu for providing water quality time-series.

We also wish to thank NIWA staff members Christian Zammit for providing catchment-average VCSN (Virtual Climate Station Network) time-series for each catchment and Elizabeth Graham for reviewing an early draft of the report.

15 Glossary of abbreviations and terms

AIC	Akaike Information Criterion, an estimator of prediction error and thereby relative quality of statistical models for a given set of data.
CFU	Colony-forming units, a unit used in microbiology to estimate the number of viable bacteria or fungal cells in a sample.
covariate	In the context of this study, a covariate is a variable in a regression relationship.
CLUES	Catchment Land Use for Environmental Sustainability, a GIS-based model that predicts the effects of land-use change and farm practice scenarios on water quality and a range of socio-economic indicators at the catchment scale.
EDF	Effective degrees of freedom, a measure of curvature of a GAM model term.
FIB	Faecal Indicator Bacteria, types of bacteria used to detect and estimate the level of faecal contamination of water.
GAM	Generalised additive model, a type of linear regression model constructed by adding together flexible curved terms.
GAMM	Generalised additive mixed model, a type of mixed linear regression model constructed by adding flexible curved terms and fixed effects.
LAWA	Land Air Water Aotearoa, a collaborative web portal for sharing New Zealand environmental data and information.
LCDB	New Zealand Land Cover Database, a multi-temporal, thematic classification of New Zealand's land cover.
LOD	Limit of detection, the lowest concentration of the analyte that can be reliably detected.
LOESS	Locally estimated scatterpoint smoothing, a method of regression analysis which creates a smooth line through a scatterplot.
mgcv	Mixed GAM computation vehicle, an R package for generalized additive modelling (GAM).
MFE	Ministry for the Environment.
MOH	Ministry of Health.
MPN	Most probable number, a statistical method used to estimate the viable numbers of bacteria in a sample.
NIWA	National Institute of Water and Atmospheric Research.
NPS-FM 2020	National Policy Statement for Freshwater Management 2020, the freshwater management policy statement of the New Zealand Government.
NRWQN	National River Water Quality Network, NIWA's network of 77 water quality monitoring sites on 35 rivers that are evenly distributed over the two main islands of New Zealand.

NSE	Nash-Sutcliffe Model Efficiency, a statistic that measures the proportion of data variance explained by a model.
NZREC	New Zealand River Environment Classification, a hierarchical classification, mapping and environmental database of New Zealand rivers.
NZWaM	New Zealand Water Model, a national hydrological model.
PET	Potential evapotranspiration, the water vapor flux under ideal conditions of complete ground cover by plants, uniform plant height and leaf coverage, and an adequate water supply.
RL	Reporting limit, the lowest concentration at which an analyte can be detected in a sample.
SOE	State of the Environment, data regularly collected on different aspects of New Zealand's environment.
SOI	Southern Oscillation Index, the difference in average air pressure measured at Tahiti and Darwin, Australia.
SU	Stock units, a method of comparing the numbers and density of livestock grazing in agriculture. In New Zealand, 1 SU is equivalent to 1 breeding ewe.
VCSN	Virtual Climate Station Network, a grid of over 11,000 virtual weather data points covering the entire New Zealand area.
WQ	Water quality, the condition of the water, including chemical, physical, and biological characteristics, usually with respect to its suitability for a particular purpose such as drinking or swimming.
WRC	Waikato Regional Council.

16 References

- Alexander, R.B., Elliott, A.H., Shankar, U., McBride, G.B. (2002) Estimating the sources and sinks of nutrients in the Waikato Basin. *Water Resources Research* 38(12), 1268-1280.
- Beck, M.W., Murphy, R.R. (2017) Numerical and qualitative contrasts of two statistical models for water quality change in tidal waters. *Journal of the American Water Resources Association*, 53(1), 197-219.
- Berthe, T., Ratajczak, M., Clermont, O., Denamur, E., Petit, F. (2013) Evidence for coexistence of distinct *Escherichia coli* populations in various aquatic environments and their survival in estuary water. *Applied & Environmental Microbiology* 79(15), 4684–4693.
- Bradford, S.A., Morales, V.L., Zhang, W., Harvey, R.W., Packman, A.I., Mohanram, A., Welty, C. (2013) Transport and fate of microbial pathogens in agricultural settings. *Critical Reviews in Environmental Science and Technology* 43, 775-893.
- Bragina, L., Sherlock, O., van Rossum, A.J., Jennings, E. (2017) Cattle exclusion using fencing reduces *Escherichia coli* (*E. coli*) level in stream sediment reservoirs in northeast Ireland. *Agriculture, Ecosystems and Environment* 239, 349-358.
<https://doi.org/10.1016/j.agee.2017.01.021>
- Byappanahalli, M.N., Shively, D.A., Nevers, M.B., Sadowsky, M.J., Whitman, R.L. (2003) Growth and survival of *Escherichia coli* and enterococci populations in the macro-alga *Cladophora* (Chlorophyta). *FEMS Microbiology Ecology* 46, 203–211.
- Byappanahalli, M.N., Whitman, R.L., Shively, D.A., Sadowsky, M.J., Ishii, S. (2006) Population structure, persistence, and seasonality of autochthonous *Escherichia coli* in temperate, coastal forest soil from a Great Lakes watershed. *Environmental Microbiology* 8(3), 504-513
- Collins, R., Elliott, S., Adams, R. (2005) Overland flow delivery of faecal bacteria to a headwater pastoral stream. *Journal of Applied Microbiology* 99(1), 126-132.
- Collins, R., McLeod, M., et al. (2007) Best management practices to mitigate faecal contamination by livestock of New Zealand waters. *New Zealand Journal of Agricultural Research* 50, 267-278. <https://doi.org/10.1080/00288230709510294>
- Craig, D.L., Fallowfield, H.J., Cromar, N.J. (2004) Use of microcosms to determine persistence of *Escherichia coli* in recreational coastal water and sediment and validation with *in situ* measurements. *J. Appl. Microbiol.* 96 (5), 922–930.
- Davies, C.M., Long, J.A.H., Donald, M., Ashbolt, N.J. (1995) Survival of fecal microorganisms in marine and freshwater sediments. *Applied Environmental Microbiology* 61, 1888–1896.
- Davies-Colley, R.J. (2013) River water quality in New Zealand: an introduction and overview. In: Dymond, J., ed. *Ecosystem Services in New Zealand: Conditions and Trends*. Wellington, Manaaki Whenua Press. Pp. 16

- Davies-Colley, R.J., Valois, A., Milne, J.M. (2018) Faecal contamination and visual clarity of New Zealand rivers: correlation of key variables affecting swimming water quality. *Journal of Water and Health* 16(3). <https://doi.org/10.2166/wh.2018.214>
- Davies-Colley, R.J., Milne, J.M., Heath, M.W. (2019) Reproducibility of river water quality measurements: inter-agency comparisons for quality assurance. *New Zealand Journal of Marine and Freshwater Research*. <https://doi.org/10.1080/00288330.2019.1585886>
- Davies-Colley, R.J., Heubeck, S., Ovenden, R., Vincent, A., Hughes, A.O. (2021) Comparison of the responses of ISO-7027-compliant turbidity sensors commonly used in NZ. Envirolink Project ELF20212. *NIWA client report 2020-282HN*.
- Davies-Colley, R.J., Hughes, A.O., Vincent, A., Heubeck, S. (2021) *in press*. Weak numerical comparability of ISO7027-compliant nephelometric turbidity sensors: ramifications for turbidity data applications. *Hydrological Processes*. Accepted 24 September 2021.
- Devane, M. (2019) Transfer of knowledge and implementation of routine analysis of environmental samples for the presence of naturalised *E. coli*. Report prepared for Northland Regional Council, p.71, ESR Christchurch
- Devane, M.L., Moriarty, E., Weaver, L., Cookson, A., Gilpin, B. (2020) Fecal indicator bacteria from environmental sources; strategies for identification to improve water quality monitoring. *Water Research* 185, 116204. <https://doi.org/10.1016/j.watres.2020.116204>
- Donnison, A.M., Ross, C., M. (1999) Animal and human faecal pollution in New Zealand Rivers. *New Zealand Journal of Marine and Freshwater Research* 33, 119-128.
- Donnison, A., Ross, C., Clark, D. (2008) *Escherichia coli* shedding by dairy cows. *New Zealand Journal of Agricultural Research* 51, 273-278. <https://doi.org/10.1080/00288230809510457>
- Fewster, R.M., Buckland, S.T., Siriwardena, G.M., Baillie, S.R., Wilson, J.D. (2000) Analysis of population trends for farmland birds using generalized additive models. *Ecology* 81(7), 1970-1984. [https://doi.org/10.1890/0012-9658\(2000\)081\[1970:AOPTFF\]2.0.CO;2](https://doi.org/10.1890/0012-9658(2000)081[1970:AOPTFF]2.0.CO;2)
- Fischer, C. (2016) Comparing the logarithmic transformation and the Box-Cox transformation for individual tree basal area increment models. *Forest Science* 62(3), 297-306. <http://dx.doi.org/10.5849/forsci.15-135>
- Fraser, C., Snelder, T., Larned, S., Whitehead, A., in prep. Untitled draft report for NIWA Envirolink Project ELF21301. NIWA, Christchurch, NZ.
- Graham, E., Jones-Todd, C., Wadhwa, S., Storey, R. (2018) Analysis of stream responses to riparian management on the Taranaki ring plain. *NIWA client report 2018051HN* prepared for Taranaki Regional Council. NIWA, Hamilton.
- Harmel, R.D., Karthikeyan, R., Gentry, T., Srinivasan, R. (2010) Effects of agricultural management, land use, and watershed scale on *E. coli* concentrations in runoff and streamflow. *Transactions of the ASABE* 53(6), 1833-1841.

- Harmel, R.D., Hathaway, J.M., Wagner, K.L., Wolfe, J.E., Karthikeyan, R., Francesconi, W., McCarthy, D.T. (2016) Uncertainty in monitoring *E. coli* concentrations in streams and stormwater runoff. *Journal of Hydrology* 534, 524-533.
<http://doi.org/10.1016/j.jhydrol.2016.01.040>
- Hastie, T.J., Tibshirani, R.J. (1986) Generalized additive models. *Statistical Science* 1, 297–310.
- Hastie, T.J., Tibshirani, R.J. (1990) *Generalized Additive Models*. Chapman & Hall/CRC, Boca Raton, FL, USA.
- Helsel, D.R., Hirsch, R.M., Ryberg, K.R., Archfield, S.A., Gilroy, E.J. (2020) Statistical methods in water resources: U.S. Geological Survey Techniques and Methods, Book 4, Chapter A3. <https://doi.org/10.3133/tm4a3>
- Hendricks, C.W., Morrison, S.M. (1967) Multiplication and growth of selected enteric bacteria in clear mountain stream water. *Water Research* 1, 567–576.
- Hipsey, M.R., Antenucci, J.P., Brookes, J.D. (2008) A generic, process-based model of microbial pollution in aquatic systems. *Water Resources Research* 44, W07408.
<https://doi.org/10.1029/2007WR00639>
- Hirsch, R.M., Slack, J.R., Smith, R.A. (1982) Techniques of trend analysis for monthly water quality data. *Water Resources Research* 18(1), 107-121.
<https://doi.org/10.1029/WR018i001p00107>
- Ishii, S., Ksoll, W.B., Hicks, R.E., Sadowsky, M.J. (2006) Presence and growth of naturalized *Escherichia coli* in temperate soils from Lake Superior watersheds. *Appl. Environ. Microbiol.* 72(1), 612-621.
- Kay, D., Crowther, J., et al. (2008) Faecal indicator organism concentrations and catchment export coefficients in the UK. *Water Research* 42, 2649-2661.
<https://doi.org/10.1016/j.watres.2008.01.017>
- Kay, D., Crowther, J., Stapleton, C.M., Wyer, M.D. (2018) Faecal indicator organism inputs to watercourses from streamside pastures grazed by cattle: before and after implementation of streambank fencing. *Water Research* 143, 229-239.
- Killick, R., Fearnhead, O., Eckley, I.A. (2012) Optimal detection of changepoints with a linear computational cost. *Journal of the American Statistical Association* 107(500), 1590-1598.
<https://doi.org/10.1080/01621459.2012.737745>
- Killick, R., Beaulieu, C., Taylor, S., Hullait, H., 2021. EnvCpt: Detection of Structural Changes in Climate and Environment Time Series. R package version 1.1.3. <https://CRAN.R-project.org/package=EnvCpt>
- Larned, S., Whitehead, A., Fraser, C., Snelder, T., Yang, J., 2019. Water quality state and trends in New Zealand rivers: analyses of national data ending in 2017. NIWA Client Report No. 2018347CH, prepared for Ministry for the Environment.
<https://environment.govt.nz/publications/water-quality-state-and-trends-in-new-zealand-rivers-analyses-of-national-data-ending-in-2017/>

- LAWA, 2021a. Land Air Water Aotearoa, Waikato Region, River Quality. <https://www.lawa.org.nz/explore-data/waikato-region/river-quality>
- LAWA, 2021b. LAWA River Water Quality National Picture Summary 2021. <https://www.lawa.org.nz/explore-data/river-quality/>
- Lee, D.K. (2020) Data transformation: a focus on the interpretation. *Korean Journal of Anesthesiology*, 73(6), 503-508. <https://doi.org/10.4097/kja.20137>
- Marra, G., Wood, S.N. (2011) Practical variable selection for generalized additive models. *Computational Statistics and Data Analysis* 55, 2372-2387. <https://doi.org/10.1016/j.csda.2011.02.004>
- McBride, G.B., Till, D., Ryan, T., Ball, A., Lewis, G., Palmer, S., Weinstein, P. (2002) Freshwater microbiology research programme report: pathogen occurrence and human health risk assessment. *Ministry for the Environment Technical Publication TR-122*. <https://environment.govt.nz/publications/freshwater-microbiology-research-programme-report-pathogen-occurrence-and-human-health-risk-assessment-analysis/>
- McBride, G., Cole, R.G., Westbrooke, I., Jowett, I. (2014) Assessing environmentally significant effects: a better strength-of-evidence than a single p value? *Environmental Monitoring and Assessment* 186, 2729–2740.
- McBride, G.B. (2019) Has water quality improved or been maintained? a quantitative assessment procedure. *Journal of Environmental Quality*.
- McCambridge, J., McMeekin, T. (1980) Effect of temperature on activity of predators of *Salmonella typhimurium* and *Escherichia coli* in estuarine water. *Marine and Freshwater Research* 31(6), 851-855.
- McCarthy, D.T., Deletic, A., Mitchell, V.G., Fletcher, T.D., Diaper, C. (2008) Uncertainties in storm water *E. coli* levels. *Water Research* 42, 1812-1824. <https://doi.org/10.1016/j.watres.2007.11.009>
- Meals, D.W., Spooner, J., Dressing, S.A., Harcum, J.B., 2011. Statistical analysis for monotonic trends, Tech Notes 6, November 2011. Developed for U.S. Environmental Protection Agency by Tetra Tech, Inc., Fairfax, VA, 23 p. Available online at <https://www.epa.gov/polluted-runoff-nonpoint-source-pollution/nonpoint-source-monitoringtechnical-notes>
- MFE and MOH, (2003) Microbiological water quality guidelines for marine and freshwater recreational areas. Ministry for the Environment and Ministry of Health, Wellington, New Zealand. <https://environment.govt.nz/publications/microbiological-water-quality-guidelines-for-marine-and-freshwater-recreational-areas/>
- Monaghan, R., Wilcock, R., Smith, L., TikkiSETTY, B., Thorrold, B., Costall, D. (2007) Linkages between land management activities and water quality in an intensively farmed catchment in southern New Zealand. *Agriculture, ecosystems & environment*, 118(1-4): 211-222.

- Moriarty, E.M., Karki, N., Mackenzie, M., Sinton, L.W., Wood, D.R., Gilpin, B.J. (2011) Faecal indicators and pathogens in selected New Zealand waterfowl. *New Zealand Journal of Marine and Freshwater Research* 45(4), 679-688.
- Moriarty, E.M., Weaver, L., Sinton, L.W., Gilpin, B. (2012) Survival of *Escherichia coli*, enterococci and *Campylobacter jejuni* in Canada goose feces on pasture. *Zoonoses Public Health* 59 (7), 490–497.
- Moriarty, E. (2015) Sources of faecal pollution in selected Waikato Rivers. Client report CSC15012 prepared for Dairy NZ by ESR, Christchurch.
- Muller, H., Geller W. (1993) Maximum growth rates of aquatic ciliated protozoa: the dependence on body size and temperature reconsidered. *Archiv fur Hydrobiologie* 126, 315–327.
- Muller, C., Stephens, T. (2021) Riparian area management scenarios for inclusion in Auckland Council’s Fresh Water Management Tool Stage 1. Final report for Auckland Council. Auckland Council. Healthy Waters Department, FWMT Report 2021/7.
- Nelson, K.L., et al. (2018) Sunlight-mediated inactivation of health-relevant microorganisms in water: a review of mechanisms and modeling approaches. *Environmental Science Processes & Impacts* 20, 1089-1122.
- New Zealand Government, 2020. National Policy Statement for Freshwater Management (2020) Wellington, August 2020.
- Norris, M, Jones, H., Kimberley, M., Borman, D. (2020) Riparian characteristics of pastoral waterways in the Waikato region, 2002-2017. *Waikato Regional Council Technical Report* 2020/12. <https://www.waikatoregion.govt.nz/assets/WRC/WRC-2019/TR202012.pdf>
- Pandey, P.K., Kass, P.H., Soupier, M.L., Biswas, S., Singh, V.P. (2014) Contamination of water resources by pathogenic bacteria. *AMB Express* 4, 1-16.
- Percec-Merien, A.M., Lewis, G.D. (2012) Naturalized *Escherichia coli* from New Zealand wetland and stream environments. *FEMS Microbiology Ecology* 83(2), 494-503.
- Ratkowsky, D.A., Lowry, R.K., McMeekin, T.A., Stokes, A.N., Chandler, R.E. (1983) Model for bacterial culture growth rate throughout the entire biokinetic temperature range. *Journal of Bacteriology* 154(3), 1222-1226.
- SAS, 2009. SAS/GRAPH 9.2: Statistical Graphics Procedures Guide, Second Edition.
- Schreiber, C., Rechenburg, A., Rind, E., Kistemann, T. (2015) The impact of land use on microbial surface water pollution. *International Journal of Hygiene and Environmental Health* 218, 181-187.
- Semadeni-Davies, A., Elliott, S., Yalden, S. (2015) Modelling *E. coli* in the Waikato and Waipa River catchments: development of a catchment-scale microbial model. *NIWA client report* AKL2015-017 prepared for Waikato Regional Council. National Institute of Water and Atmospheric Research, Auckland.

- Semadeni-Davies, A., Greenwood, M., Elliott, S. (2016) Modelling *E. coli* for the Hauraki Plains and Coromandel Peninsula: development and calibration of catchment-scale microbial models for load and concentration. *NIWA client report 2016060AK* prepared for Waikato Regional Council. National Institute of Water and Atmospheric Research, Auckland.
- Simpson, G.L. (2018) Modelling palaeoecological time series using Generalised Additive Models. *Frontiers in Ecology and Evolution* 6, 149. <https://doi.org/10.3389/fevo.2018.00149>
- Smith, D.G., McBride, G.B., Bryers, G.G., Wisse, J., Mink, D.F.J. (1996) Trends in New Zealand's national river water quality network. *New Zealand Journal of Marine and Freshwater Research* 30, 485-500. <https://doi.org/10.1080/00288330.1996.9516737>
- Soller, J.A., Schoen, M.E., Bartrand, T., Ravenscroft, J.E., Ashbolt, N.J. (2010) Estimated human health risks from exposure to recreational waters impacted by human and non-human sources of faecal contamination. *Water Research* 44, 4674-4691.
- Snelder, T. (2018) Assessment of recent reductions in *E. coli* and sediment in rivers of the Manawatū-Whanganui Region: including associations between water quality trends and management interventions. Land Water People (LWP) Client Report 2017-06, prepared for Horizons Regional Council.
- Snelder, T., Biggs, B., Weatherhead, M. (2010) New Zealand River Environment Classification User Guide, revised 2 March 2015. Ministry for the Environment, Wellington, New Zealand. Document ID 11123. <https://data.mfe.govt.nz/document/11123-river-environment-classification-user-guide-2010/>
- Stott, R., Davies-Colley, R., Nagels, J., Donnison, A., Ross, C., Muirhead, R. (2011) Differential behaviour of *Escherichia coli* and *Campylobacter* spp. in a stream draining dairy pasture. *Journal of Water and Health* 9(1), 59-69. <https://doi.org/10.2166/wh.2010.061>
- Vant, B. (2014) Sources of the nitrogen and phosphorus in the Waikato and Waipa rivers, 2003-12. Waikato Regional Council Technical Report 2014/56. Hamilton, Waikato Regional Council. <https://waikatoregion.govt.nz/services/publications/tr201456/>
- Vant, B. (2016) Water quality and sources of nitrogen and phosphorus in the Hauraki rivers, 2006-15. *Waikato Regional Council Technical Report 2016/17*. Hamilton, Waikato Regional Council. <https://waikatoregion.govt.nz/services/publications/tr201617/>
- Vant, B. (2018) Trends in river water quality in the Waikato region, 1993-2017. *Waikato Regional Council Technical Report 2018/30*. Hamilton, Waikato Regional Council. <https://www.waikatoregion.govt.nz/services/publications/tr201830/>
- Vermuelen, L.C., Hofstra, N., 2014. Influence of climate variables on the concentration of *Escherichia coli* in the Rhine, Meuse, and Drentse Aa during 1985–2010. *Regional Environmental Change* 14, 307-319. <https://doi.org/10.1007/s10113-013-0492-9>
- Wilcock, B. (2006) Assessing the relative importance of faecal pollution sources in rural catchments. *NIWA Client Report: HAM2006-104* prepared for Environment Waikato.

- Wilcock, R.J., Monaghan, R.M., Quinn, J.M., Srinivasan, M.S., Houlbrooke, D.J., Duncan, M.J., Wright-Stow, A.E., Scarsbrook, M.R. (2013) Trends in water quality of five dairy farming streams in response to adoption of best practice and benefits of long-term monitoring at the catchment scale. *Marine and Freshwater Research* 64, 401-412.
<https://doi.org/10.1071/Mf12155>
- Wood, D., Horn, B., Moriarty, E.M. (2018) Faecal pollution source risks. Report No. CSC18003 prepared for Dairy NZ by ESR, Christchurch, NZ.
- Waikato Regional Council, 2019. Stock Density. Accessed on 21 September 2021 at <https://www.waikatoregion.govt.nz/environment/land-and-soil/land-and-soil-monitoring/riv9-report-card/>
- Yang, G.X., Moyer, D.L. (2020) Estimation of nonlinear water-quality trends in high-frequency monitoring data. *Science of the Total Environment* 715.
<https://doi.org/10.1016/j.scitotenv.2020.136686>

Appendix A Handling of censored values

Censored data refer to measurements whose values are only partially known. For environmental data, this most often occurs with very low values (e.g., concentrations) that are below the limits of reliable detection of the equipment or procedure being used. Such values are called “left-censored” and reported with a “<” sign (e.g., < 1). Censoring may also occur with very high values (e.g., concentrations) that are above the operating limits of the equipment or procedure, in which case they are called “right-censored”, and reported with a “>” sign (e.g., > 1000). Censored data require special handling when used in statistical calculations. Fraser et al. (in prep.) discuss handling of censored values in data at length, but do not recommend a particular approach. The common approach of replacing left-censored values with 0.5 of the censoring level works well in many instances but is not appropriate when measurement does not have a natural lower bound at zero (e.g., for temperatures), or when the censoring level changes through time (as in the case of Waikato *E. coli* data as illustrated in Figure 6).

Another option, “imputation”, replaces the censored values with an estimate of their original value. In this case the average of all data values below the censorship level (including already imputed values) is used. Censored values with no data values below them are replaced with the censoring level itself. For least-squares-based fitting this prevents introducing an artefactual trend. Therefore, imputation should be applied after data transformation. This method can also be applied to right-censored data.

We compared several methods for handling censored values and compared them in Figure 51. A synthetic data set was created (ostensibly with no trend) and censoring was then applied to points < 1 prior 2010 and < 3 thereafter. The effect of the following approaches to using the censored points in trend analysis was then tested—the objective was to recreate the original trend:

1. Original – original data with no censorship and the original (near zero) trend.
2. Censored – use the censorship level as reported, resulting in an artefactual increasing trend.
3. Exclude – delete the censored data, resulting in an even more pronounced artefactual increasing trend.
4. Half – replace the censored data with half the censorship level (this is a common approach), resulting in a (slightly) negative trend relative to the original.
5. Impute - replace the censored data with the average of all data values below the censorship level (including already imputed values), resulting in a trend that is very close to the original.

Figure 51 shows that the “half” and “impute” methods recreate the original trend well in this case. Based on this preliminary analysis of censorship approaches, we used the “impute” method to reposition left- and right-censored values in the *E. coli* data. This method was applied after Box-Cox transformation.

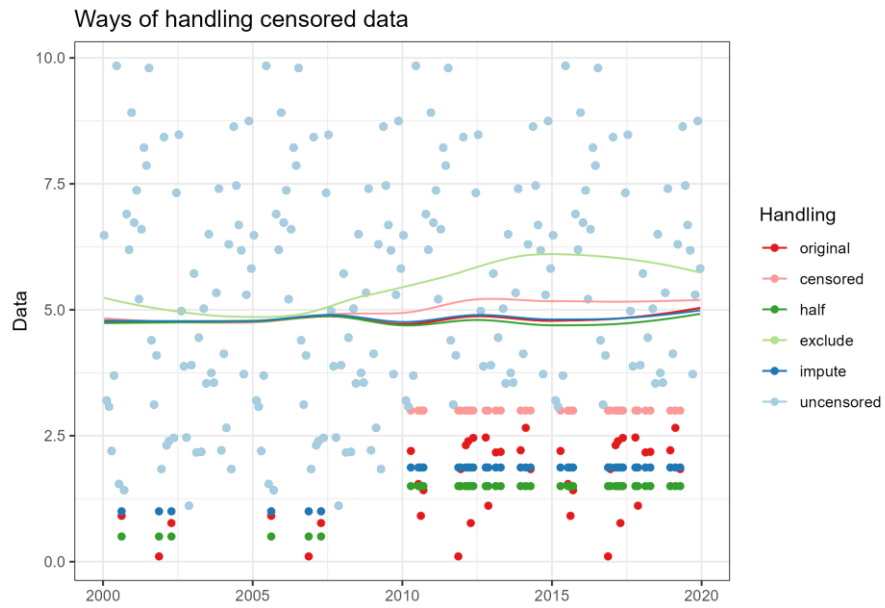


Figure 51: Comparison of methods for handling censored data in trend analysis. The “uncensored” points were included in all methods; methods differed only in their handling (or exclusion) of the “original” points.